Extracting Fire Behaviour Data from Georeferenced Oblique Aerial Wildfire Photographs

by

Henry G. Hart

A Thesis Submitted in Partial Fulfillment of the
Requirements for the Degree of

MASTER OF SCIENCE

In the Department of Geography

We acknowledge and respect the lək̓ʷəŋən peoples on whose traditional territory the university stands, and the Songhees, Esquimalt and W̱SÁNEĆ peoples whose historical relationships with the land continue to this day.

Extracting Fire Behaviour Data from Georeferenced Oblique Aerial Wildfire Photographs

by

Henry G. Hart

Supervisory Committee

Dr. Christopher Bone, Co-Supervisor
Department of Geography

Dr. Daniel Perrakis, Co-Supervisor
Department of Geography

Abstract

Wildfires are a natural process critical to the health of forests around the world. However, recent decades have witnessed unprecedented wildfire seasons in many forested regions, leading to a range of unprecedented socio-economic, environmental, and human health impacts. Mitigating these impacts relies in part on fire behaviour prediction systems, which provide information to assist operational wildfire managers with addressing wildfire risk and prioritizing wildfire fighting efforts. A key aspect of fire behaviour prediction systems are rate of spread models that rely on observational and experimental fire behaviour data from naturally occurring wildfires and prescribed burns, respectively. Given the challenge with observing and measuring wildfires in situ, rate of spread models typically rely on a small set of data inputs that are not always representative of the range of wildfires occurring in certain forest types. Furthermore, existing fire behaviour models often lack empirical data on forests that have more recently experienced significant compositional shifts due to climate change or various ecological or anthropogenic disturbances.

To address these shortcomings, the objective of this thesis is to establish a method of acquiring empirical fire behaviour data to enhance fire behaviour prediction science through two distinct studies. The first evaluates the utility of monophotogrammetry to extract fire behaviour data from oblique aerial wildfire photographs. The results demonstrate how this approach can provide new and accurate fire spread observations to inform fire behaviour prediction or other aspects of wildland fire science where databases of such wildfire photos exist. The second study is an empirical wildfire spread analysis in forest stands affected by mountain pine beetle (MPB), and utilizes the method of monoplotting to acquire spread rate data from wildfire photographs of grey-attack MPB-affected forest stands. Results from this study further demonstrate the efficacy

of the previously established monoplotting technique while providing novel empirical evidence of fire behaviour in grey attack MPB-affected forest stands.

Overall, the research results presented in this thesis demonstrate the potential of monophotogrammetry for the acquisition of fire behaviour data and evaluating the results derived from fire behaviour prediction systems in different ecological contexts. This thesis exhibits the potential for this method to expand into other areas of fire behaviour, such as flame or smoke plume dimensions, spotting, and the relationship between fire behaviour and disturbance events such as pest insect outbreaks.

Table of Contents

List of Tables

List of Figures

Acknowledgements

I would like to first thank my supervisory committee for their mentorship, patience, and trust throughout the entirety of this project. Thank you Chris Bone for the opportunity pursue this research while opening many doors for me along the way. I truly appreciate all that you have done for me and I feel grateful to have been apart of the SURREAL Lab. Thank you Dan Perrakis and Steve Taylor for your interest in collaborating and for patiently showing me the ropes of fire behaviour. I have a long way to go, but your enthusiasm and passion for research continue to inspire me.

This project would not have been possible without the support from many individuals and organizations along the way. Thank you to the Natural Resources Canada-Canadian Forest Service's Emergency Management System program for funding for this research and to the British Columbia Wildfire Service for providing access to the wildfire image archive. I would also like to thank Chris Stockdale and Claudio Bozzini for hosting the WSL Monoplotting course in Edmonton, Alberta which was key to the success of this project.

To my parents and sister, thank you for your never ending support, I would not be here without you. Finally, thank you Milly for always being there for me throughout this journey. Having you by my side has meant more to me than you will ever know.

Chapter 1: Introduction

1.1 Background

Wildfire is a critical process that plays a significant role in maintaining healthy forest ecosystems (Tymstra et al., 2020). There are vital symbioses between fire and the forest succession of individual tree species, such as lodgepole pine (*Pinus contorta*) where fire creates optimal seedbed conditions, promotes maximum release of stored seed, and reduces competition from understory vegetation (Lotan et al., 1985). This association is further emphasized in tree species such as jack pine (*Pinus banksiana*), which would cease to exist without the periodic presence of wildfire due to the heat of fire causing seed crop release (Weber & Stocks, 1998). Furthermore, wildfire has been demonstrated as an essential component of maintaining a vegetation mosaic in the landscape and responsible for the success of evolutionary novelties and biodiversity of forest ecosystems, while providing effective natural control for managing vegetation, parasites and disease that negatively affect forest ecosystems (Pausas & Keeley, 2019; Scasta, 2015; Weber & Stocks, 1998).

While the positive impacts of wildfire on forest ecosystems are abundant, climate change and broadscale forest management policies have collectively altered the scale and intensity of wildfires around the world (Calkin et al., 2015; Kirchmeier-Young et al., 2019; Liu et al., 2010; Settele et al., 2015; Westerling et al., 2006), resulting in an array of socio-economic, environmental, and human health consequences (Jolly et al., 2015; Reid et al., 2016). Warmer and drier conditions due to the rising temperatures are contributing to an increase in the frequency, severity, and extent of wildfires and longer fire seasons (Cleetus & Kranti, 2014). Furthermore, while fire suppression policies have been effective in reducing the number of fire

historically they have also led to a significant increase in fuel accumulation and forest density across landscapes which in turn has increased the frequency of extreme fire risk conditions (Calkin et al., 2015). The severity of these impacts continue to rise. In recent years, the increase in global wildfire activity in countries such as the United States, Australia, and Canada has resulted in unprecedented area burned, fire suppression costs, human displacement, and building loss (BC Wildfire Service, 2020; Filkov et al., 2020; Higuera & Abatzoglou, 2020; Statistics Canada, 2019; Xu et al., 2020). Although the causes of recent fire disasters are complex, most consequences appear to result from the way climate change and forest management policies have altered ecological process and forest composition (Parisien et al., 2020; Schoennagel et al., 2017). This presents a critical challenge for wildfire science as conventional methods for predicting wildfire behaviour may become limited under novel forest conditions and emphasizes the need for advancing fire management systems in order to better understand and predict fire behaviour (Taylor et al., 2013).

Currently, fire danger rating systems (FDRS) represent the primary approach used for forecasting wildfire danger and behaviour within national fire management agencies (Taylor & Alexander, 2006). FDRS typically produce qualitative or numeric indices of fire potential representing the risk of a wildfire occurring at a given time and place (Taylor & Alexander, 2006). These danger ratings consider various factors that influence fire behaviour, such as weather, topography, and fuel characteristics. In addition to producing overall fire danger ratings, these indices predict a variety of wildfire characteristics, such as head fire rate of spread, i.e. the predicted speed of the fire front in meters per minute, to wildfire management organizations for supporting their tactical and operational decision making during a wildfire (Martell, 1982; Taylor et al., 2013). Although FDRS have been implemented to predict wildfire risk in forests around

the world (Lin, 2000; Mirto et al., 2015; San-Miguel-Ayanz et al., 2003), a universal FDRS standard does not exist (Taylor & Alexander, 2006). That being said, Canada, being one of the early pioneers in FDRS and fire danger research in general, launched the Canadian Forest Fire Danger Rating System (CFFDRS) in 1968, and its continued development has led it to become one of the most well developed and widely applied FDRS in the world (Di Giuseppe et al., 2016; Xiao-rui et al., 2005). Countries such as Argentina, Fiji, Mexico, and New Zealand, as well as parts of Europe have adopted this system largely because of its simplicity and customizable application (Taylor & Alexander, 2006). However, changes in observed wildfire behaviour in recent years coupled with the availability of new forms of wildfire monitoring data provide opportunities for improving the CFFDRS to assist with more contemporary methods in wildfire management.

In British Columbia (BC), Canada, the CFFDRS plays a critical role in predicting and understanding wildfire behaviour. Understanding the changing nature of BC wildfires is increasingly important due to their complex relationship with climate change. Rising temperatures increase evapotranspiration and reduce the fuel moisture of forest landscapes in turn increasing fire risk (Halofsky et al., 2020). In addition, warming temperatures translate to an increase in lighting activity, thus increasing wildfire lightning strike ignitions, while lengthening fire seasons and area burned (Coogan et al., 2020; Romps et al., 2014). Climate change is also expected to increase the frequency of summer-dry climates and droughts, resulting in reduced fuel moisture and increased fire activity (Littell et al., 2016). Similarly, research in BC has found a positive feedback relationship between mountain pine beetle (MPB) and climate change, which has been found to be a significant factor in increasing the extent and severity of pest outbreaks (Kurz et al., 2008). Rising temperatures due to climate change alter the seasonal temperatures

which are responsible for limiting the extent and severity of pest insect outbreaks (Sambaraju et al., 2012). Conditions of drought and above-average temperatures can result in a bark beetle population transitioning from endemic to outbreak levels when host trees become stressed and overwinter beetle mortality declines (Aukema et al., 2008). For example, BC has seen an unprecedented MPB outbreak in recent decades, impacting more than 18 million hectares of forest across the province (Natural Resources Canada, 2022). The increasing severity, frequency, and extent of wildfire in BC combined with the unprecedented number of MPB-affected trees over the last two decades presents researchers with a time sensitive issue regarding the relationship between such disturbance events. Research has shown that MPB significantly effects the resilience of forest stand with respect to wildfire through altering fuel conditions, such as reducing the foliar moisture content of needles in the canopy and increasing the amount and dryness of forest floor fuels (Jenkins et al., 2014; Jolly et al., 2012). These alterations have the potential to increase the risk, severity, and extent of wildfire in MPB-affected forest stands (Dhar et al., 2016). Yet, there are crucial gaps in the knowledge of MPB's effect on fire behaviour, specifically the lack of empirical evidence necessary for providing real world observations of fire behaviour in MPB-affected forest stands and advancing fire behaviour models (Alexander & Cruz, 2013; Hoffman et al., 2015; Stephens et al., 2018). For fire managers using the CFFDRS, this introduces unaccounted factors, such as increased forest floor fuels and decreased foliar moisture content in the canopy, which may not be considered while predicting fire behaviour in MPB-affected forest stands. In the context of wildfire management, errors in predicting fire behaviour can result in uninformed decision making with significant consequences.

To address these issues, the overall goal of this thesis is to establish a method for acquiring fire behaviour data to further inform fire behaviour prediction. One underutilized

source of fire behaviour data comes from individually georeferenced oblique angle photographs of wildfires taken during air reconnaissance missions. Specifically, this is accomplished by evaluating the utility of technique known as mono-photogrammetry to extract fire behaviour data from oblique aerial wildfire photographs. Mono-photogrammetry, also known as monoplotting, is a method used to georeference oblique aerial photographs for the purpose of extracting spatial measurements from such photographs. In this thesis, monoplotting is evaluated regarding its ability to acquire fire behaviour data from operational aerial wildfire photographs. This proposed method is evaluated by performing an empirical wildfire spread analysis in two contexts, one examining wildfires from 2009 to 2014 across various regions of BC to develop and document the methodology, while the second examines wildfires from 2017 to 2018 in forests impacted by MPB. It is expected that the results from this study will contribute to our understanding of fire behaviour and assist in improving fire behaviour prediction systems.

This thesis is organized in five chapters. Following this introduction (Chapter 1), Chapter 2 provides a brief literature review on the CFFDRS and methods of acquiring fire behaviour data. Chapter 3 represents a study that explores the use of mono-photogrammetry for georeferencing oblique aerial wildfire photographs in order to extract fire behaviour data. Specifically, this study employs the software program WSL Monoplotting Tool (MPT) to georeference operational oblique aerial wildfire photographs taken during airtanker response in BC.

Chapter 4 comprises a study utilizing the method of monoplotting to acquire observed headfire rate of spread (HROS) data from wildfire photographs containing grey-attack stage MPB-affected forest stands. This study compares the observed HROS with the Canadian Fire Behaviour Prediction (FBP) System predicted HROS for healthy non-MPB affected stands to

determine the effects of MPB attack on fire spread. This study also explores if site-specific conditions are related to the differences in observed and predicted HROS. Similar to Chapter 2, this study is focused on BC, again using photographs taken during airtanker response.

Chapter 5 is the concluding chapter of the thesis that provides a summary of the results and discusses the sources of uncertainty from the two completed studies. Additionally, this chapter discusses the future applications and overall contributions of this research to the scientific community.

References

Alexander, M. E., & Cruz, M. G. (2013). Are the applications of wildland fire behaviour models getting ahead of their evaluation again? *Environmental Modelling and Software*, *41*, 65–71. https://doi.org/10.1016/j.envsoft.2012.11.001

Aukema, B.H, L. Carroll, A., Zheng, Y., Zhu, J., F. Raffa, K., Dan Moore, R., Stahl, K., & Taylor, S.W. (2008). Movement of outbreak populations of mountain pine beetle: influences of spatiotemporal patterns and climate. *Ecography*, *31*(3), 348–358. https://doi.org/10.1111/j.2007.0906-7590.05453.x

BC Wildfire Service. (2020). *2017 Wildfire Season*. Available online: https://www2.gov.bc.ca/gov/content/safety/wildfire-status/about-bcws/wildfire-history/wildfire-season-summary (accessed on 15 March 2022).

Calkin, D. E., Thompson, M. P., & Finney, M. A. (2015). Negative consequences of positive feedbacks in us wildfire management. *Forest Ecosystems*, *2*(9). https://doi.org/10.1186/s40663-015-0033-8

Cleetus, R., & Kranti, M. (2014). *Playing with fire: how climate change and development patterns are contributing to the soaring costs of western wildfires*. Union of Concerned Scientists.

Coogan, S. C. P., Cai, X., Jain, P., & Flannigan, M. D. (2020). Seasonality and trends in human- A nd lightning-caused wildfires ≥ 2 ha in Canada, 1959-2018. *International Journal of Wildland Fire*, *29*(6), 473–485. https://doi.org/10.1071/WF19129

Dhar, A., Parrott, L., & Heckbert, S. (2016). Consequences of mountain pine beetle outbreak on forest ecosystem services in western Canada. *Canadian Journal of Forest Research*, *46*(8), 987–999. https://doi.org/10.1139/cjfr-2016-0137

Di Giuseppe, F., Pappenberger, F., Wetterhall, F., Krzeminski, B., Camia, A., Libertá, G., & Miguel, J. S. (2016). The potential predictability of fire danger provided by numerical weather prediction. *Journal of Applied Meteorology and Climatology*, *55*(11), 2469–2491. https://doi.org/10.1175/JAMC-D-15-0297.1

Filkov, A. I., Ngo, T., Matthews, S., Telfer, S., & Penman, T. D. (2020). Impact of Australia's catastrophic 2019/20 bushfire season on communities and environment. Retrospective analysis and current trends. *Journal of Safety Science and Resilience*, *1*(1), 44–56. https://doi.org/10.1016/j.jnlssr.2020.06.009

Halofsky, J. E., Peterson, D. L., & Harvey, B. J. (2020). Changing wildfire, changing forests: the effects of climate change on fire regimes and vegetation in the Pacific Northwest, USA. *Fire Ecology*, *16*(4). https://doi.org/10.1186/s42408-019-0062-8

Higuera, P. E., & Abatzoglou, J. T. (2020). Record-setting climate enabled the extraordinary 2020 fire season in the western United States. *Global Change Biology*, *27*(1), 1–2. https://doi.org/10.1111/gcb.15388

Hoffman, C. M., Linn, R., Parsons, R., Sieg, C., & Winterkamp, J. (2015). Modeling spatial and temporal dynamics of wind flow and potential fire behavior following a mountain pine beetle outbreak in a lodgepole pine forest. *Agricultural and Forest Meteorology*, *204*, 79–93. https://doi.org/10.1016/j.agrformet.2015.01.018

Jenkins, M. J., Runyon, J. B., Fettig, C. J., Page, W. G., & Bentz, B. J. (2014). Interactions among the mountain pine beetle, fires, and fuels. *Forest Science*, *60*(3), 489–501. https://doi.org/10.5849/forsci.13-017

Jolly, W. M., Cochrane, M. A., Freeborn, P. H., Holden, Z. A., Brown, T. J., Williamson, G. J., & Bowman, D. M. J. S. (2015). Climate-induced variations in global wildfire danger from 1979 to 2013. *Nature Communications*, *6*, 7537. https://doi.org/10.1038/ncomms8537

Jolly, W. M., Parsons, R. A., Hadlow, A. M., Cohn, G. M., McAllister, S. S., Popp, J. B., Hubbard, R. M., & Negron, J. F. (2012). Relationships between moisture, chemistry, and ignition of Pinus contorta needles during the early stages of mountain pine beetle attack. *Forest Ecology and Management*, *269*, 52–59. https://doi.org/10.1016/j.foreco.2011.12.022

Kirchmeier-Young, M. C., Gillett, N. P., Zwiers, F. W., Cannon, A. J., & Anslow, F. S. (2019). Attribution of the Influence of Human-Induced Climate Change on an Extreme Fire Season. *Earth's Future*, *7*(1), 2–10. https://doi.org/10.1029/2018EF001050

Kurz, W. A., Dymond, C. C., Stinson, G., Rampley, G. J., Neilson, E. T., Carroll, A. L., Ebata, T., & Safranyik, L. (2008). Mountain pine beetle and forest carbon feedback to climate change. *Nature*, *452*, 987–990. https://doi.org/10.1038/nature06777

Lin, C. C. (2000). The development, systems, and evaluation of forest fire danger rating: A review. *Taiwan Journal of Forest Science*, *15*(4), 507–520. https://doi.org/10.7075/TJFS.200012.0507

Littell, J. S., Peterson, D. L., Riley, K. L., Liu, Y., & Luce, C. H. (2016). A review of the relationships between drought and forest fire in the United States. *Global Change Biology*, *22*(7), 2353–2369. https://doi.org/10.1111/gcb.13275

Liu, Y., Stanturf, J., & Goodrick, S. (2010). Trends in global wildfire potential in a changing climate. *Forest Ecology and Management*, *259*(4), 685–697. https://doi.org/10.1016/j.foreco.2009.09.002

Lotan, J. E., Brown, J. K., & Neuenschwander, L. F. (1985). Role of Fire in Lodgepole Pine Forests. In Proceedings of the Lodgepole Pine the Species and its Management Symposium, Spokane, Washinton, USA, 134–152 May 1984.

Martell, D. L. (1982). A review of operational research studies in forest fire management. *Canadian Journal of Forest Research*, *12*(2), 119–140. https://doi.org/10.1139/x82-020

Mirto, M., Mariello, A., Nuzzo, A., Mancini, M., Raolil, A., Marra, O., Fiore, S., Sirca, C., Salis, M., Bacciu, V., Spano, D., & Aloisio, G. (2015). *The OFIDIA Fire Danger Rating System*. 10th International Conference on P2P, Parallel, Grid, Cloud and Internet Computing (3PGCIC), 695–700. https://doi.org/10.1109/3PGCIC.2015.115

Natural Resources Canada. (2022). *Mountain pine beetle (factsheet)*. Available online: https://www.nrcan.gc.ca/forests/fire-insects-disturbances/top-insects/13397 (accessed on 15 March 2022)

Parisien, M. A., Barber, Q. E., Hirsch, K. G., Stockdale, C. A., Erni, S., Wang, X., Arseneault, D., & Parks, S. A. (2020). Fire deficit increases wildfire risk for many communities in the Canadian boreal forest. *Nature Communications*, *11*(2121), 1–9. https://doi.org/10.1038/s41467-020-15961-y

Pausas, J. G., & Keeley, J. E. (2019). Wildfires as an ecosystem service. *Frontiers in Ecology and the Environment*, *17*(5), 289–295. https://doi.org/10.1002/fee.2044

Reid, C. E., Brauer, M., Johnston, F. H., Jerrett, M., Balmes, J. R., & Elliott, C. T. (2016). Critical Review of Health Impacts of Wildfire Smoke Exposure. *Environmental Health Perspectives*, *124*(9), 1334–1343. https://doi.org/10.1289/ehp.1409277

Romps, D. M., Seeley, J. T., Vollaro, D., Molinari, J., Romps, D. M., Seeley, J. T., Vollaro, D., & Molinari, J. (2014). Projected increase in lightning strikes in the United States due to global warming. *Science*. *346*(6211), 851–854. https://doi.org/10.1126/science.1259100

Sambaraju, K. R., Carroll, A. L., Zhu, J., Stahl, K., Moore, R. D., & Aukema, B. H. (2012). Climate change could alter the distribution of mountain pine beetle outbreaks in western Canada. *Ecography*, *35*(3), 211–223. https://doi.org/10.1111/j.1600-0587.2011.06847.x

San-Miguel-Ayanz, J., Carlson, J. D., Alexander, M., Tolhurst, K., Morgan, G., Sneeuwjagt, R., & Dudley, M. (2003). Current Methods to Assess Fire Danger Potential. *Wildland Fire Danger Estimation and Mapping*, *4*, 21–61. https://doi.org/10.1142/9789812791177_0002

Scasta, J. D. (2015). Fire and Parasites: An Under-Recognized Form of Anthropogenic Land Use Change and Mechanism of Disease Exposure. *EcoHealth*, *12*(3), 398–403. https://doi.org/10.1007/s10393-015-1024-5

Schoennagel, T., Balch, J. K., Brenkert-Smith, H., Dennison, P. E., Harvey, B. J., Krawchuk, M. A., Mietkiewicz, N., Morgan, P., Moritz, M. A., Rasker, R., Turner, M. G., & Whitlock, C. (2017). Adapt tomore wildfire in western North American forests as climate changes. *Proceedings of the National Academy of Sciences of the United States of America*, *114*(18), 4582–4590. https://doi.org/10.1073/pnas.1617464114

Settele, J., Scholes, R., Betts, R. A., Bunn, S., Leadley, P., Nepstad, D., Overpeck, J. T., Taboada, M. A., Fischlin, A., Moreno, J. M., Root, T., Musche, M., & Winter, M. (2015). Terrestrial and Inland water systems. *Climate Change 2014 Impacts, Adaptation and Vulnerability: Part A: Global and Sectoral Aspects* (pp. 271–360). Cambridge University Press. https://doi.org/10.1017/CBO9781107415379.009

Statistics Canada. (2019). *Environment Facts Sheet: British Columbia's forest fires, 2018*. Available online: https://www150.statcan.gc.ca/n1/en/pub/16-508-x/16-508-x2019002-eng.pdf?st=HAo2klaO (accessed 15 March 2022).

Stephens, S. L., Collins, B. M., Fettig, C. J., Finney, M. A., Hoffman, C. M., Knapp, E. E., North, M. P., Safford, H., & Wayman, R. B. (2018). Drought, Tree Mortality, and Wildfire in Forests Adapted to Frequent Fire. *BioScience*, *68*(2), 77–88. https://doi.org/10.1093/biosci/bix146

Taylor, S.W., & Alexander, M.E. (2006). Science, technology, and human factors in fire danger rating: the Canadian experience. *International Journal of Wildland Fire*, *15*(1), 121. https://doi.org/10.1071/WF05021

Taylor, S. W., Woolford, D. G., Dean, C. B., & Martell, D. L. (2013). Wildfire Prediction to Inform Fire Management: Statistical Science Challenges. *Statistical Science*, *28*(4), 586–615. https://doi.org/10.1214/13-STS451

Tymstra, C., Stocks, B. J., Cai, X., & Flannigan, M. D. (2020). Wildfire management in Canada: Review, challenges and opportunities. *Progress in Disaster Science*, *5*, 100045. https://doi.org/10.1016/J.PDISAS.2019.100045

Weber, M. G., & Stocks, B. J. (1998). Forest fires and sustainability in the boreal forests of Canada. *Ambio*, *27*(7), 545–550.

Westerling, A. L., Hidalgo, H. G., Cayan, D. R., & Swetnam, T. W. (2006). Warming and earlier spring increase Western U.S. forest wildfire activity. *Science*, *313*(5789), 940–943. https://doi.org/10.1126/science.1128834

Xiao-rui, T., Mcrae, D. J., Boychuk, D., Ji-zhong, J., Cheng-da, G., Li-fu, S., & Ming-yu, W. (2005). Comparisons and assessment of forest fire danger systems. *Forestry Studies in China*, *7*, 53–61. https://doi.org/10.1007/s11632-005-0058-0

Xu, R., Yu, P., Abramson, M. J., Johnston, F. H., Samet, J. M., Bell, M. L., Haines, A., Ebi, K. L., Li, S., & Guo, Y. (2020). Wildfires, Global Climate Change, and Human Health. *New England Journal of Medicine*, *383*(22), 2173–2181. https://doi.org/10.1056/NEJMsr2028985

Chapter 2: Literature Review

2.1 Canadian Forest Fire Danger Rating System

Throughout early logging and settlement in Canada, various forms of unregulated fire management have always been present (Van Wagner, 1990). However, it was not until 1925 that James G. Wright, the originator of Canadian forest fire research, proposed a program to develop an early form of a fire danger rating system (Beall, 1990). Over the course of the next 15 years, further research and development led Wright, and his assistant Herbert W. Beall to produce their first set of fire danger tables in 1933 (Taylor & Alexander, 2006). By the mid-20th century, an expanding Canadian forest industry led to renewed interest in fire research and resulted in the development of a fire danger working group composed of fire researchers from across the country. In 1968, this group worked towards unifying existing regional fire danger rating tables in Canada into a singular national system, now known as the Canadian Forest Fire Danger Rating System (CFFDRS). Nearly fifty years later, the CCFDRS is the primary system used for forecasting wildfire danger and behaviour across Canada (Stocks et al., 1989; Taylor & Alexander, 2006).

Forecasted wildfire conditions are based on outputs from sub-models within the CFFDRS, primarily the Fire Weather Index (FWI) and Fire Behaviour Prediction (FBP) Systems (Forestry Canada Fire Danger Group, 1992; Van Wagner, 1987). The core of the FBP System consists of empirical functions for predicting rate of spread (ROS) and fuel consumption, and various physical and quasi-empirical equations for estimating fire intensity and other outputs based on fire weather and vegetative fuel type inputs. These provide intelligence to support tactical and operational decision making within wildfire management organizations (Martell,

1982; Stocks et al., 1989; Taylor et al., 2013). Today, the CFFDRS and FBP System are also used in stochastic simulation modelling environments as key elements in sophisticated landscape fire risk analyses (Johnston et al., 2020; Parisien et al., 2019). The CFFDRS has five primary outputs that provide information on various fire characteristics: ROS, fuel consumption, headfire intensity, crown faction burned, and fire description. However, the predicted headfire ROS has become one of the most widely used variables in wildfire management today due to its essential role in making critical wildfire suppression decisions (Plucinski et al., 2017).

In the FBP System, predicted headfire ROS values are calculated from empirical models related to weather conditions, fuel type, and topography. Sigmoidal regression functions were developed by fitting ROS data to the Initial Spread Index (ISI), a dimensionless index of wildfire spread (part of the FWI System) derived from wind speed and estimated fine litter moisture (FCFDG, 1992; Stocks et al., 1989; Wotton, 2009). ROS must also be calculated in order to estimate other fire behaviour characteristics including type of fire (surface, intermittent crown, continuous crown) and headfire intensity (FCFDG, 1992). Figure 2.1 shows ROS models and the underlying data in two different forest ecosystems referred to as fuel types. The initial intention with the FBP System when it was published was that additional experimental and observational data would surface allowing for proper validation of existing models and potentially the creation of new ROS models representing unexplored fuel type complexes (FCFDG, 1992; Wotton et al., 2009). Although there has been some progress in this respect (Pepin & Wotton, 2020; Perrakis et al., 2014; Wilkinson et al., 2018), the challenge of validating and acquiring new empirical data has limited the improvements to the FBP System.

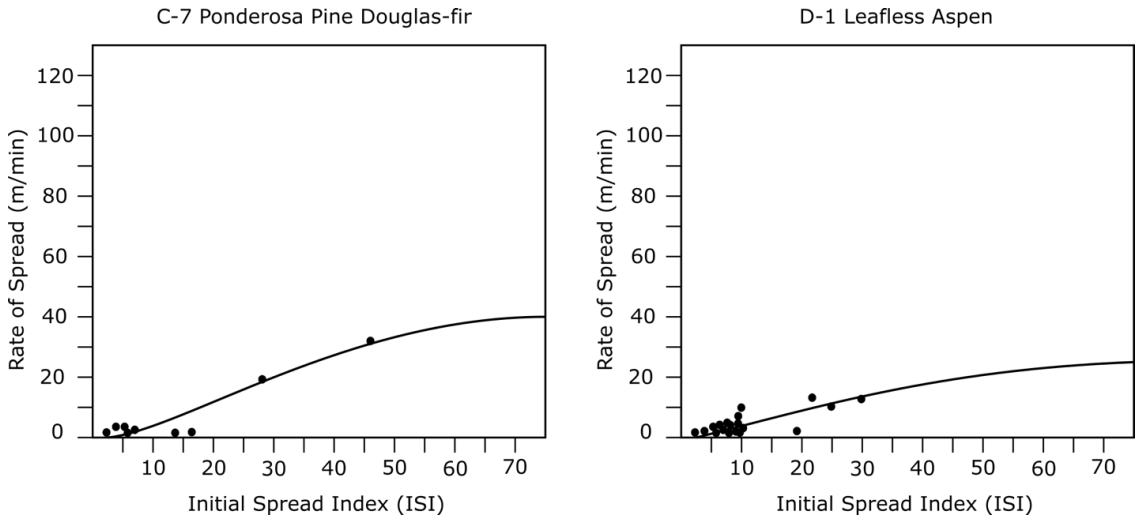

Figure 2.1 Example replica ROS-ISI scatterplots of the C-7 and D-1 fuel types (FCFDG 1992).

The FBP System database contains several hundred experimental fires and wildfire observations distributed among 14 fuel types for establishing ROS and fuel consumption models (Hirsch, 1996). Experimental fire observations, with carefully measured and monitored fire environment variables (e.g Alexander et al., 1991; Stocks, 1989), provide the most reliable and accurate fire behaviour data, but tend to be conducted under lower danger (moister) weather conditions to minimize escapes and maintain safety. Documented wildfire observations therefore provide valuable 'real world' fire behaviour data under high and extreme danger conditions (Alexander & Thomas, 2003), filling the right side of the data space in ROS functions (Figure 2.1). Although some experimental burns associated with the FBP System did take place under very high fire danger conditions (e.g. Stocks & Hartley, 1995), it is unrealistic to imagine that the logistics of field experiments would allow them to be conducted or adequately replicated under the most extreme conditions – driest fuel, strongest wind – for all fuel types (Taylor et al., 2013).

As a result, clustering at low ROS-ISI values occurs, and higher end (high ISI) predictions have great uncertainty (Figure 2.1). For several fuel types, such as C-5 ('Red and White pine), C-6 ('Conifer Plantation), M-3 and M-4 ('Dead balsam fir mixedwood', leafless

and green conditions), and slash types (S-1 and S-3 in particular), no high to extreme data (ISI greater than 20) exists in the models whatsoever (FCFDG, 1992). Furthermore, the M-1 and M-2 fuel types ('Boreal Mixedwood', leafless and green conditions) are not based on empirical models (Hirsch, 1996) and are arguably in even greater need of validation data.

Considering the aforementioned issues, it is clear that the FBP System ROS models would benefit from additional validation at all levels of fire danger and ROS. This is a well-known challenge, and one that has existed for some time (Albini, 1976). Similar difficulties, such as data and models largely derived from low-spread conditions and a paucity of validation studies, are known to exist for most other fire behaviour modelling systems (Cruz & Alexander, 2013; Gould et al., 2011; Sullivan, 2009). For wildfire management decision makers, low accuracy ROS models could lead to critically underestimating the growth of a wildfire with dangerous consequences. Conversely, overestimating wildfire ROS, while not as dangerous, could lead to wasteful allocation or false prioritization of resources. In order to address the lack of observational fire data, subsequently improving the ROS models and identifying a more complete range of wildfire behaviour, new sources of wildfire data need to be explored. Additional observational data will not only result in more reliable and validated ROS models, but may also potentially establish new ROS models of unexplored fuel complexes (Perrakis et al., 2014).

2.2 Fire Behaviour Data Acquisition

In order to improve the ROS models and represent a more complete range of potential wildfire behaviour, two methods of acquiring and validating observational data wildfire are possible, remote sensing and photogrammetry. Recent advances in sensors and remote sensing techniques, such as satellite imagery, LiDAR, and aerial imagery, offer potential solutions for

acquiring validated observational wildfire behaviour data (Xiao-rui et al., 2005). In the past, satellite data from passive sensors such as MODIS and LANDSAT have been primarily used for the detection of wildfires, estimating burned areas, and mapping fuel types (Li et al., 2003; Szpakowski & Jensen, 2019). Although the high temporal resolution of earth observation satellites, such as MODIS, are helpful in the pre-fire and post-fire analysis stages, the low spatial resolution of this data is not sufficient for determining the headfire ROS of wildfires (Xie et al., 2018). Polar orbiting satellites, such as LANDSAT, have high spatial resolution; however, the temporal resolution (i.e. return intervals) of these satellites is not high enough to collect near real-time observational data, such as headfire ROS, due to the temporally stochastic nature of wildfires (Liu et al., 2018; Xie et al., 2018). With respect to the active remote sensing systems such as LiDAR, due to the high cost and complexity of acquiring the data, a majority of the studies have focused on the pre-fire and post-fire analysis of wildfires, such as surface fuel mapping, burn severity, and vegetation recovery (Szpakowski & Jensen, 2019). As such, the use of satellite imagery and LiDAR data has revealed multiple challenges in addressing the issue of acquiring near real-time observational data to determine the headfire ROS of wildfires. However, minimal research has yet to examine the utility of conventional oblique aerial imagery for assessing ROS, which may hold promise given recent advancements in photogrammetric software.

Although operational personnel are often well-situated to collect fire behaviour data from wildfires, such as field observations or aerial imagery (e.g. Moriarty et al., 2019), this is typically a low priority during high stress events such as evolving wildfire emergencies. Consequently, fire behaviour data collected from wildfires are typically infrequent, unreliable or unverifiable in the absence of explicit data collection standards (Filkov et al., 2018). When opportunistic data

are successfully collected, including oblique aerial images, extensive processing is required in order to extract the details required for spatial analysis. For example, one potential source of additional observational data is from imagery collected by fire management organizations such as the BC Wildfire Service (BCWS). Using this archive, previous studies (i.e. Perrakis et al., 2014) were able to manually georeference the timestamped aerial wildfire images and extract spatial data, including headfire position, spread distance, and burning period; using this technique a preliminary ROS could be calculated for a given wildfire. Unfortunately, this manual georeferencing process was time consuming, subjective (limited to trained experts using their individual judgment), and difficult to reproduce. As a result, this rich source of traditional remote sensing data has been underutilized as a source of observational wildfire data. Although wildfire studies have thus far focused on manually georeferencing aerial images, other areas of research such as aerial archaeology have georeferenced oblique aerial images digitally using advanced photogrammetric software and techniques (Doneus et al., 2016; Verhoeven & Sevara, 2016).

Several Aerial Archaeology studies have focused on the use of stereo-photogrammetry algorithms, such as Structure from Motion (SfM) or Multi-View Stereo (MVS; Verhoeven et al., 2012). These have the ability to construct 3D models from 2D scenes, for example generating a georeferenced 3D model of a potential archaeological site from oblique aerial imagery taken from around the study area (Doneus et al., 2011). However, both SfM and MVS algorithms require multiple clear, overlapping images from various view points around the study area (Mertes et al., 2017; Warrick et al., 2017). This is problematic for the wildfire image archive due to the impromptu nature of how these aerial wildfire images were collected. A majority of the wildfire images have limited visibility due to smoke and vary in terms of location, position, and resolution, and thus do not meet the requirements for stereo-photogrammetry.

An alternative digital photogrammetry technique for georeferencing oblique aerial images is mono-photogrammetry. A monoplotting system aims to precisely estimate the original camera system of the aerial image through the definition of control points in both the aerial image and corresponding Digital Elevation Model (DEM). The principle of this theory is given that the original camera system, digital image, and DEM lie in a straight line in the world space, it can be said that a ray starting from the camera centre will pass through a set of pixel coordinates in the digital image (image control point) and intersect with the DEM at the corresponding world coordinates (DEM control point).

Although progress in monoplotting technology has been limited thus far, recent advancements have facilitated the development of an open-access monoplotting software package called the WSL Monoplotting Tool (MPT; Bozzini et al., 2012). This software has the ability to precisely estimate the original camera setup of the aerial image by defining ground control points (GCP) in the aerial image and the respective DEM of the same area. In doing so, each point on the aerial image is provided with its corresponding real world point, allowing for 3D spatial measurements and analysis. As described in the following chapter, this technique proved effective for analyzing and extracting the headfire front positions of individual wildfire runs in order to calculate the respective headfire ROS.

References

Albini, F. (1976). Estimating Wildfire Behavior and Effects (General Technical Report INT-30). USDA Forest Service, Intermountain Forest and Range Experiment Station: Ogden, Utah, USA. https://digitalcommons.usu.edu/barkbeetles/147

Alexander, M. E., Stocks, B. J., & Lawson, B. D. (1991). Fire behavior in black spruce-lichen woodland: the Porter Lake project (Information Report NOR-X-310). Forestry Canada, Northwest Region, Northern Forestry Centre: Edmonton, Alberta, Canada. https://cfs.nrcan.gc.ca/pubwarehouse/pdfs/11563.pdf

Alexander, M. E., & Thomas, D. A. (2003). Wildland fire behavior case studies and analyses: other examples, methods, reporting standards, and some practical advice. *Fire Management Today*, *63*(4), 4–12.

Beall, H. W. (1990). The art and science of fire management (Information Report NOR-X-309). In Proceedings of the First Interior West Fire Council Annual Meeting and Workshop, Kananaskis Village, Alberta, Canada 24-27 October 1988. Forestry Canada, Northwest Region, Northern Forestry Centre: Edmonton, Alberta, Canada. https://citeseerx.ist.psu.edu/viewdoc/download?doi=10.1.1.978.4395&rep=rep1&type=pdf

Bozzini, C., Conedera, M., & Krebs, P. (2012). A New Monoplotting Tool to Extract Georeferenced Vector Data and Orthorectified Raster Data from Oblique Non-Metric Photographs. *International Journal of Heritage in the Digital Era*, *1*(3), 499–518. https://doi.org/10.1260/2047-4970.1.3.499

Cruz, M. G., & Alexander, M. E. (2013). Uncertainty associated with model predictions of surface and crown fire rates of spread. *Environmental Modelling and Software*, *47*, 16–28. https://doi.org/10.1016/j.envsoft.2013.04.004

Doneus, M., Verhoeven, G., Fera, M., Briese, C., Kucera, M., & Neubauer, W. (2011). From Deposit to Point Cloud – a Study of Low-Cost Computer Vision Approaches for the Straightforward Documentation of Archaeological Excavations. *Geoinformatics FCE CTU*, *6*, 81–88. https://doi.org/10.14311/gi.6.11

Doneus, Michael, Wieser, M., Verhoeven, G., Karel, W., Fera, M., & Pfeifer, N. (2016). Automated Archiving of Archaeological Aerial Images. *Remote Sensing*, *8*(3), 209. https://doi.org/10.3390/rs8030209

Forestry Canada Fire Danger Group. (1992). Development and structure of the Canadian Forest Fire Behavior Prediction System (Information Report ST-X-3). Forestry Canada, Science and Sustainable Development Directorate: Ottawa, Ontario, Canada. https://cfs.nrcan.gc.ca/publications?id=10068

Filkov, A., Duff, T., & Penman, T. (2018). Improving Fire Behaviour Data Obtained from Wildfires. *Forests*, *9*(2), 81. https://doi.org/10.3390/f9020081

Gould, J., McCaw, M., Cruz, M. ., & Anderson, W. (2011). How good are fire behaviour models? Validation of eucalypt forest fire spread model (unpublished conference paper). Wildfire 2011, the 5th International Wildland Fire Conference, Sun City, South Africa.

Hirsch, K. . (1996). Canadian Forest Fire Behavior Prediction (FBP) System: User's Guide (Special Report 7). Natural Resources Canada, Canadian Forest Service, Northwest Region, Northern Forestry Centre: Edmonton, Alberta, Canada. https://www.frames.gov/documents/catalog/hirsch_1996.pdf

Johnston, L. M., Wang, X., Erni, S., Taylor, S. W., McFayden, C. B., Oliver, J. A., Stockdale, C., Christianson, A., Boulanger, Y., Gauthier, S., Arseneault, D., Wotton, B. M., Parisien, M. A., & Flannigan, M. D. (2020). Wildland fire risk research in Canada. *Environmental Reviews*, *28*(2), 164–186. https://doi.org/10.1139/er-2019-0046

Li, Z., Fraser, R., Jin, J., Abuelgasim, A. A., Csiszar, I., Gong, P., Pu, R., & Hao, W. (2003). Evaluation of algorithms for fire detection and mapping across North America from satellite. *Journal of Geophysical Research: Atmospheres*, *108*(D2). https://doi.org/10.1029/2001jd001377

Liu, X., He, B., Quan, X., Yebra, M., Qiu, S., Yin, C., Liao, Z., & Zhang, H. (2018). Near Real-Time Extracting Wildfire Spread Rate from Himawari-8 Satellite Data. *Remote Sensing*, *10*(10), 1654. https://doi.org/10.3390/rs10101654

Martell, D. L. (1982). A review of operational research studies in forest fire management. *Canadian Journal of Forest Research*, *12*(2), 119–140. https://doi.org/10.1139/x82-020

Mertes, J. R., Gulley, J. D., Benn, D. I., Thompson, S. S., & Nicholson, L. I. (2017). Using structure-from-motion to create glacier DEMs and orthoimagery from historical terrestrial and oblique aerial imagery. *Earth Surface Processes and Landforms*, *42*(14), 2350–2364. https://doi.org/10.1002/esp.4188

Moriarty, K., Cheng, A. S., Hoffman, C. M., Cottrell, S. P., & Alexander, M. E. (2019). Firefighter Observations of "Surprising" Fire Behavior in Mountain Pine Beetle-Attacked Lodgepole Pine Forests. *Fire*, *2*(2), 34. https://doi.org/10.3390/fire2020034

Parisien, M.-A., Dawe, D. A., Miller, C., Stockdale, C. A., & Armitage, O. B. (2019). Applications of simulation-based burn probability modelling: a review. *International Journal of Wildland Fire*, *28*(12), 913. https://doi.org/10.1071/WF19069

Pepin, A.-C., & Wotton, M. (2020). Fire Behaviour Observation in Shrublands in Nova Scotia, Canada and Assessment of Aids to Operational Fire Behaviour Prediction. *Fire*, *3*(3), 34. https://doi.org/10.3390/fire3030034

Perrakis, D. B., Lanoville, R. A., Taylor, S. W., & Hicks, D. (2014). Modeling wildfire spread in mountain pine beetle-affected forest stands, British Columbia, Canada. *Fire Ecology*, *10*(2), 10–35. https://doi.org/10.4996/fireecology.1002010

Plucinski, M. P., Sullivan, A. L., Rucinski, C. J., & Prakash, M. (2017). Improving the reliability and utility of operational bushfire behaviour predictions in Australian vegetation. *Environmental Modelling and Software*, *91*, 1–12. https://doi.org/10.1016/j.envsoft.2017.01.019

Stocks, B. J. (1989). Fire behavior in mature jack pine. *Canadian Journal of Forest Research*, *19*(6), 783-790. https://doi.org/10.1139/x89-119

Stocks, B. J., & Hartley, G. R. (1995). Fire behavior in three jack pine fuel complexes (Poster with text). Natural Resources Canada, Canadian Forest Service, Great Lakes Forestry Centre: Sault Ste. Marie, Ontario, Canada. https://cfs.nrcan.gc.ca/publications?id=29043

Stocks, B. J., Lynham, T. J., Lawson, B. D., Alexander, M. E., Wagner, C. E. Van, McAlpine, R. S., & Dubé, D. E. (1989). The Canadian Forest Fire Danger Rating System: An Overview. *The Forestry Chronicle*, *65*(6), 450–457. https://doi.org/10.5558/tfc65450-6

Sullivan, A. L. (2009). Wildland surface fire spread modelling, 1990 - 2007. 2: Empirical and quasi-empirical models. *International Journal of Wildland Fire*, *18*(4), 369-386. https://doi.org/10.1071/wf06142

Szpakowski, D. M., & Jensen, J. L. R. (2019). A review of the applications of remote sensing in fire ecology. *Remote Sensing*, *11*(22), 2638. https://doi.org/10.3390/rs11222638

Taylor, S.W., & Alexander, M.E. (2006). Science, technology, and human factors in fire danger rating: the Canadian experience. *International Journal of Wildland Fire*, *15*(1), 121-135. https://doi.org/10.1071/WF05021

Taylor, S. W., Woolford, D. G., Dean, C. B., & Martell, D. L. (2013). Wildfire Prediction to Inform Fire Management: Statistical Science Challenges. *Statistical Science*, *28*(4), 586–615. https://doi.org/10.1214/13-STS451

Van Wagner, C. E. (1987). Development and structure of the Canadian forest fire weather index system (Forestry Technical Report 35). Natural Resources Canada, Canadian Forest Service: Ottawa, Ontario, Canada. https://cfs.nrcan.gc.ca/pubwarehouse/pdfs/19927.pdf

Van Wagner, C. E. (1990). Six Decades of Forest Fire Science in Canada. *The Forestry Chronicle*, *66*(2), 133–137. https://doi.org/10.5558/tfc66133-2

Verhoeven, G., Doneus, M., Briese, C., & Vermeulen, F. (2012). Mapping by matching: A computer vision-based approach to fast and accurate georeferencing of archaeological aerial photographs. *Journal of Archaeological Science*, *39*(7), 2060–2070. https://doi.org/10.1016/j.jas.2012.02.022

Verhoeven, Geert, & Sevara, C. (2016). Trying to Break New Ground in Aerial Archaeology. *Remote Sensing*, *8*(11), 918. https://doi.org/10.3390/rs8110918

Warrick, J. A., Ritchie, A. C., Adelman, G., Adelman, K., & Limber, P. W. (2017). New Techniques to Measure Cliff Change from Historical Oblique Aerial Photographs and Structure-from-Motion Photogrammetry. *Journal of Coastal Research*, *33*(1), 39-55. https://doi.org/10.2112/jcoastres-d-16-00095.1

Wilkinson, S. L., Moore, P. A., Thompson, D. K., Wotton, B. M., Hvenegaard, S., Schroeder, D., & Waddington, J. M. (2018). The effects of black spruce fuel management on surface fuel condition and peat burn severity in an experimental fire. *Canadian Journal of Forest Research*, *48*(12), 1433–1440. https://doi.org/10.1139/cjfr-2018-0217

Wotton, B. M., Alexander, M. E., & Taylor, S. W. (2009). Updates and revisions to the 1992 Canadian Forest Fire Behavior Prediction System (Information Report GLC-X-10). Natural Resources Canada, Canadian Forest Service, Great Lakes Forestry Centre: Sault Ste. Marie, Ontario, Canada. https://cfs.nrcan.gc.ca/pubwarehouse/pdfs/31414.pdf

Wotton, B. Mike. (2009). Interpreting and using outputs from the Canadian Forest Fire Danger Rating System in research applications. *Environmental and Ecological Statistics*, *16*(2), 107–131. https://doi.org/10.1007/s10651-007-0084-2

Xiao-rui, T., Mcrae, D. J., Li-fu, S., Ming-yu, W., & Hong, L. (2005). Satellite remote-sensing technologies used in forest fire management. *Journal of Forestry Research*, *16*(1), 73–78. https://doi.org/10.1007/bf02856861

Xie, Z., Song, W., Ba, R., Li, X., & Xia, L. (2018). A Spatiotemporal Contextual Model for Forest Fire Detection Using Himawari-8 Satellite Data. *Remote Sensing*, *10*(12), 1992. https://doi.org/10.3390/rs10121992

Chapter 3: Georeferencing Oblique Aerial Wildfire Photographs: An Untapped Source of Fire Behaviour Data[1]

Abstract

In this study, we investigate a novel application of the photogrammetric monoplotting technique for assessing wildfires. We demonstrate the use of the software program WSL MonoplottingTool (MPT) to georeference operational oblique aerial wildfire photographs taken during airtanker response in the early stages of fire growth. We located the position of the fire front in georeferenced pairs of photos from five fires taken 31–118 min apart, and calculated the head fire spread distance and head fire rate of spread (HROS). Our example photos were taken 0.7 to 4.7 km from fire fronts, with camera angles of incidence from −19º to −50º to image centre. Using high quality images with detailed landscape features, it is possible to identify fire front positions with high precision; in our example data, the mean 3D error was 0.533 m and the maximum 3D error for individual fire runs was less than 3 m. This resulted in a maximum HROS error due to monoplotting of only ~0.5%. We then compared HROS estimates with predictions from the Canadian Fire Behavior Prediction System, with differences mainly attributed to model error or uncertainty in weather and fuel inputs. This method can be used to obtain observations to validate fire spread models or create new empirical relationships where databases of such wildfire photos exist. Our initial work suggests that monophotogrammetry can provide reproducible estimates of fire front position, spread distance and rate of spread with high accuracy, and could potentially be used to characterize other fire features such as flame and smoke plume dimensions and spotting.

[1] The following chapter has been published as:
Hart, H., Perrakis, D.D.B., Taylor, S.W., Bone, C., Bozzini, C. (2021). Georeferencing Oblique Aerial Wildfire Photographs: An Untapped Source of Fire Behaviour Data. Fire, 4(4), 81. https://doi.org/10.3390/fire4040081

3.1 Introduction

Fire behaviour prediction is important to operational wildfire decision-making and fire fighter safety (Taylor et al., 2013). Wildfire spread rates in conifer forests may vary from less than 1 m/min to more than 100 m/min, while spread in grasslands and other open fuels may exceed 200 m/min (Forestry Canada Fire Danger Group, 1992). Fire spread rate relationships are used in both aspatial and spatial fire growth models and are also incorporated in risk assessments (Johnston et al., 2020; Parisien et al., 2019). Observations of the position of the origin, head, flank and back of a fire over time, and the corresponding spread rates, are important for developing empirical fire behaviour models, validating any kind of fire behaviour model in real world conditions, and in wildfire cause investigations (Hirsch, 1996; Plucinski et al., 2017; Wotton et al., 2009).

In the Canadian Fire Behaviour Prediction (FBP) System, for example, the predicted head fire rate of spread (HROS) is estimated using nonlinear regression relationships between observed HROS and the Initial Spread Index (ISI) of the Canadian Forest Fire Weather Index (FWI) System obtained from several hundred experimental fires and wildfires in 14 different fuel types (FCFDG, 1992; Hirsch, 1996; Johnston et al., 2020; Parisien et al., 2019; Plucinski et al., 2017; Van Wagner, 1987; Wotton et al., 2009). While estimates of HROS from experimental fires using direct observation or indirect measures using electronic timers or imagery are most accurate (Alexander et al., 1991; Stocks, 1989), such experiments are rare, and, when they do occur, are typically conducted during low to moderate fire danger conditions. As a result, spread measurements in high danger conditions have been mainly obtained from wildfires (Alexander & Thomas, 2003). However, obtaining reliable wildfire observations through research or operational activities is dilemmatic. While researchers have used infrared sensors among other

methods to obtain accurate wildfire observations (Allison et al., 2016; Moriarty et al., 2019), they face many obstacles, including difficulty in getting to incidents while notable fire activity is occurring or before suppression has influenced fire growth, or getting into favourable positions to observe fire behaviour when response actions restrict access. On the other hand, while firefighters and officers are often positioned to observe noteworthy fire behaviour, they often lack the time, training or resources to make careful observations or measurements while carrying out their main duties (Filkov et al., 2018). Thus, there is a paucity of reliable wildfire spread observations to evaluate the FBP System HROS models, or indeed all types of fire spread and growth models (Alexander & Cruz, 2013; Gould et al., 2011; Sullivan, 2009).

In this paper, we demonstrate a method to extract wildfire spread observations from oblique aerial photographs taken during wildfire response in the province of British Columbia, Canada. We focus on photographs that were obtained by observers in reconnaissance aircraft accompanying air tankers to document evolving fire conditions and airtanker operations early in the first burning period for training and accountability purposes. The photographs were taken at close range (less than 1 km) and at varying angles, providing unobstructed views of the fire front position and flame zone depth. The use of these photos has the obvious advantage that airtankers and 'bird dog' spotter planes are in the right place at the right time, and no additional resources are required. In a previous study, Perrakis et al. (2014) estimated fire spread from similar images. However, the methods used to georeference points on the photos were difficult to reproduce and contained unknown error. Therefore, our objectives in this study were as follows:

1. Develop an efficient, systematic, repeatable procedure to determine the geographic coordinates of wildfire features captured in oblique photographs.

2. Demonstrate the use of the procedure to obtain estimates of wildfire spread rates and validate fire behaviour models, using the FBP System models as an example.

To address these objectives, we investigated a novel application of a conventional photogrammetric method called monoplotting to extract fire behaviour data from oblique aerial images. Although the theory of monoplotting was first described in the early 1970s (Makarovic, 1973), its application has been limited in the past due to the lack of computing power and the availability of high resolution Digital Elevation Models (DEM) that are necessary to achieve accurate results (Bozzini et al., 2012). Advances in these areas led to several monoplotting software packages, but their limited flexibility, complicated user interfaces and closed-access platforms prevented their widespread use (Stockdale et al., 2015). More recently, Bozzini et al. (2012) developed an open-access monoplotting software package (Monoplotting Tool, 2021), the WSL Monoplotting Tool (MPT), at the Swiss Federal Institute for Forest, Snow and Landscape Research WSL in Birmensdorf, Switzerland that georeferences single oblique aerial images without the need for multiple, and overlapping images that are typically required for conventional photogrammetrical georeferencing practices (Bozzini et al., 2012). The MPT has subsequently been used for a wide range of 3D spatial measurements and analysis, including documenting avalanches (Conedera et al., 2018) and extracting ecological information from historical landscape imagery (Stockdale et al., 2015). This paper extends the application of the technique to the fire behaviour context.

A brief description of the monoplotting process and its implementation in MPT are provided in Section 2. In Section 3, we document the application of the method to wildfire image series in order to calculate the spread distance and HROS of five wildfires that occurred in British Columbia, Canada between 2009 and 2014. In Section 4, we analyze the accuracy of the

georeferencing process and compare the observed fire spread with predicted values. While our immediate goal was to investigate the utility and limitations of this method to obtain observations to validate HROS models within the Canadian FBP System, the method can be used to georeference oblique wildfire photographs for other fire behaviour or management applications.

3.2 Materials and Methods

3.2.1 Monoplotting Process

Mono-photogrammetry, also known as monoplotting, is the process of georeferencing a single oblique photograph by relating it to a digital elevation model (DEM; Bozzini et al., 2012). This process involves camera calibration which provides a reconstruction of the camera parameters at the shooting time, thus allowing for matching of each point of the image with its corresponding ground point (and vice versa).

In other words, georeferencing consists of positioning the camera, the image and the DEM in such a way that, for each point on the image, the ray starting from the origin of the camera and passing through this point intersects the DEM at the corresponding ground point (Figure 3.1).

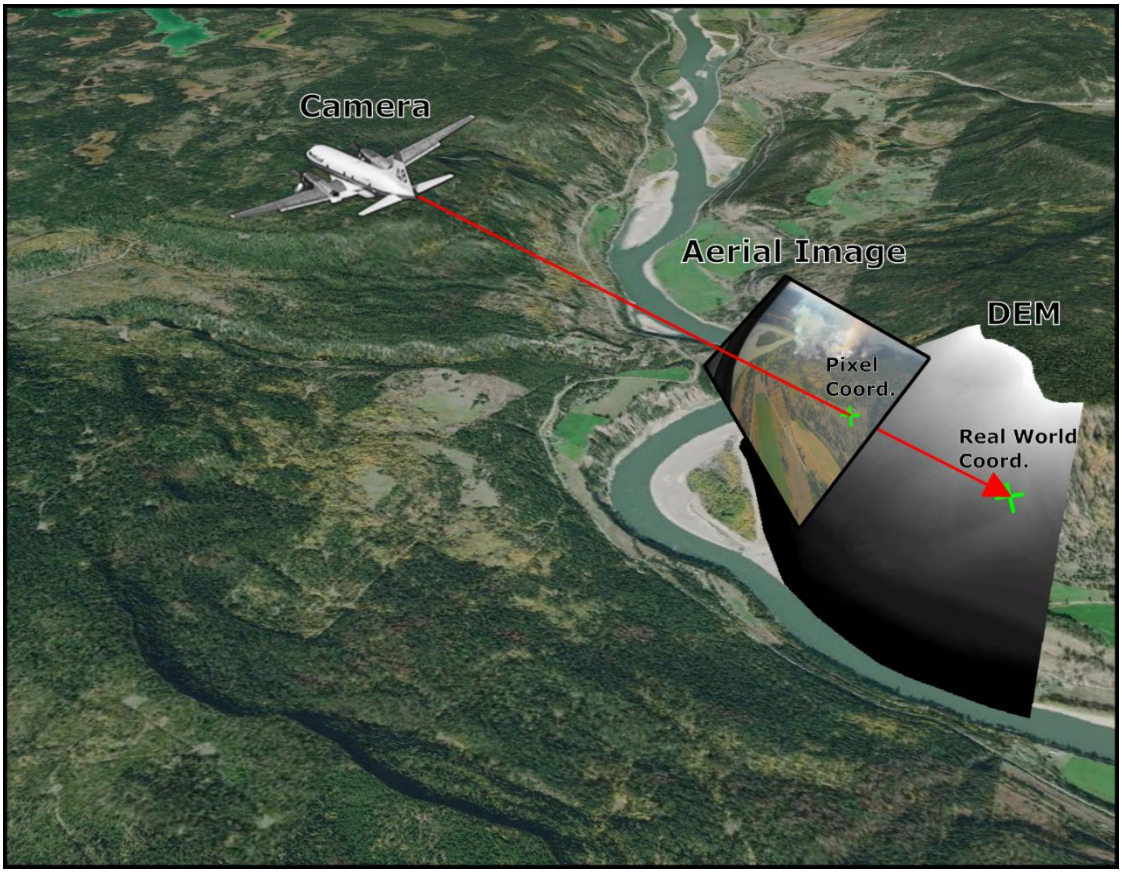

Figure 3.1. Monoplotting principle, displaying the relationship between the camera, photo and DEM.

A monoplotting system requires a digital image, DEM, camera system parameters and an additional georeferenced source, such as an orthoimage, from which Ground Control Points (GCPs) are determined. GCPs are points for which both the position in pixels on the image and the position in real world coordinates with respect to the DEM are known. Examples of suitable points are building corners or other stationary landscape features.

The MPT software incorporates a camera calibration algorithm, which estimates the intrinsic (image center, focal distance, radial and tangential distortion) and extrinsic (Euler rotation angle corresponding to the camera orientation, camera position coordinates) parameters of the camera system (Bozzini et al., 2012). The camera calibration is an iterative process based on the method of least squares after a linearization of the collinearity equations (Bozzini et al.,

2012), that relies on the identification of precise GCPs and high resolution input data and is essential to the success and accuracy of georeferencing digital images using MPT. As noted by Stockdale et al. (2015), exact GCP placement in the 2D and 3D space, flawless DEM quality and zero film or lens distortion would result in a perfectly georeferenced image; however, this is rarely the case. Therefore, the camera calibration algorithm produces error values for each GCP pair and utilizes these values to determine the best solution of the intrinsic and extrinsic camera parameters that minimize the calculated errors using the least square method (Table 3.1). It should be noted that the calculated parameters correspond to the best configuration of the camera according to the defined points, so it is possible that some parameters (e.g., camera position, image center, etc.) do not correspond perfectly with the actual values when the photo was taken. Figure 3.2 visually describes the camera calibration algorithm and derivation of the error values used to calculate the final camera system parameters (Bozzini et al., 2012; Bozzini, 2018; Steiner, 2012).

Table 3.1 Summary of MPT camera calibration errors as shown in the software.

Error	**Unit**	**Symbol**	**Description**
Pixels	px	d	Distance from user defined image GCP (p) coordinates to MPT calculated image point (p') coordinates given in pixels
Angle	º	α(r, r')	The angle between the two light rays (r, r')
Radius	m	R	Distance from MPT calculated ground point (P") to user defined ground GCP (P)
World 3D	m	D	Distance from MPT calculated ground point (P') to the user defined ground GCP (P)
World 2D	m	D2d	Projection of the World 3D error (D) on the horizontal plane

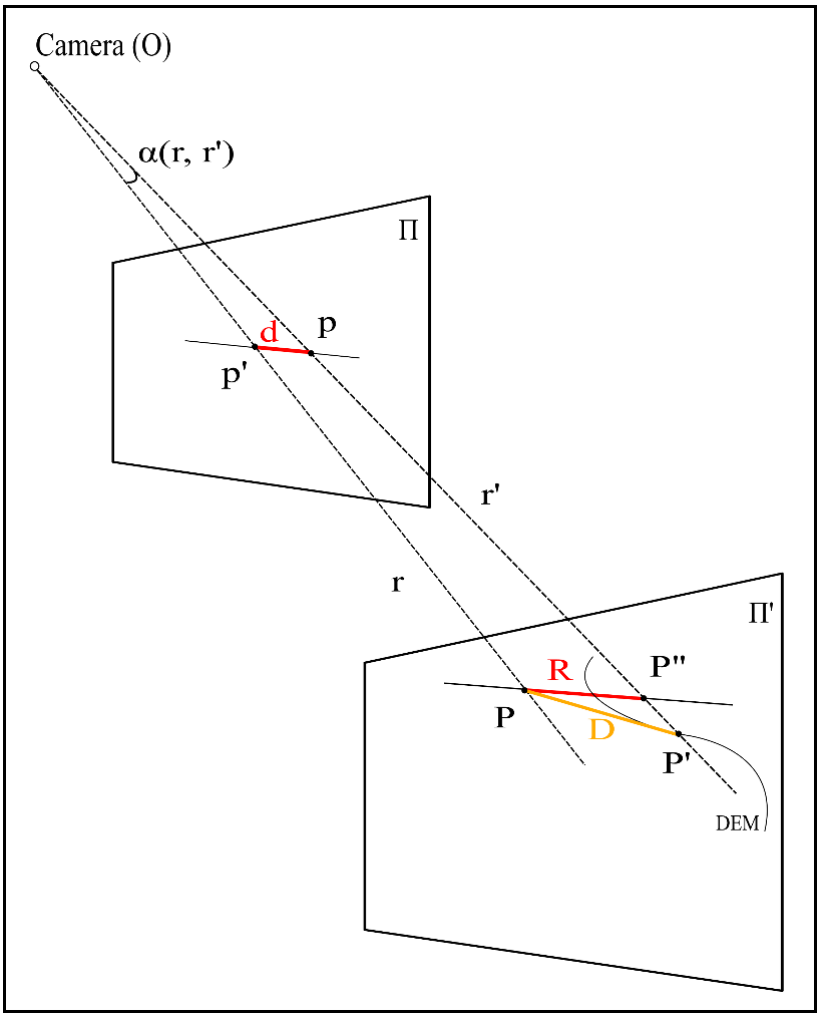

Figure 3.2: Visual representation of the camera calibration algorithm and derivation of error values used by MPT; figure adapted from (Steiner, 2012; Stockdale et al., 2015). The symbols are defined in the following paragraph and in Table 3.1.

During the camera calibration algorithm, the user first selects a location on the orthophoto (in combination with the DEM) to estimate the initial real-world coordinates of the camera position (O) and defines a precise GCP on the image (p) and GCP on the corresponding DEM (P). Some additional elements help in evaluating the accuracy of the camera calibration. ∏ is the image plane, ∏' is a plane parallel to ∏ containing P. O and P define the ray r, while O and P' define r'. p' (projection of P on ∏) is the pixel point calculated from P. P" (intersection of r' and ∏') is the ground point on ∏' calculated from p, and P' (intersection of r' and the DEM) is the ground point on the DEM calculated from p. Differences between the two rays (α), the MPT

calculated points (d), and the user defined GCPs (R and D) represent a matrix of error types that describe the overall accuracy of the georeferencing (Table 3.1).

The iterative camera calibration process is based on the principle of monoplotting; more specifically, the mathematical model in which two collinearity equations are used to solve the intrinsic and extrinsic parameters of the camera system simultaneously:

$$x = -c \times \frac{r_{11}(X_P - X_C) + r_{21}(Y_P - Y_C) + r_{31}(Z_P - Z_C)}{r_{13}(X_P - X_C) + r_{23}(Y_P - Y_C) + r_{33}(Z_P - Z_C)} \quad (1)$$

$$y = -c \times \frac{r_{12}(X_P - X_C) + r_{22}(Y_P - Y_C) + r_{32}(Z_P - Z_C)}{r_{13}(X_P - X_C) + r_{23}(Y_P - Y_C) + r_{33}(Z_P - Z_C)} \quad (2)$$

where x, y are image coordinates; c is the focal length; X_C, Y_C and Z_C are the real world coordinates of camera position; r_{11} r_{33} are the coefficients of the rotation matrix defining the camera rotation parameters; and X_P, Y_P and Z_P are the known coordinates of the GCP (Bozzini et al., 2012; Schenk, 2005). Once the camera system parameters are estimated, the correspondence between image and ground points are determined by MPT using Equations (1) and (2) and the DEM (the DEM is needed for calculation from pixel to real coordinates).

3.2.2 Study Area, Image Selection and Data Compilation

The BC Wildfire Service (BCWS) has the primary responsibility to manage wildfires in the province of British Columbia, Canada. On average, 1600 fires occur each year in the province within a land area of about 94 million ha (BC Wildfire Service, 2020). Airtankers are used in an initial attack on an average of 15% of fires in BC when fire behaviour is beyond ground crew capacity, or to initiate initial attack when the arrival of ground crews is delayed. BCWS Air Attack Officers, who carry out an initial assessment from reconnaissance aircraft and guide the air tankers towards the fire, take digital photographs of each incident to document the

fire behaviour and air tanker effectiveness. Photographs are typically captured with consumer-grade hand-held cameras or smartphones (more recent images are of increasing quality). Digital images acquired since 2000 are archived in a central database.

We selected ten images from five wildfires in the BCWS archive that occurred between 2009 and 2014 (Figure 3.3) within a wide range of landscape features and vegetation types (Table 3.2). The selected photographs contained a suitable perspective of the fire front location in successive images separated by at least 30 min, as well as landscape features suitable for georeferencing (Figure 3.4).

As noted in Section 2.1, in order to georeference the photographs, the monoplotting procedure requires GCPs visible in both the oblique photographs and in an orthoimage, and a digital elevation model (DEM; Bozzini, 2018). We obtained a 25 m DEM from the British Columbia Data Catalogue and orthoimages, all of which are under 0.5 m resolution, from various satellite sources within the ESRI World Imagery layer (BC Data Catalogue, 2020; ESRI 2020). The wildfire photographs and orthoimages associated with each fire site are shown in Figure 3.4. Although the orthoimages for Sites 1, 2, 4 and 5 were captured after the fires had occurred, the GCPs were not affected by the fires.

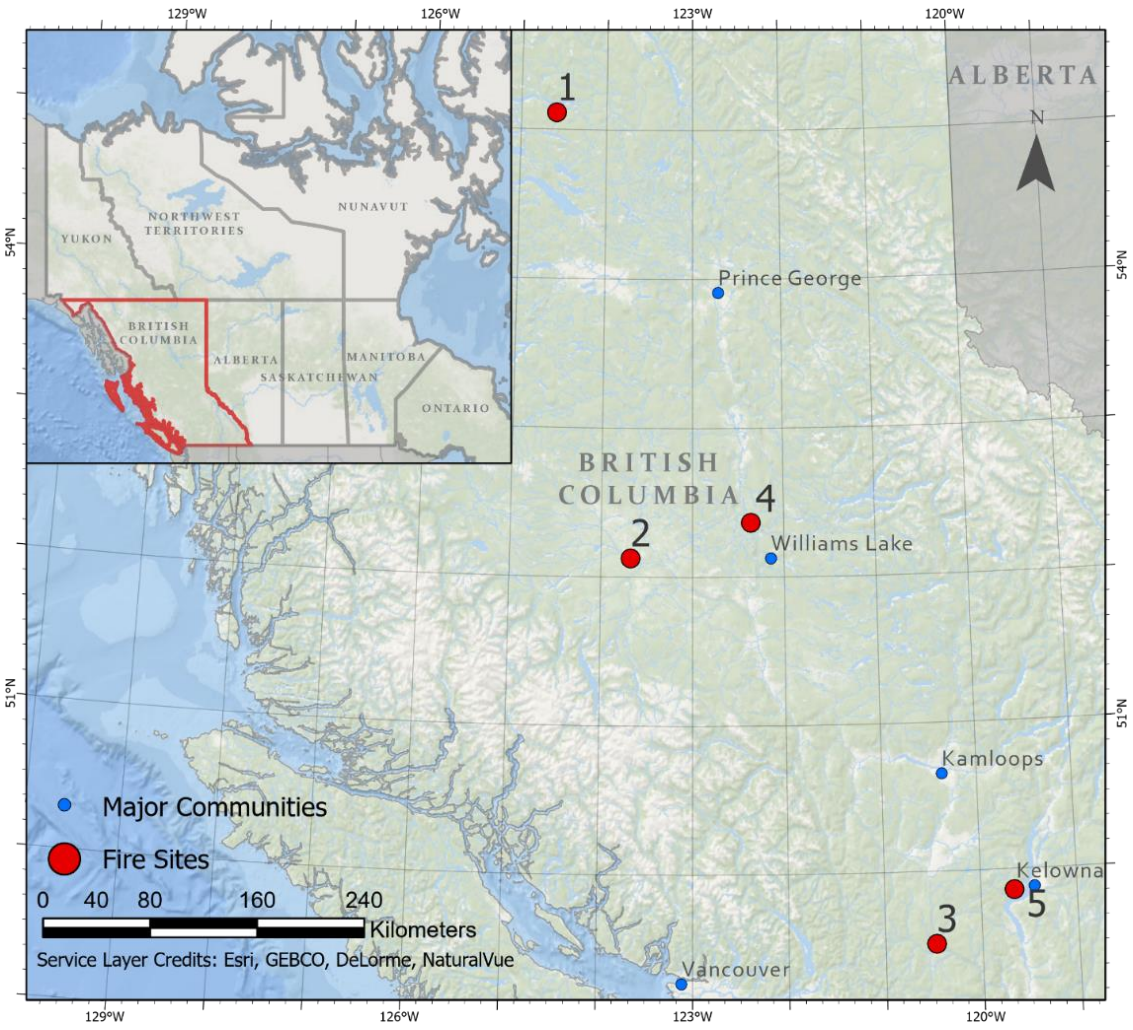

Figure 3.3. The location of the fire sites used in this study in British Columbia.

Table 3.2. Study Site descriptions, including landscape features and vegetation descriptions.

Site Number	Landscape Features	Vegetation Type
1	Flat riparian landscape, open areas with shrubs, patchy forest	Engelmann spruce—Subalpine fir forest
2	Flat landscape, two building structures, open areas with shrubs, forest and agricultural areas	Ponderosa Pine—Douglas-fir
3	Moderately sloped landscape, open grass field with lone standing trees	Interior grassland, cured
4	Steeply sloped landscape, two buildings, patchy forested sections with lone standing trees	Grassland—Ponderosa pine forest transition
5	A: Moderately sloped landscape, many buildings, sports fields, forested areas B: Moderately sloped landscape, two buildings, densely forested with open disturbance patches	Closed Douglas-fir forest

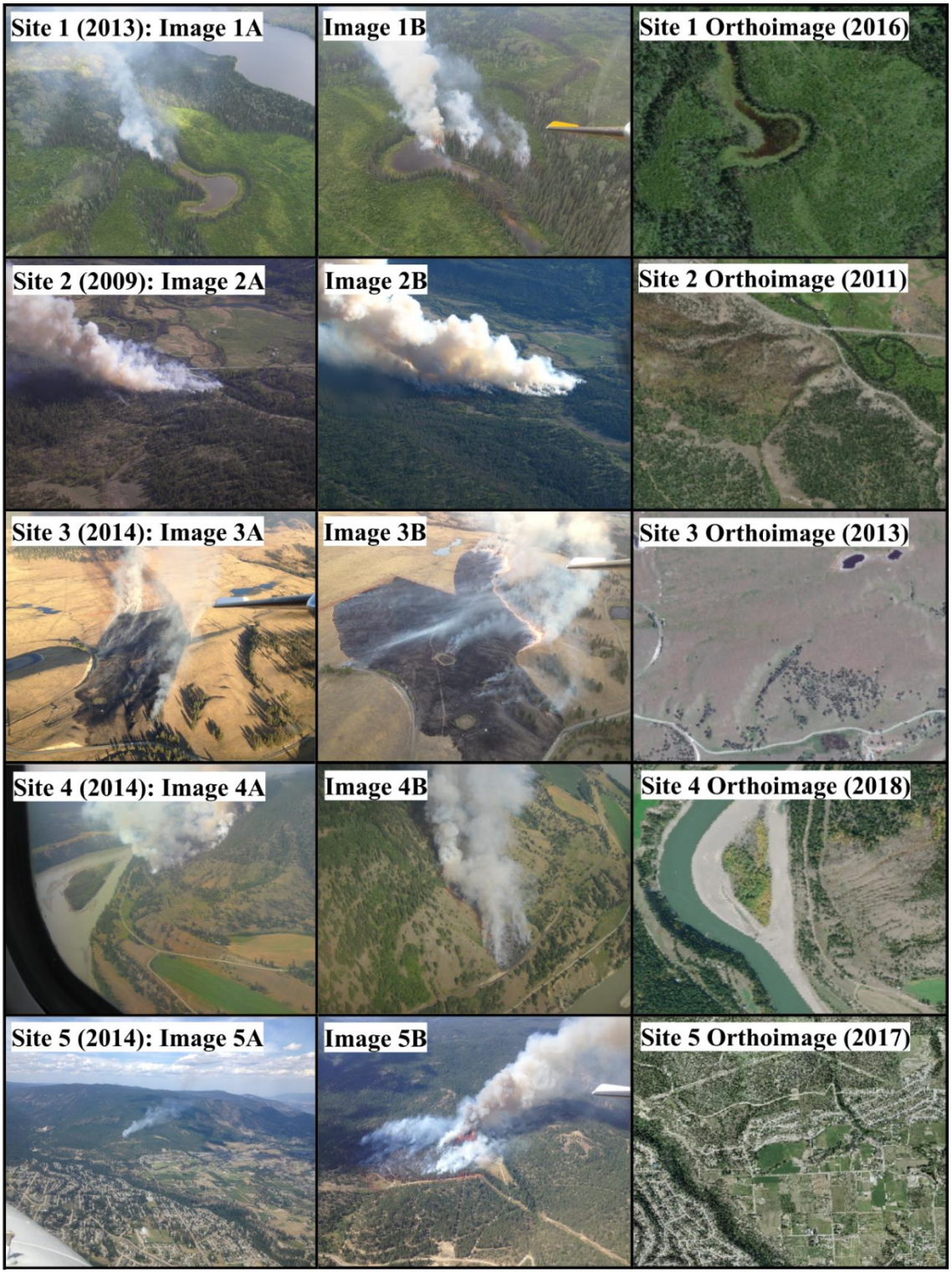

Figure 3.4. Study site image pairs with their respective orthoimages. Images were captured at the following Pacific Daylight times: 1A 14:31, 1B 15:13, 2A 18:16, 2B 19:13, 3A 18:33, 3B 19:04, 4A 14:56, 4B 16:09, 5A 13:48 and 5B 15:46.

3.2.3 Georeferencing Oblique Aerial Wildfire Images Using MPT

After assembling the oblique photo pairs, orthophotos and DEM for each site, we selected 5 GCPs in each photo pair that could also be located in the corresponding orthophoto. To work effectively, GCPs need to be located in a dispersed pattern across the oblique photos; when this is not possible, it is necessary at least to find the required control points around the feature or features of interest in the (Conedera et al., 2018; Steiner, 2012; Stockdale et al., 2015)—in this case, the fire front position. As suggested by Stockdale et al. (2015), we avoided using GCPs on hill tops or terrain breaks where there is a higher risk of points being displaced across large horizontal distances (e.g., infinitely beyond the horizon line or on a mistaken hill peak beyond the correct one). In addition, GCPs should be located close to the features of interest, as precision decreases with distance from the camera. We note that it is not necessary that the same GCPs be used in the successive images. We evaluated the accuracy of each selected GCP and adjusted or replaced those with unacceptable accuracy where possible. GCPs consisted primarily of individual identifiable trees, shrubs and building corners (Table 3.2). A GCP was considered acceptable if it had a three-dimensional error (World 3D Error) less than 5 m (i.e., the distance from MPT calculated GCP to the user defined GCP in real-world space; Table 3.1). Furthermore, following Bozzini (2018), the GCP must have an angle error less than or near 0.01º. Examples of GCPs with low error values are shown in Figure 3.5.

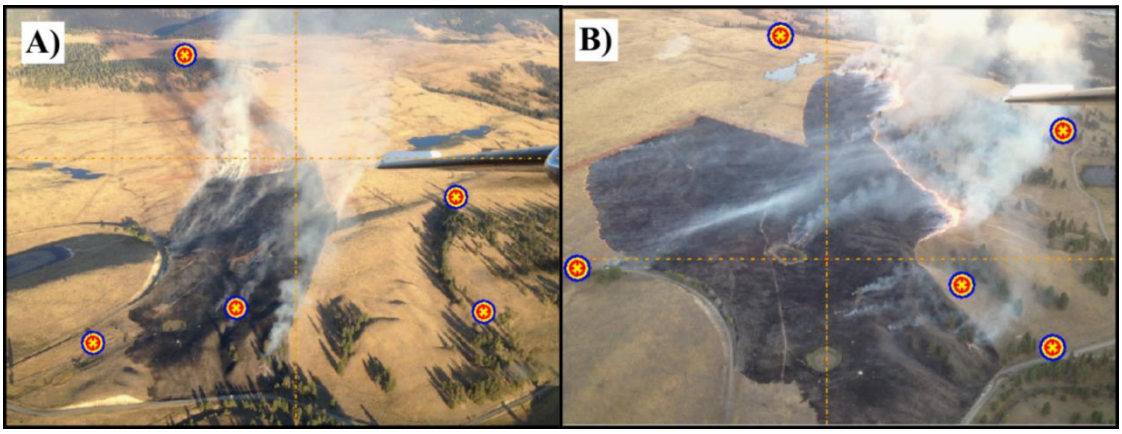

Figure 3.5. Overlapping user defined (yellow X's), MPT computed GCPs (blue circles) and computed image centre (dotted line crosshairs) displaying successfully calibrated wildfire images for Site 3: image 3A (A) and 3B (B).

Before determining the headfire position and HROS, we extracted the angle of incidence of each image using their respective viewshed parameters and the real-world coordinates of the image centre. Specifically, we calculated the angle between a ray from the camera centre and the slope of a 10 m segment of ground at the image centre (Stockdale et al., 2015).

3.2.4 Headfire Position Interpretation and Rate of Spread Calculation

Our aim was to determine the Head Fire Spread Distance (HSD) and HROS in successive images. In order to make meaningful interpretations of HROS from HSD, images must be selected where the fuels and topography are relative uniform between the successive fire front positions. After georeferencing the digital images, we used the annotation feature in MPT to digitize custom georeferenced vectors (polylines) on the digital image to represent the fire front position. The head of a fire typically develops a curved front due to the distribution of radiation ahead of the fire (Weber, 1989). Where fire growth is approximated by the elliptical model (Van Wagner, 1969), the apex of the ellipse represents the head of the fire. Thus, there is a point (the head) at the fire front where the HROS (and so the fireline intensity, flame length and flame zone depth) are at a maximum, and the flame tilt towards the unburned fuel is also at a maximum (N.

Cheney & Gould, 1995). The location of the head fire (front) was determined visually, based on the shape of the fire perimeter, the flame zone depth, flame height, angle and smoke direction, when they could be observed (Figure 3.6). For the purpose of estimating HROS, only the furthest leeward segments of fireline are required; in certain cases (e.g., Figure 3.6B), fire suppression actions or fuel discontinuities may determine which segments of fireline produce subsequent fire growth.

The fire front positions were exported from MPT as individual shapefiles and imported into ArcPro (ESRI, Redlands, CA, USA). The HSD was calculated using the 'Near' tool, as the Euclidian distance between the heads on successive arcs and can be seen as the perpendicular Hausdorff distance between two successive curves (the maximum of all minimum distances between two curves). The HSD is typically normal to the head fire front (Cheney & Gould, 1995; and the head fire front is typically normal to the spread direction). In cases when it is difficult to identify the head based on flame zone properties, we estimated the position in relation to the smoke column base, tilt angle, and spread direction. Using the HSD, we then estimated the headfire rate of spread as:

$$HROS = \frac{HSD}{(T2 - T1)} \quad (3)$$

where HSD is the head fire spread distance and T1 and T2 are the times of photo capture. To demonstrate the use of the data to validate fire spread models, we determined the vegetation and FBP System fuel type associated with each fire from the BC Forest Service's vegetation resource inventory (VRI) data and fuel type layer (Perrakis et al., 2018) and obtained fire weather information from weather station data. See the Appendix A for more information on the FBP System HROS predictions.

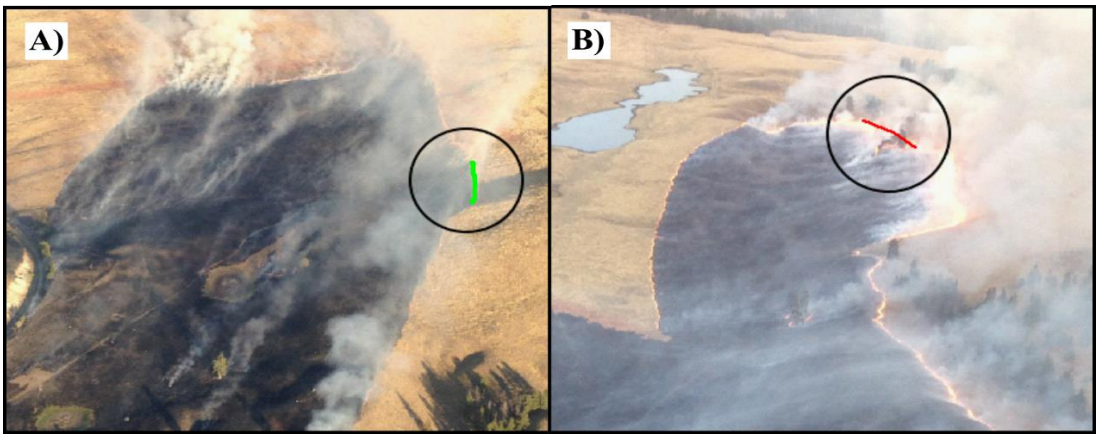

Figure 3.6. (A) Start fire front position (green line); (B) end fire front position (red line) at Site #3.

3.3 Results

3.3.1 Fire Front Locations and Accuracy Assessment

We used the monoplotting technique to estimate the position of fire fronts in 10 images of five fires in British Columbia. The estimated position of the fire fronts and the GCPs used to georeference each image are shown in Figure 3.7. The positional accuracy of the fire front locations (or of other features) depends greatly on the error in GCP locations and the camera angle of incidence. The error values of the GCPs for each image are shown in Table 3.3.

Table 3.3. The GCP errors for each georeferenced wildfire image.

Image #	Aerial Image Time Stamp	Mean Angle Error (º)	3D Error (m) Min.	3D Error (m) Max.	3D Error (m) Mean
1A	14:31	0.008	0.033	0.388	0.244
1B	15:13	0.011	0.033	0.382	0.253
2A	18:16	0.009	0.053	1.034	0.600
2B	19:13	0.002	0.087	0.822	0.500
3A	18:33	0.001	0.137	1.127	0.555
3B	19:04	0.001	0.102	0.672	0.322
4A	14:56	0.009	0.327	0.691	0.475
4B	16:09	0.012	0.234	0.962	0.706
5A	13:48	0.014	0.133	2.030	1.197
5B	15:46	0.011	0.103	0.959	0.477
Mean or *Extreme*	NA	0.008	*0.033*	*2.030*	0.533

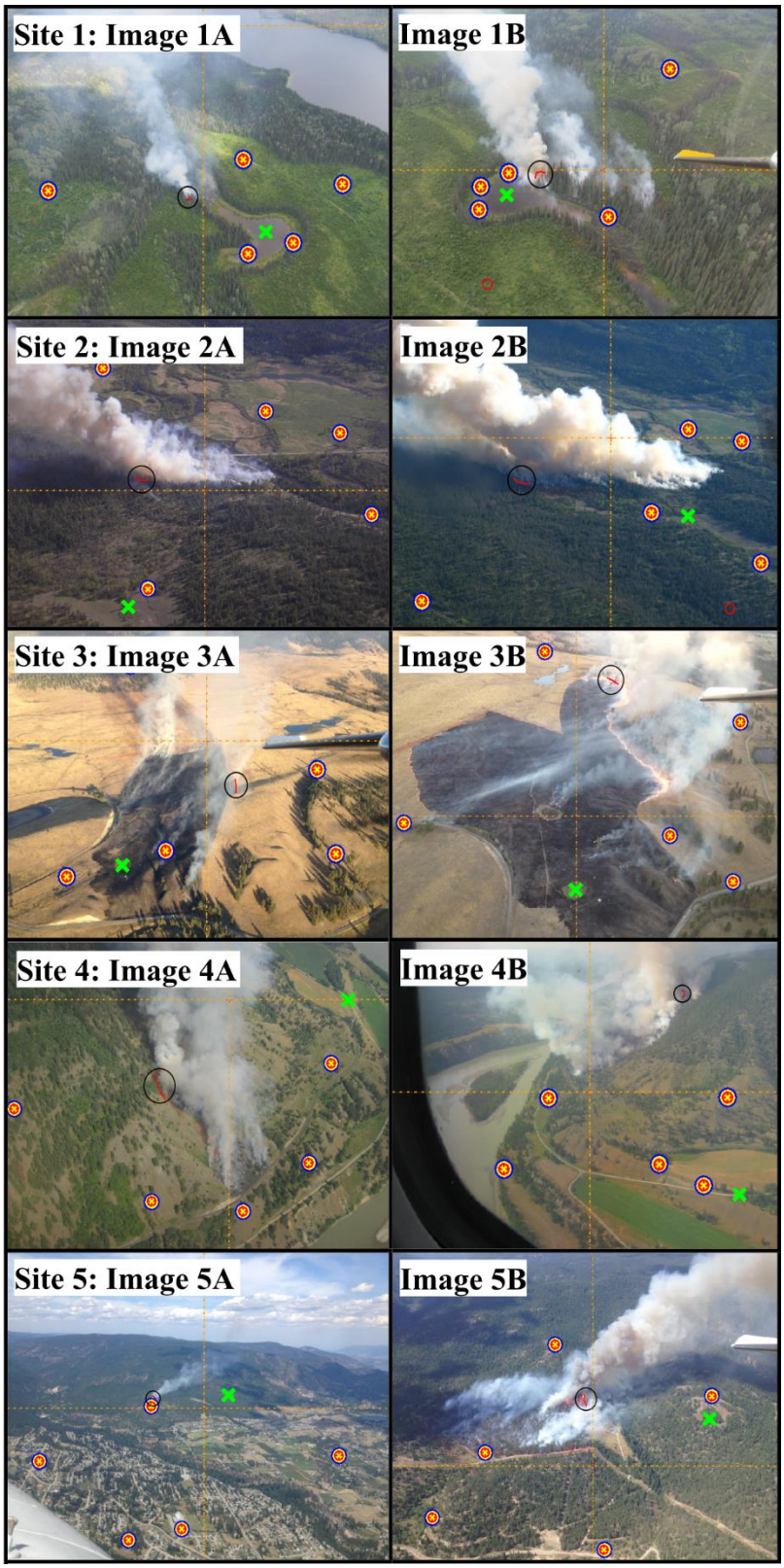

Figure 3.7. Georeferenced photographs, with identified GCPs (targets), fire front positions (red line in black circle) and green ‘X’ representing a reference feature visible in both images.

The mean and maximum 3D error of each of the five image pairs were all under the initial requirement of less than 5 m indicating successful georeferencing. Six of the images also met the angle error target of less than 0.01º, with the remaining four images not exceeding 0.014º, which we considered to be within a reasonable range.

The distance to fire front, elevation above ground level and camera angle of incidence all vary from image to image (Table 3.4). The azimuth of each camera direction is provided for clarity.

Table 3.4. The estimated camera characteristics for each georeferenced image.

Image #	Approx. Distance to Fire Front (m)	Elevation above Ground Level (m)	Angle of Incidence (º)	Azimuth (º)
1A	1040	587.63	−42.02	85.44
1B	650	360.16	−43.40	290.86
2A	1725	836.29	−31.95	205.09
2B	3720	1443.46	−25.67	224.78
3A	1720	794.27	−36.32	114.35
3B	2130	516.12	−42.52	153.80
4A	1275	1024.43	−49.52	104.10
4B	2420	631.57	−31.54	332.08
5A	4665	810.97	−18.82	11.80
5B	1575	772.71	−37.09	352.91
Mean	2092	777.76	−35.89	NA

The distance to fire front, camera elevation and angle of incidence ranged between 650 to 4665 m, 365 to 1443 m and −18 to −49º, respectively. There was a significant correlation between the angle of incidence and the 3D accuracy ($r = 0.63$) but no significant relationship between angle of incidence and angle error (Figure 3.8).

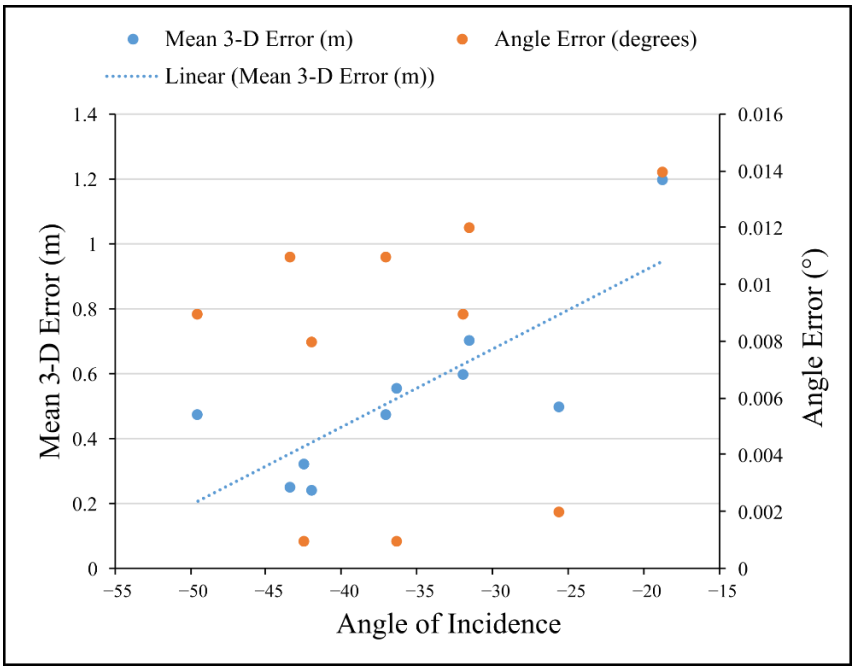

Figure 3.8. Relationship between angle of incidence and mean 3D error, and angle error in 10 wildfire images.

3.3.2 Fire Spread Distance and Rate Estimates

Spread distances and HROS (Equation (3)) are shown in Table 3.5. Spread distances ranged from 201 to 846 m over burning periods of 31 to 118 min, resulting in HROS values from 4.7 to 27.3 m/min. The max total 3D error refers to the sum of the maximum 3D error of each GCP (provided by MPT software) of both images. The max HROS error refers to the maximum possible error associated each Site due to monoplotting and is calculated by dividing the max total 3D error by fire spread distance.

Table 3.5. Fire behaviour parameters determined from the georeferenced wildfire images.

Site #	Fire Year	Fire Spread Distance (m)	Burning Period (min)	Max Total 3D Error (m)	Max HROS Error (%)	HROS (m/min)
1	2013	200.63	42	0.770	0.38	4.78
2	2009	581.13	57	1.856	0.32	10.20[a]
3	2014	845.77	31	1.799	0.21	27.28
4	2014	377.42	73	1.653	0.44	5.17
5	2014	554.30	118	2.989	0.54	4.70

[a] See Appendix A for a recalculation of Site 2 based on a different starting segment.

We calculated the rate of spread predicted by the FBP System using the closest-match FBP System fuel type for each fire, and the weather indices from interpolated surfaces (Nadeem et al., 2019). The differences between the rate of spread in the oblique photos and the predicted spread ranged between 1.0 to 6.10 m/min with a % difference RMSE of 4.258 (Table 3.6). For Site 2, the calculations were repeated using an initially unidentified spot fire (see below), which reduced the fire spread distance considerably, improving the fit between observed and predicted HROS. Details are provided in the Appendix A.

Table 3.6. The observed and FBP System predicted fire spread rates for the fire behaviour parameters from the georeferenced wildfire imagery. HROSp and HROSO refer to predicted and observed rate of spread. See the Appendix A for FBP System calculation details.

Fire Obs. #	FBP Fuel Type	$HROS_p$ (m/min)	$HROS_o$ (m/min)	Difference (m/min)	Difference (%)
1	C-2, C-3	5.80	4.78	+1.02	21.33
2	C-7	4.10	10.20	-6.10	-59.80[a]
3	O1-b	22.0	27.28	-5.28	-19.35
4	C-7 (O1-b)	3.10	5.17	-2.07	-40.03
5	C-7	9.20	4.70	+4.50	+95.74

Notes: [a] Recalculated using spot fire start position, resulting in $HROS_o$ of 4.8 m/min, absolute difference of -0.74m and relative difference of -15.29%; see Appendix A for details.

At Site 3, retardant lines (visible in Figure 3.5B) were clearly effective at stopping fire spread along the most active portion of the head. The resultant spread between A and B images was due to the escape of a portion of the flank (green line in Figure 3.6A).

Additional fire behaviour characteristics can sometimes be observed in these images and offer opportunities for measurement and documentation. The depth of the flaming front, for example, is often visible in non-forested fire images (e.g., Figure 3.6, image 3B). Figure 3.9 shows the flame front depth ranging from 4.76 m to 21.47 m. The flame residence time (Wotton et al., 2012) can also be calculated as the quotient of the flame front depth and HROS; for the

latter example with a 27.28 m/min spread rate, this was approximately 47 s using the average maximum fire front depth measurements from both images.

Many fires also exhibit short- or medium-range spotting (ember lofting; Werth et al., 2016), which can also potentially be studied using monoplotting. For Site 2, we identified the development of a secondary head caused by downwind spotting (Figure 3.10A) and measured the minimum spotting distance, assuming instantaneous ignition (298 m; Figure 3.10B). See also the Appendix A for a recalculation of HROS based on the spot fire positions.

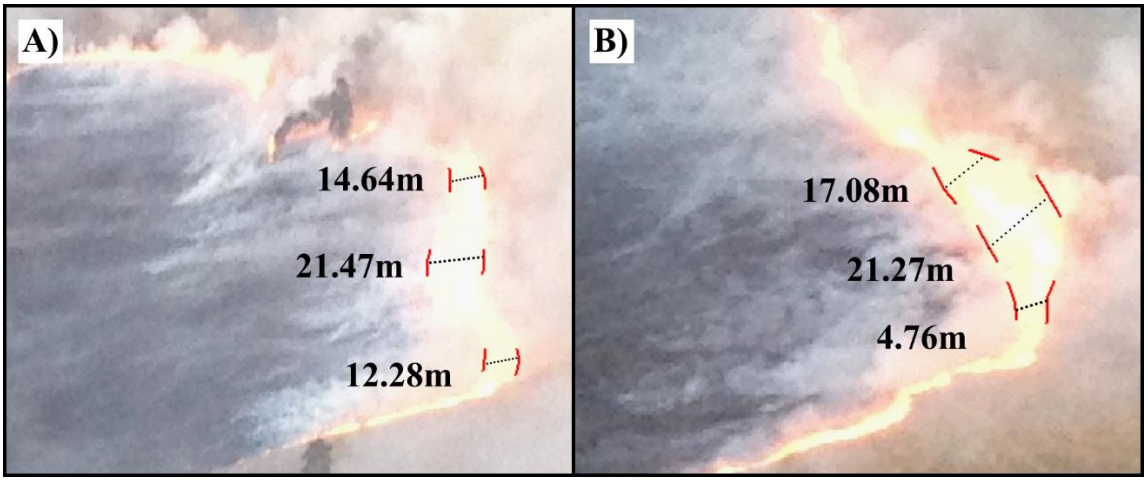

Figure 3.9. Two flaming fronts in image 3B, displaying measurable flaming front depths (red).

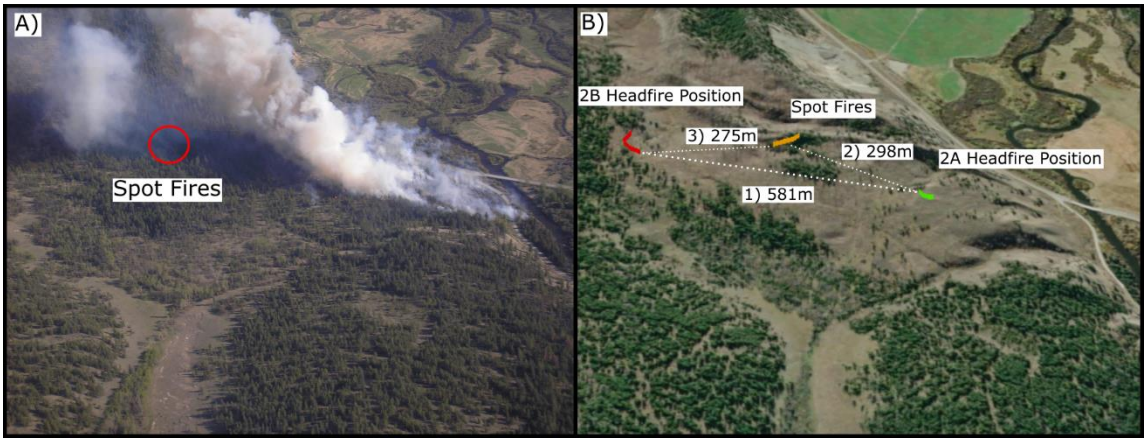

Figure 3.10. (A) Spot fires identified (red circle) on the Site 2 image at 18:16; (B) the headfire position at image 2A (green line), image 2B (red line) and the spot fire position (orange line); spread distances (1,3) and minimum spotting distance (2) are as indicated.

3.4 Discussion

The goal of this study was to evaluate the use of monoplotting to geolocate the fire front position and estimate fire spread rates using oblique aerial photographs of wildfires. While the potential uses for this process are numerous, our main intention is to provide real world observations for validating and improving existing fire behaviour models. We made novel use of the monoplotting software program MPT to georeference image pairs from five wildfires, extracted fire front positions, and calculated the spread rate of the fire runs. While the process is only semi-automated (i.e., GCPs are selected and the fire front position is manually identified by a human interpreter), the systematic nature of the method should yield relatively reproducible results between users. Although skill in matching GCPs in the obliques and orthophotos, and in locating the fire front position will likely vary between individual interpreters, the method also provides an estimate of the angular and positional error of the GCPs that are indicative of the accuracy of each observation. The quality of our wildfire images and resolution of our orthoimages and DEM yielded good results; in our examples the total max 3D error of the observations ranged from 0.770 to 2.989 m with spread distances of 200 to 846 m resulting in max HROS errors of approximately 0.21–0.54%, a very low degree of uncertainty for wildfire position data.

3.4.1 Factors Affecting MPT Accuracy

Previous research shows that the quality of the photographs, the angle of incidence of the camera and the resolution of the DEM and orthoimage used in the monoplotting process all influence the placement and precision of GCPs, and significantly affect the accuracy of a georeferenced image (Bozzini et al., 2012; Gabellieri & Watkins, 2019; Steiner, 2012; Stockdale et al., 2015). However, because these factors were very similar between our five sites, we were

not able to evaluate their influence in this wildfire application. Rather, we examined the influence of landscape features, fuel type, distance of camera to the fire front position, camera elevation above ground level and camera angle of incidence (Tables 3.2 and 3.4). Our analysis suggests that the camera angle of incidence (determined by the distance between the camera and the image centre, the camera elevation above ground and ground slope in the DEM) strongly influenced the accuracy of georeferencing among 10 images, which is consistent with earlier work (Conedera et al., 2018; Stockdale et al., 2015).

The visible landscape in all of our ten images provided sufficient GCP locations (5) for accurate georeferencing of the images. However, variation in the vegetation and landscape features in the images often influence the availability of GCPs. In our sites, open non-forested areas and areas of patchy forest in otherwise forested landscapes allowed for individual trees or shrubs to be identified in both the oblique images and orthoimages with a high degree of precision. The presence of built structures also provided precise GCPs, particularly building corners. It is apparent that heterogeneous landscapes will yield more precise GCPs than landscapes with continuous forest or grassland vegetation. Our tests on a range of fire photographs also suggested certain cases (not shown) where images were unsuitable or unreliable for analysis by monoplotting.

All wildfire images used in this study were taken from aircraft at moderate angles of incidence, which likely contributed to their level of accuracy (Table 3.4). This finding supports the relationship between angle of incidence and accuracy, because when the angle of incidence increases, the overall accuracy of the georeferenced image increases (Bozzini et al., 2012; Gabellieri & Watkins, 2019). The angle of incidence is dependent on the position of the camera and the DEM at which it intersects; therefore, the angle of incidence can be heavily influenced

by the terrain of the landscape present in the image, as well as the height and angle of obliquity of the camera when the image was taken. Due to this relationship, MPT works equally well in mountainous or flat areas, provided photographs are taken from a high vantage with a sufficiently oblique angle. For wildfire photography, this must be balanced with the obvious advantages of an unobstructed view of the flame front (see below). In our study, we observed that the mean 3D error increased as the angle of incidence decreased, but it is difficult to be certain that this had a significant impact on the accuracy of each image. Furthermore, the distance to fire front and elevation at which the wildfire images were captured in this study had varying influences on MPT accuracy. Relative to the other wildfire images, the camera closest to the fire front and at the lowest elevation above ground level resulted in the lowest mean 3D error out of all ten images. In general, the image resolution increased when the camera was closer to the fire front and at a lower elevation, which resulted in less pixelation while 'zooming in' on unique landscape features. This allowed the GCPs to be selected with greater precision, thus increasing the accuracy, a finding that is consistent with previous research (Stockdale et al., 2015). However, in some cases, within the limits of the resulting image resolution, images with clearly identifiable GCPs, favourable fire front locations and high incidence angles may reduce the impact of the distance and elevation on MPT errors.

A unique challenge associated with monoplotting wildfire imagery involves the obscuring effect of the smoke plume on the fire head. Note that some authors have proposed a broader definition of the head that includes perimeter segments below the maximum ROS, e.g., greater than 50% of maximum ROS, for fireline communication and safety purposes (Planas et al., 2011). Our focus, however, was on the single point of maximum fire intensity and ROS (in relatively homogenous fuels and topography). In very high angle (near-nadir) photographs, the

position of the fire's head is often partly or fully hidden; this can undermine much of the precision gained from the high angle, as estimating fire front position in these cases can be highly subjective. A camera angle of incidence near -45 degrees, aimed underneath the smoke plume appears to be a good compromise. However, the best camera angle of incidence and position for a given fire will depend on the fire and plume behaviour, and, on some fires (e.g., surface fires with very strong winds and smoke plumes attached to the ground), identifying an accurate frontal position from photographs will be difficult. Confidence can be increased when multiple photographs show the fire head from different vantage points within a short time span (few seconds to ~1–2 min). Future studies will explore the use of infrared sensors and machine learning approaches to assist with tracing the fire front and perimeter on oblique wildfire imagery. The final step in our exploratory analysis involved comparing spread rates estimated from the monoplotted fire position locations with FBP System predictions. Analyzing each fire run included best estimates of fire environment inputs given the available data. While the full details and sensitivity of these decisions are beyond the scope of this study, some details are provided in Appendix A. The error between predicted and observed spread rates in our fires ranged from 19% to 96%, which is not unusual for a small number of observations, particularly slower-spreading surface fires in conifer stands (Cheney et al., 2012). Interestingly, three out of five examples were in fuel complexes most similar to the C-7 fuel type ('Ponderosa pine—Douglas-fir'), a less well-documented type in the FBP System (FCFDG, 1992). Assuming a similar definition of HSD (i.e., the minimum Hausdorff distance between perimeters), differences between observed and predicted values can result from five sources: interpreter and methodological error in estimating the location of GCPs; interpreter error in observing or locating the true fire front position; unobserved processes such as spotting that occurs between

photographs; model error in the prediction system (e.g., due to uncertainty in the spread model); and error in weather and fuel moisture inputs, particularly the wind speed and direction at the fire location. Other studies have discussed these uncertainties (Cheney et al., 2012; Filkov et al., 2018; Gould et al., 2011), but they are not easily resolved post-hoc. It is not possible to have perfect knowledge of the condition of fuels and the state of the atmosphere affecting wildfire fronts. As we improve our techniques for measuring and characterizing the fire environment, so will we also improve our fire behaviour models, using methods such as those described here (Albini & Anderson, 1982; Finney, 2000).

3.4.2 Recommendations for Future Research and Application

Based on our experience with applying the monoplotting method to oblique aerial images of wildfires taken in the first few hours following an ignition, we recommend the following practices:

1. When selecting wildfire images for monoplotting, the fire front position must be visible or at least interpretable with a high degree of confidence and the visible landscape and resolution of the images must permit precise location of at least five GCPs. Monoplotting to determine the position of fire features will be most successful in heterogeneous landscapes. Accuracy may be higher in mountainous terrain.
2. The accuracy of georeferencing increases with the resolution of the available orthophotos and DEM as well as the distance from camera to ground and camera settings, which influence the pixel resolution. The monoplotting method will be more accurate in regions where orthophotos of half meter resolution and an underlying DEM of at least 25 m resolution are available (for very irregular terrain a DEM with higher resolution is recommended).

3. Images captured from close distance to the fire and at a lower elevation allow for more precise location of GCPs. However, this also reduces the field of view and may restrict the number of GCPs. We recommend a distance range between 650 and 2500 m, and an elevation range of 350 to 1050 m to yield angles of incidence from about -30 to -50º and a good field of view and perspective of the fire front. Ideally, the view of the flaming front is unobscured by the smoke plume, although it is not always possible. Bird dog aircraft attached to air tanker groups are often in this airspace and can provide a good platform for acquiring wildfire spread imagery.
4. Care must be taken in locating fire fronts in oblique photos with regard to the depth of visible flame, the shape of the fire front, the location of the smoke plume base and direction of smoke spread; this requires some training and experience. Complex fire spread patterns, particularly when fuels or terrain are highly heterogeneous or spotting is a significant factor, may be georeferenced using monoplotting, but will be much more difficult to relate to the fire environment. Such considerations are beyond the scope of this article.

Based on the success of this pilot study, we are currently expanding our research to obtain more wildfire spread observations from the historic database. Consideration should also be given to mounting dedicated cameras with overlapping IR sensors on operational aircraft that would capture imagery in a more systematic manner, such as georeferencing the standard image while extracting the fire front from the IR image. In addition, analysis of GIS tracking data on airtankers would provide insights into the field of view from the airtanker airspace (Clark & Martell, 2021).

With increasing severity and variability of wildfires, knowledge of wildfire behaviour has never been more important. Monoplotting of oblique air photos of wildfires, often acquired during the early stages of wildfire growth and response, can provide new and accurate fire spread observations to inform fire behaviour prediction or other aspects of wildland fire science.

Appendix A

The main data used to calculate HROS for conifer forests in the FBP System presented in Tables 3.6 and A1 include the following inputs: Fuel type, ISI, BUI and foliar moisture content; degree of curing is also included for the grass fuel type. ISI in turn is calculated and adjusted to represent the effect of slope relative to wind on spread based on the Fine Fuel Moisture Code (FFMC), wind speed and direction, slope and slope azimuth. We determined the fuel type at the fire locations from the BC provincial forest inventory layers (fuel structure and FBP fuel type; (Perrakis et al., 2018) and the slope and slope azimuth from the DEM. The daily FFMC and BUI were obtained from a dataset of FWI System station observations interpolated to fire locations using procedures in (Nadeem et al., 2019). Values interpolated from several weather stations were used because fires can be up to 50 km or more from the nearest station. However, we used the wind speed and direction observed at the nearest hour to the time of the photographs at the nearest BC Wildfire Service weather station and the interpolated daily FFMC to calculate ISI, which was then adjusted for slope effects. All calculations were completed using RedApp 6.2.4, a software developed by the RedApp Development Team in Canada (The Universal Fire Behaviour Calculator, 2021). We made a number of modifications to the general procedure to reflect local site conditions and data availability for Sites 1–3 as follows:

Site 1. The fuel type at this location consisted of subalpine conifer forest of Engelmann spruce and subalpine fir. Fire behaviour analysts in BC have observed that fire spread in these stands

tends to behave somewhere between the predictions of the C-3 and C-2 fuel types, thus we used the mean of the predicted HROS for C-2 and C-3.

Site 2. After completing the main analysis, we noted spot fires ~300 m from the main flame front that may have influenced the spread pattern between images; this would result in a much lower spread distance and HROS than originally predicted. Spotting to 300 m is close to the prediction (RedApp's implementation of Albini's model; Albini, 1983) of intermediate-range spotting distance of 340–360 m from a surface fire (assuming downwind cover height of 15–20 m and wind speed of 18.5 km/h). According to the Alexander and Cruz spotting separation distance model (Alexander & Cruz, 2006), ember transport distances of 46–89 m would be required to allow a new front to develop and spread that would not be overrun by the main flame front (Calculations assume an ignition delay (ID) of 1–10 min, acceleration coefficient (a_a) of 0.115, observed HROS (assuming fire spread from the spot fires) of 4.84 m/min and steady state buildup time (T_{ss}) of 30 min). Thus, we assume that the Site 2 spot fires would generate a new independent front, and so we used their position to estimate HROS. The spread rate based on the spot fire position (4.8 m/min) is much closer to the C-7 HROS prediction (4.1 m/min).

Site 3. This fire was less than 10 km and at a similar elevation to a nearby weather station; therefore, we used the hourly FFMC from that station rather than the interpolated daily FFMC.

We further note that the Site 4 fire spread through open grassland on the lower slope before spreading uphill into the very open Douglas-fir (C-7) stand. Although the analyzed fire run only encompasses the forested portion of the slope, the fire environment is complex, making estimation of FBP System inputs challenging. The fire environment includes a steep slope with changing aspect, heterogeneous fuels and a significant body of water directly below the slope (the Fraser River). Furthermore, nearby weather stations are more than 40 km away and show

different wind directions during the fire run. Considering these factors, the 40% discrepancy between predicted and observed HROS (Table 3.6) seems quite good. Alternative methods for estimating wind speed affecting fires could include use of the length to breadth ratio (Taylor & Alexander, 2018) or using terrain-influenced wind models (e.g., Forthofer et al., 2014), although these methods were not explored here.

Despite their importance, there are few validation studies of fire behaviour models. In particular, further evaluation of the C-7 fuel type may be merited, as this type is based on relatively few data points (FCFDG, 1992). Monoplotting can be useful in providing precise and unbiased estimates of the fireline position at different times. Estimating fire environment inputs is a necessary task in these efforts that can range from simple to complex depending on the circumstance.

Table A1. Fire environment inputs and predicted headfire rate of spread for five example fires. ISI_{sw} is the slope-wind adjusted ISI; and $HROS_p$ is the predicted rate of spread.

Site #	FFMC	Wind Speed (km/h)	Wind Observation (LST)	Distance (km)	Slope, Azimuth	ISI_{sw}	BUI	Fuel Type	$HROS_p$
1	89.0	14.5	1500	23	< 5%	7.7	57	C-2, C-3 [a]	5.8
2	91.0	18.5	1900	28	< 5%	12.6	42	C-7	4.1 [b]
3	93.6 [c]	1.8 [d]	1900	9	< 5%	7.9	-	O-1b	22.0
4	94.0	7.7 [e]	1500	46	32%, 215 [e]	10.0	94	C-7 (O-1b) [e]	3.1
5	95.0	16.1	1400-1500 [f]	25	< 5%	19.5	146	C-7	9.2

Notes: [a] Used 'dual-fuel' concept; ROS_P is calculated from 50% of each C-2, C-3 (9.0 m/min, 2.6 m/min); [b] Using spot fire location as a starting point; see text for details; [c] Weather station was <10 km from fire and in the same valley; therefore, station hFFMC was used; [d] Smoke plume characteristics suggest higher wind speed at the fire than at the station; [e] Variable wind speed and direction, aspect, wind-slope vectoring and heterogeneous fuel type; ROS_p was based on a single wind speed and direction (3º) and single fuel type (C-7); [f] Wind speed used was average of 1400 and 1500 (LST) readings.

References

Albini, F. A. (1983). Potential Spotting Distance from Wind-Driven Surface Fires (Research Paper INT-309). United States Department of Agriculture, Forest Service, Intermountain Forest and Range Experiment Station: Ogden, Utah, USA. https://www.frames.gov/documents/behaveplus/publications/Albini_1983_INT-RP-309_ocr.pdf

Albini, F. A., & Anderson, E. B. (1982). Predicting fire behavior in US Mediterranean ecosystems (General Technical Report PSW-GTR-58). In Proceedings of the Symposium on Dynamics and Management of Mediterranean-type Ecosystems, June 1981, San Diego, California. Pacific Southwest Forest and Range Experiment Station, Forest Service, U.S. Department of Agriculture. https://www.fs.usda.gov/treesearch/pubs/45222

Alexander, M. E., & Thomas, D. A. (2003). Wildland fire behavior case studies and analyses: value, approaches, and practical uses. *Fire Management Today*, *63*(3), 4–8.

Alexander, M.E., Stocks, B. J., & Lawson, B. D. (1991). Fire behavior in black spruce-lichen woodland: the Porter Lake project (Information Report NOR-X-310). Forestry Canada, Northwest Region, Northern Forestry Centre: Edmonton, Alberta, Canada. https://cfs.nrcan.gc.ca/pubwarehouse/pdfs/11563.pdf

Alexander, Martin E., & Cruz, M. G. (2006). Evaluating a model for predicting active crown fire rate of spread using wildfire observations. *Canadian Journal of Forest Research*, *36*(11), 3015–3028. https://doi.org/10.1139/X06-174

Alexander, Martin E., & Cruz, M. G. (2013). Are the applications of wildland fire behaviour models getting ahead of their evaluation again? *Environmental Modelling and Software*, *41*, 65–71. https://doi.org/10.1016/j.envsoft.2012.11.001

Allison, R. S., Johnston, J. M., Craig, G., & Jennings, S. (2016). Airborne optical and thermal remote sensing for wildfire detection and monitoring. *Sensors*, *16*(8), 1310. https://doi.org/10.3390/s16081310

BC Data Catalogue. (2022). *VRI Data*. Available online: https://catalogue.data.gov.bc.ca/dataset/vri-historical-vegetation-resource-inventory-2002-2019- (accessed 15 March 2022)

BC Wildfire Service. (2020). *2017 Wildfire Season*. Available online: https://www2.gov.bc.ca/gov/content/safety/wildfire-status/about-bcws/wildfire-history/wildfire-season-summary (accessed 15 March 2022)

Bozzini, C., Conedera, M., & Krebs, P. (2012). A New Monoplotting Tool to Extract Georeferenced Vector Data and Orthorectified Raster Data from Oblique Non-Metric Photographs. *International Journal of Heritage in the Digital Era*, *1*(3), 499–518. https://doi.org/10.1260/2047-4970.1.3.499

Bozzini, Claudio. (2018). *WSL Monoplotting Tool: User Manual*. Swiss Federal Research Institute WSL. Available Online: https://www.wsl.ch/fileadmin/user_upload/WSL/Services_Produkte/Software_Apps/Monoplotting/MPT_-_2.0_-_User_manual_-_E.pdf (accessed 15 March 2022).

Cheney, N., & Gould, J. (1995). Fire Growth in Grassland Fuels. *International Journal of Wildland Fire*, *5*(4), 237–247. https://doi.org/10.1071/WF9950237

Cheney, N. P., Gould, J. S., McCaw, W. L., & Anderson, W. R. (2012). Predicting fire behaviour in dry eucalypt forest in southern Australia. *Forest Ecology and Management*, *280*, 120–131. https://doi.org/10.1016/j.foreco.2012.06.012

Clark, N. A., & Martell, D. L. (2021). The use of aircraft tracking GPS data to develop models of the use of airtankers in forest fire management. *INFOR*, *57*(4), 535–562. https://doi.org/10.1080/03155986.2019.1706398

Conedera, M., Bozzini, C., Ryter, U., Bertschinger, T., & Krebs, P. (2018). Using the Monoplotting Technique for Documenting and Analyzing Natural Hazard Events. *Natural Hazards - Risk Assessment and Vulnerability Reduction*. IntechOpen. https://doi.org/10.5772/intechopen.77321

ESRI. (2020). *ESRI World Imagery (For Export).* Available online: https://www.arcgis.com/home/item.html?id=226d23f076da478bba4589e7eae95952 (accessed 15 March 2022).

Forestry Canada Fire Danger Group. (1992). Development and structure of the Canadian Forest Fire Behavior Prediction System (Information Report ST-X-3). Forestry Canada, Science and Sustainable Development Directorate: Ottawa, Ontario, Canada. https://cfs.nrcan.gc.ca/publications?id=10068

Filkov, A., Duff, T., & Penman, T. (2018). Improving Fire Behaviour Data Obtained from Wildfires. *Forests*, *9*(2), 81. https://doi.org/10.3390/f9020081

Finney, M. A. (2000). Efforts at Comparing Simulated and Observed Fire Growth Patterns (Final Report INT-95066-RJVA). USDA Forest Service, Rocky Mountain Research Station, Fire Science Laboratory: Fort Collins, Colorado, USA. https://www.firelab.org/sites/default/files/2021-05/Finney_2000_FarsiteValidation_FinalReport.pdf

Forthofer, J. M., Butler, B. W., & Wagenbrenner, N. S. (2014). A comparison of three approaches for simulating fine-scale surface winds in support of wildland fire management. Part I. Model formulation and comparison against measurements. *International Journal of Wildland Fire*, *23*(7), 969–981. https://doi.org/10.1071/WF12089

Gabellieri, N., & Watkins, C. (2019). Measuring long-term landscape change using historical photographs and the WSL Monoplotting Tool. *Landscape History*, *40*(1), 93–109. https://doi.org/10.1080/01433768.2019.1600946

Gould, J., McCaw, M., Cruz, M. ., & Anderson, W. (2011). How good are fire behaviour models? Validation of eucalypt forest fire spread model (unpublished conference paper). Wildfire 2011, the 5th International Wildland Fire Conference, Sun City, South Africa.

Hirsch, K. . (1996). Canadian Forest Fire Behavior Prediction (FBP) System: User's Guide (Special Report 7). Natural Resources Canada, Canadian Forest Service, Northwest Region, Northern Forestry Centre: Edmonton, Alberta, Canada. https://www.frames.gov/documents/catalog/hirsch_1996.pdf

Johnston, L. M., Wang, X., Erni, S., Taylor, S. W., McFayden, C. B., Oliver, J. A., Stockdale, C., Christianson, A., Boulanger, Y., Gauthier, S., Arseneault, D., Wotton, B. M., Parisien, M. A., & Flannigan, M. D. (2020). Wildland fire risk research in Canada. *Environmental Reviews*, *28*(2), 164–186. https://doi.org/10.1139/er-2019-0046

Makarovic, B. (1973). Digital Monoplotters. *The ITC Journal*, *4*, 583–600.

Monoplotting Tool. (2021). *Monoplotting Tool*. Available online: https://www.wsl.ch/monoplotting (accessed 15 March 2020).

Moriarty, K., Cheng, A. S., Hoffman, C. M., Cottrell, S. P., & Alexander, M. E. (2019). Firefighter Observations of "Surprising" Fire Behavior in Mountain Pine Beetle-Attacked Lodgepole Pine Forests. *Fire*, *2*(2), 34. https://doi.org/10.3390/fire2020034

Nadeem, K., Taylor, S. W., Woolford, D. G., & Dean, C. B. (2019). Mesoscale spatiotemporal predictive models of daily human- and lightning-caused wildland fire occurrence in British Columbia. *International Journal of Wildland Fire*, *29*(1), 11–27. https://doi.org/10.1071/WF19058

Parisien, M.-A., Dawe, D. A., Miller, C., Stockdale, C. A., & Armitage, O. B. (2019). Applications of simulation-based burn probability modelling: a review. *International Journal of Wildland Fire*, *28*(12), 913. https://doi.org/10.1071/WF19069

Perrakis, D. B., Eade, G., & Hicks, D. (2018). British Columbia Wildfire Fuel Typing and Fuel Type Layer Description (Information Report BC-X-444). Natural Resources Canada, Canadian Forest Service. Pacific Forestry Centre: Victoria, British Columbia, Canada. https://cfs.nrcan.gc.ca/publications?id=39432

Perrakis, D. B., Lanoville, R. A., Taylor, S. W., & Hicks, D. (2014). Modeling wildfire spread in mountain pine beetle-affected forest stands, British Columbia, Canada. *Fire Ecology*, *10*(2), 10–35. https://doi.org/10.4996/fireecology.1002010

Planas, E., Cubells, M., & Pastor, E. (2011). Different approaches for the head fire perimeter definition in wildland fires. *Fire Safety Science*, *10*, 1425–1435. https://doi.org/10.3801/IAFSS.FSS.10-1425

Plucinski, M. P., Sullivan, A. L., Rucinski, C. J., & Prakash, M. (2017). Improving the reliability and utility of operational bushfire behaviour predictions in Australian vegetation. *Environmental Modelling and Software*, *91*, 1–12. https://doi.org/10.1016/j.envsoft.2017.01.019

Schenk, T. (2005). *Introduction to Photogrammetry*. Department of Civil and Environmental Engineering and Geodetic Science, The Ohio State University: Columbus, Ohio, USA, 59-61.

Steiner, L. (2012). *Reconstruction of Glacier States from Geo-Referenced, Historical Postcards*. Master's Thesis, Institut für Kartographie und Geoinformatik: Hannover, Germany.

Stockdale, C. A., Bozzini, C., Macdonald, S. E., & Higgs, E. (2015). Extracting ecological information from oblique angle terrestrial landscape photographs: Performance evaluation of the WSL Monoplotting Tool. *Applied Geography, 63*, 315–325. https://doi.org/10.1016/j.apgeog.2015.07.012

Stocks, B. J. (1989). Fire behavior in mature jack pine. *Canadian Journal of Forest Research, 19*(6), 783-790. https://doi.org/10.1139/x89-119

Sullivan, A. L. (2009). Wildland surface fire spread modelling, 1990 - 2007. 2: Empirical and quasi-empirical models. *International Journal of Wildland Fire, 18*(4), 369-386. https://doi.org/10.1071/wf06142

Taylor, S. W., & Alexander, M. E. (2018). *Field guide to the Canadian Forest Fire Behavior Prediction (FBP) System.* 3rd edition. Northern Forestry Centre, Canadian Forest Service.

Taylor, S. W., Woolford, D. G., Dean, C. B., & Martell, D. L. (2013). Wildfire Prediction to Inform Fire Management: Statistical Science Challenges. *Statistical Science*, *28*(4), 586–615. https://doi.org/10.1214/13-STS451

The Universal Fire Behaviour Calculator. (2021). *The Universal Fire Behaviour Calculator*. Available online: https://redapp.org/ (accessed 15 March 2020).

Van Wagner, C. E. (1969). A simple fire-growth model. *Forestry Chronicle, 45*, 103-104. https://doi.org/10.5558/tfc45103-2

Van Wagner, C. E. (1987). Development and structure of the Canadian forest fire weather index system (Forestry Technical Report 35). Natural Resources Canada, Canadian Forest Service: Ottawa, Ontario, Canada https://cfs.nrcan.gc.ca/pubwarehouse/pdfs/19927.pdf

Weber, R. O. (1989). Analytical models for fire spread due to radiation. *Combustion and Flame, 78*(3–4), 398–408. https://doi.org/10.1016/0010-2180(89)90027-8

Werth, P. A., Potter, B. E., Alexander, M. E., Clements, C. B., Cruz, M. G., Finney, M. A., Forthofer, J. M., Goodrick, S. L., Hoffman, C., Jolly, W. M., McAllister, S. S., Ottmar, R. D., & Parsons, R. A. (2016). Synthesis of knowledge of extreme fire behavior: volume 2 for fire behavior specialists, researchers, and meteorologists (General Technical Report PNW-GTR-891). U.S. Department of Agriculture, Forest Service, Pacific Northwest Research Station: Portland, Oregon, USA. https://doi.org/10.2737/PNW-GTR-891

Wotton, B. Mike, Gould, J. S., McCaw, W. L., Cheney, N. P., & Taylor, S. W. (2012). Flame temperature and residence time of fires in dry eucalypt forest. *International Journal of Wildland Fire, 21*(3), 270–281. https://doi.org/10.1071/WF10127

Wotton, B. M., Alexander, M. E., & Taylor, S. W. (2009). Updates and revisions to the 1992 Canadian Forest Fire Behavior Prediction System (Information Report GLC-X-10). Natural Resources Canada, Canadian Forest Service, Great Lakes Forestry Centre: Sault Ste. Marie, Ontario, Canada. https://cfs.nrcan.gc.ca/pubwarehouse/pdfs/31414.pdf

Chapter 4: Empirical Wildfire Spread Analysis in Grey-Attack Mountain Pine Beetle-Affected Forest Stands

4.1 Introduction

Ecological disturbances such as insect outbreaks and wildfire are primary factors shaping forest ecosystems in Western North America (Hessburg et al., 2019; Jenkins et al., 2014; Schoennagel et al., 2017). Insect outbreaks, particularly those related to bark beetles in the subfamily Scolytinae, are a fundamental process of forest landscape dynamics impacting forest composition, structure, and ecosystem function (Canelles et al., 2021). However, severe outbreaks can result in epidemic levels of tree mortality, loss in forest resiliency, and adverse consequences for biodiversity (Pureswaran et al., 2018). The increasing extent and frequency of bark beetle outbreaks in western North America in recent decades has resulted in significant declines in timber revenue, impacting both regional economies and local communities (Corbett et al., 2016; Saab et al., 2014). Over roughly the same time period, wildfire seasons have become more severe with many jurisdictions experiencing unprecedented levels of area burned, critical health risks due to declining air quality, and infrastructure loss. Furthermore, larger and more intense wildfires are challenging conventional forms of wildfire management, thus increasing risks to human life and property (Martin et al., 2016; McGee et al., 2015).

Understanding interactions between insect and wildfire disturbances is becoming increasingly important due to their complex relationship with global climate change (Jactel et al., 2019; Seidl et al., 2011; Xu et al., 2020). In British Columbia (BC), Canada, climate change is one of the most important drivers in the rise of forest disturbances in recent decades (Kirchmeier-Young et al., 2019; Woods et al., 2010). Bark beetle populations transition from

endemic to outbreak levels under conditions of drought and above-average temperatures that cause host trees to become stressed and overwinter beetle mortality to decline (Aukema et al., 2008). For example, the ongoing outbreak of mountain pine beetle (*Dendroctonus ponderosae*; MPB hereafter) in BC have reached unprecedented levels under warming conditions since the late 1990's, impacting more than 18 million hectares across the range of host species *Pinus contorta* (lodgepole pine) and *Pinus ponderosa* (ponderosa pine) in the province (BC Ministry of Forests Lands & Natural Resource Operations, 2022) . Similarly, warming temperatures and summer drought conditions have resulted in decreased soil and fuel moisture in the US Pacific Northwest, thus increasing the likelihood of ignition and length of fire seasons, contributing to an increase in the extent and frequency of wildfires (Halofsky et al., 2020). In 2017 and 2018 for example, BC experienced back-to-back record fire seasons burning a combined 2.57 million hectares (BC Wildfire Service, 2020; Statistics Canada, 2019). The novel conditions created from the impacts of climate change and the unprecedented disturbance events that follow constrain the ability to utilize existing approaches for modelling how future events will unfold. Complicating this further is that the influence of one disturbance agent on another is likely to increase as scale of such events intensifies. Of particular importance is how MPB-impacted forests influence wildfire behaviour.

Previous research has shown that time since MPB attack alters the fuel conditions of forest stands and may affect future fire risk and behaviour (Dhar et al., 2016). For example, a previous study (Jolly et al., 2012) determined that the foliar moisture content, i.e. the moisture content of live needles in the canopy, drops from greater than 100% in healthy green trees to ~12% in red-attack (1 to 3 years since MPB). The foliar moisture content of a forest stand can affect the ability of wildfire to transition to crowning (Van Wagner, 1977) and has serious

implications in terms of wildfire management as crown fires have the ability to become much more intense and difficult to control. A review study (Jenkins et al., 2014) describes how needles drop off during the final grey-attack stage (greater than 4 years since MPB), reducing the canopy fuels while increasing the forest floor fuels, wind speed, and drying of surface fuels. Although this results in a reduction of canopy fuel load, the resulting increase to the surface fuel complex and wind speed are theorized to increase the surface fire spread rate, flame height, and potential transition to crown fire (Jenkins et al., 2012). Similarly, previous research conducting interviews with fire fighters provides alternative evidence that MPB-impacted stands experience faster fire spread rates, increased intensity and spotting, and faster surface to crown fire transitions than non-MPB-affected stands (Moriarty et al., 2019).

However, there are known gaps in the knowledge of the effect of MPB on fire behaviour (Coogan et al., 2019; Johnston et al., 2020), with several studies attempting to model the effects of MPB having been subject to uncertain and contradictory results (as per Dhar et al., 2016; Stephens et al., 2018). In addition, there are limited studies using empirical evidence (as per Meigs et al., 2015; Moriarty et al., 2019) largely due to the difficulty of collecting observational wildfire data (Hart & Preston, 2020). Yet, empirical data are necessary for providing rare real world measurements on MPB-affected stands and further developing existing or new empirical models (Hoffman et al., 2015; Perrakis et al., 2014).

One of the initial studies showing empirical evidence of fire behaviour in recently MPB-affected forest stands in British Columbia, Canada was provided by Perrakis et al. (2014). They extracted empirical fire behaviour data from aerial wildfire photographs and utilized the Canadian Forest Fire Danger Rating System (CFFDRS) empirical approach to develop a new headfire rate of spread (ROS) model for recently attacked (1-5 years) MPB-affected forest stands

from 2004 to 2010. In Canada, the CFFDRS is the primary system that forecasts wildfire conditions, evaluates the risk of wildfires, and predicts fire behaviour based on outputs from two subsystems: the Fire Weather Index (FWI) and Fire Behaviour Prediction (FBP) System (Stocks et al., 1989). The first subsystem, the FWI, relies on daily weather observations (i.e. temperature, relative humidity, wind speed, and precipitation) taken at 1200 Local Standard Time (LST) to provide FWI indices representing daily fire potential ratings for different regions. The second subsystem, the FBP, assesses fire behaviour characteristics, i.e. headfire rate of spread (ROS), for various wildfire scenarios with consideration of the fuel type, topography, and weather (Hirsch, 1996). In their study, Perrakis et al. determined that the observed ROS of 16 MPB-affected fire sites burned on average 2.7 times faster than the predicted ROS of unaffected pine forests. This study provided evidence of increased headfire ROS in recently MPB-affected pine stands and developed ROS models to reduce the uncertainty associated with fire behaviour in MPB-affected pine stands. For wildfire management, accurate ROS models are essential to making safe and efficient wildfire suppression decisions (Plucinski et al., 2017). However, in BC the prevalence of red-attack stage stands has significantly declined since the epidemic outbreak peak in 2005 when approximately 140 million cubic meters of forests was impacted (BC FLNRO, 2022). Most affected stands have now lost their red needles and entered the grey attack stage consisting of standing beetle-killed trees with no foliage, some loss of small branches, and potential loss of significant crown mass (Schoennagel et al., 2012). In the context of wildfire, forests in the grey attack stage are expected to have less available crown fuel and greater spacing between tree crowns than in the red attack stage, thus decreasing the probability of active crown fire. However, the transition from red to grey-attack forests increases the quantity and drying of surface fuel loads, and increases the wind speed as a result of a more open canopy promoting

faster surface spread rates (Hicke et al., 2012). Nevertheless, research that analyzes the impacts of grey attack on wildfire behaviour, notably case studies or other field evidence of headfire ROS, is limited. Empirically-based fire behaviour observations of grey-attack stage forest stands are needed given the increase in size, severity, and frequency of wildfires in recent years. The expansion of knowledge on fire behaviour in grey-attack forest stands will further advance wildfire management strategies, preparedness, and prediction systems.

Therefore, the objective of this study is to estimate the headfire ROS in several forest sites across BC that were in the grey attack stage when a recent wildfire event took place. Using oblique photographs of wildfire events, I identified a set of fires that took place in grey-attack forest stands in 2017 and 2018 and employed a mono-photogrammetric approach (Hart et al., 2021) to estimate the headfire front positions at two time periods during each fire, which allowed for calculating the observed ROS. I compared these results to ROS estimates from the Canadian FBP System using the C-3 fuel type, which represents the fuel structure of healthy green pine stands. The results from this comparison quantified the effects of grey-attack stage dead trees on the spread rate of wildfires in BC. Furthermore, I analyzed if differences in the observed versus predicted ROS were related to MPB attributes such as the severity of MPB attack, the number of years since peak MPB-outbreak, stand percentage of lodgepole pine, and stand percentage of dead trees. In addition, I analyzed the effects of site-specific forest conditions on the differences in observed and predicted ROS, namely, the forest crown closure percentage, forest stand heights, and tree age. The intent of this study was to help fire management personnel and researchers better understand and predict fire behaviour in grey-attack MPB-affected forest stands.

4.2 Materials and Methods

4.2.1 Study Area and Data

The study area for this research consisted of ten MPB-affected wildfire sites across the province of British Columbia (BC), Canada (Figure 4.1).

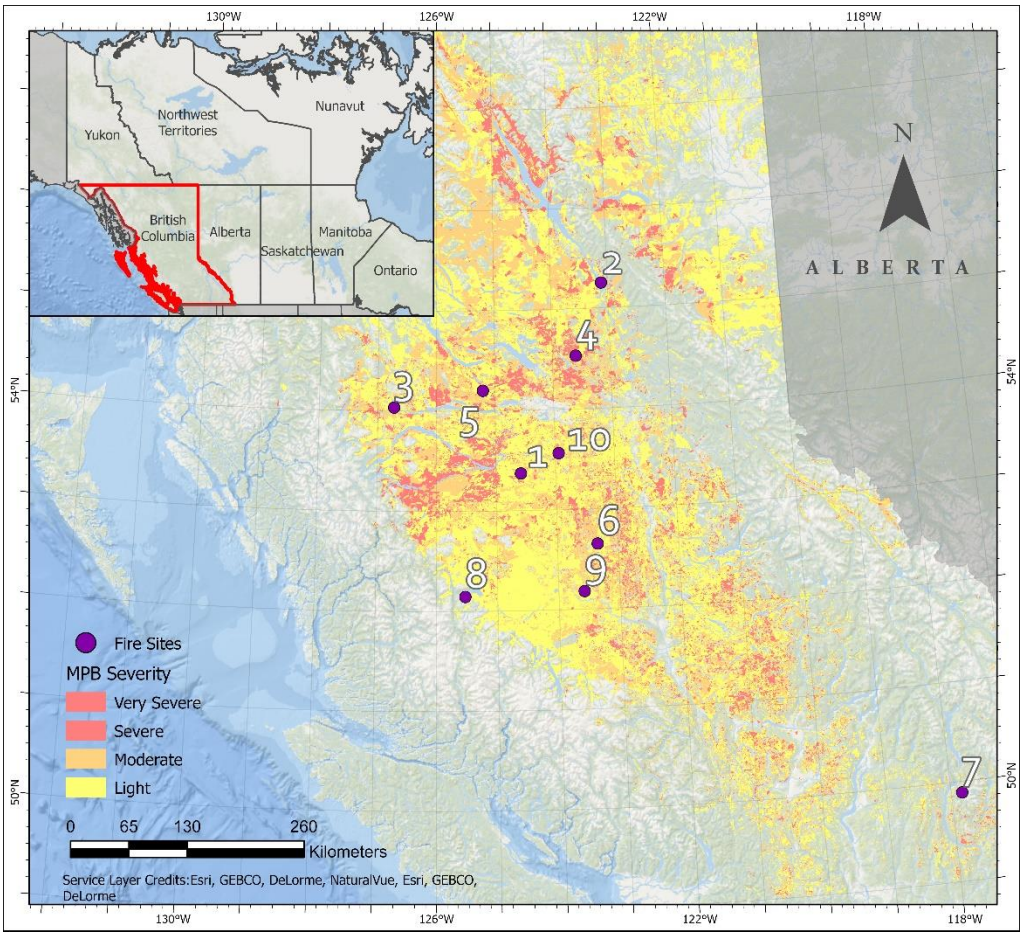

Figure 4.1. Study area map displaying the location of the numbered fire sites, coded 1-10, used in this study across British Columbia, Canada. Coloured shading represents MPB severity levels as indicated (BC Data Catalogue, 2022b).

The selected wildfire sites and their respective photographs contain MPB-affected forest stands in the grey-attack stage and represent a variety of ecological characteristics across a range of elevations, slopes, and BEC (biogeoclimatic) zones (Figure A1, A2, and A3; Table 4.1). The aerial wildfire photographs were selected from the BC Wildfire Service (BCWS) image archive,

courtesy of the Ministry of Forests, Lands, Natural Resource Operations and Rural Development (FLNRORD), containing 668 wildfires and 8,750 timestamped photographs across BC over the 2017 and 2018 fire seasons. The BCWS air attack officers capture aerial wildfire photographs during air tanker operations or reconnaissance missions over active wildfires. I validated the MPB-status of each wildfire site using MPB pest outbreak datasets from the BC Data Catalogue (BC Data Catalogue, 2022b). I further validated the MPB-status by confirming the forest stand composition of each Site using the Vegetative Resource Inventory (VRI) dataset (BC Data Catalogue, 2022c).

Table 4.1. The ecological characteristics of each site, including elevation, slope, BEC zone, and subzone.

Site #	Elevation (m)	Slope (%)	BEC Zone[a]	BEC Subzone[b]
1	1365	27.8	ESSF	mv
2	685	2.7	SBS	mk
3A	828	3.4	SBS	dk
3B	828	4.6	SBS	dk
4	810	0.4	SBS	mk
5	829	26.9	SBS	dw
6	1252	2.8	MS	xv
7	1682	38.7	ESSF	wc
8	1348	2.2	MS	xv
9	1172	4.9	IDF	dk
10	922	1.4	SBS	dw

Notes: [a] Acronyms designate BEC Zones: ESSF = Engelmann Spruce – Subapline Fir; IDF = Interior Douglas-fir; MS = Montane Spruce; SBS = Sub-Boreal – Spruce.
[b] Acronyms designate BEC Subzones: dk = Dry Cool; dw = Dry Warm; mk = Moist Cool; mv = Moist Very Cold; wc = Wet Cold; xv = Very Dry Very Cold.

Extracting the observed ROS using MPT required a digital elevation model (DEM) and orthoimagery. I used a 25 m DEM from the British Columbia Data Catalogue and orthoimages under 0.5 m resolution from the ESRI World Imagery Layer (BC Data Catalogue, 2022a; ESRI, 2020). To determine the predicted ROS of each site, I required the initial fire season starting FWI codes and the daily fire weather data from the start of the fire season to the wildfire date (temperature, wind speed, precipitation, and relative humidity). The FLNRO-WMB weather

station closest to each fire was manually identified and the BC Wildfire Service provided the station startup codes; daily weather data (1200 LST) was extracted from the Pacific Climate Impacts Consortium (PCIC) data portal (Pacific Climate Impacts Consortium, 2022).

Data was also required to analyze if the difference between observed and predicted ROS were related to site specific MPB or forest stand attributes. For the MPB analysis I acquired data on the MPB severity rating at the peak of the attack at each location, time since peak MPB-outbreak, and percentage of lodgepole pine and dead trees in the forest stand. The severity related factors were extracted from the aforementioned Pest Infestation dataset and the percentages of lodgepole pine and dead trees were extracted from the VRI layer. Forest stand attribute analysis factors including crown closure percentage, forest stand heights, and tree age were also extracted from the VRI dataset. Both the MPB and forest stand attributes involving the VRI dataset were extracted in the year prior to the associated wildfire year to ensure that the forest structure factors were representative of the forest stand at the time of the wildfire.

4.2.2 Defining Grey Attack Stands and Monoplotting Process

First I visually identified all wildfire sites in the 2017 and 2018 BCWS image archive that had areas or clusters of grey-attack MPB-affected forest stands (Figure 4.2). I then overlaid the spatial location of each site's headfire positions (start and end position) with the MPB and VRI data to confirm that the corresponding fuel complex was in fact in a grey-attack MPB-affected area dominated by a lodgepole pine forest stand.

Following the method described by Hart et al. (2021), I used MPT to georeference the wildfire photographs for extracting the headfire front positions. Essentially, the MPT software replicates the original extrinsic and intrinsic camera parameters that were used to capture the

wildfire photograph through the placement of Ground Control Points (GCP) in the wildfire photograph and respective orthoimage with associated DEM data. Specifically, MPT requires five GCPs, i.e. identifiable features such as building corners or other landscape features (Stockdale et al., 2015), that are visible in both the wildfire photograph and respective orthoimage (Bozzini, 2018). The resulting camera system places the wildfire photograph into the real world, where a ray originating from the simulated camera centre will pass through a pixel coordinate on the oblique photograph and intersect with the real world coordinate on the DEM. This provides each set of pixel coordinates in the wildfire photograph with corresponding world coordinates from the DEM, allowing for 3D spatial measurements and analysis. Once the wildfire photographs were georeferenced, I visually identified the headfire front positions in the photographs based on the smoke column and flame characteristics, and extracted the headfire front positions as individual shapefiles (Hart et al., 2021).

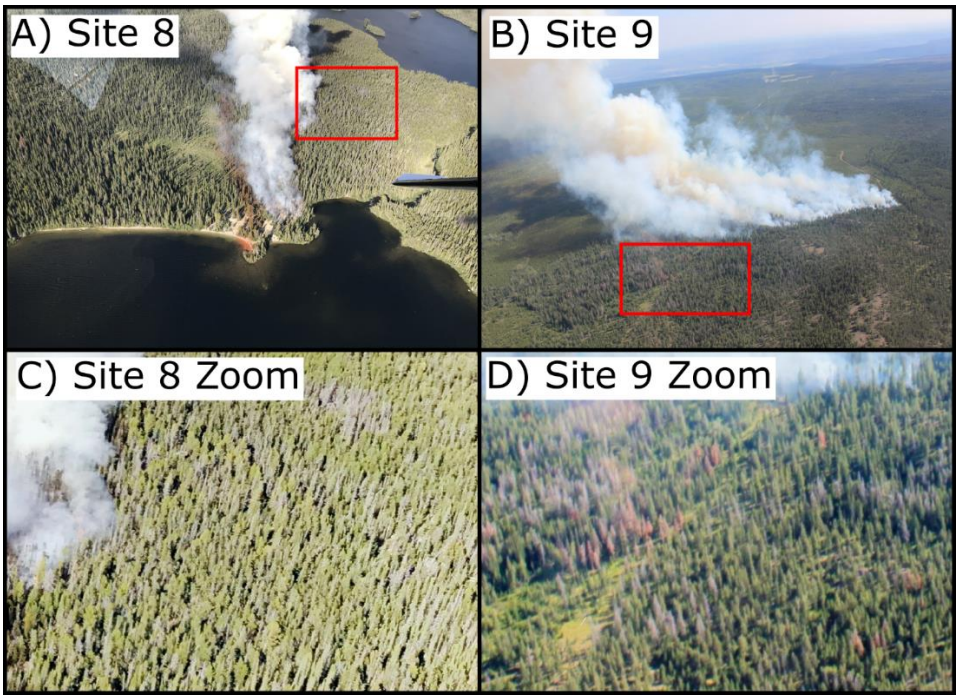

Figure 4.2. A/B) Areas of final stage grey-attack MPB identified in sites 8 and 9. C/D) MPB-affected areas (red square) zoomed in for easier observation.

I overlaid the extracted headfire front positions on the MPB dataset (i.e. polygon representations of MPB disturbance boundaries from 1907 – 2020) to determine the severity level and year of outbreak of each site. I considered sites with headfire front positions that overlapped MPB-affected areas (between 5 and 15 years since peak MPB-severity) to ensure the MPB-attack stage was grey-attack at the time of the wildfire. In addition, I ensured that the area burned of each site overlapped MPB-affected areas to ensure the entirety of the fire run was in MPB-affected forest stands.

The selected sites at this point underwent an additional analysis using the VRI dataset to quantify the proportion of lodgepole pine and MPB-caused mortality in each stand. Similar to the previous MPB validation, I overlaid the headfire front positions on the VRI polygons to determine the estimated forest stand composition and MPB disturbance history of each site. The VRI dataset provides polygon data representing surveyed areas with information such as forest stand composition and pest outbreak history. Sites 2, 3, 5, 6, and 8 were dominated by, i.e. greater than 63%, lodgepole pine (Figure 4.3A). In contrast, Sites 1, 4, 7, 9, and 10 had a lodgepole pine stand composition ranging from 46% to 53%, suggesting a more heterogeneous stand composition, dominated by two or more significant species. As mentioned previously, in addition to containing significant portions of lodgepole pine, the pine also had to contain significant grey-attack MPB impact. Sites 2, 3, 5, 6, and 10 had quantified proportions of MPB-caused pine mortality in the VRI attributes, estimated by VRI interpreters (Figure 4.3B). In contrast, Sites 1, 4, 7, 8, and 9, had missing data on the proportion of stands that were killed. In the latter, I manually estimated the proportion of dead trees based on the photographs.

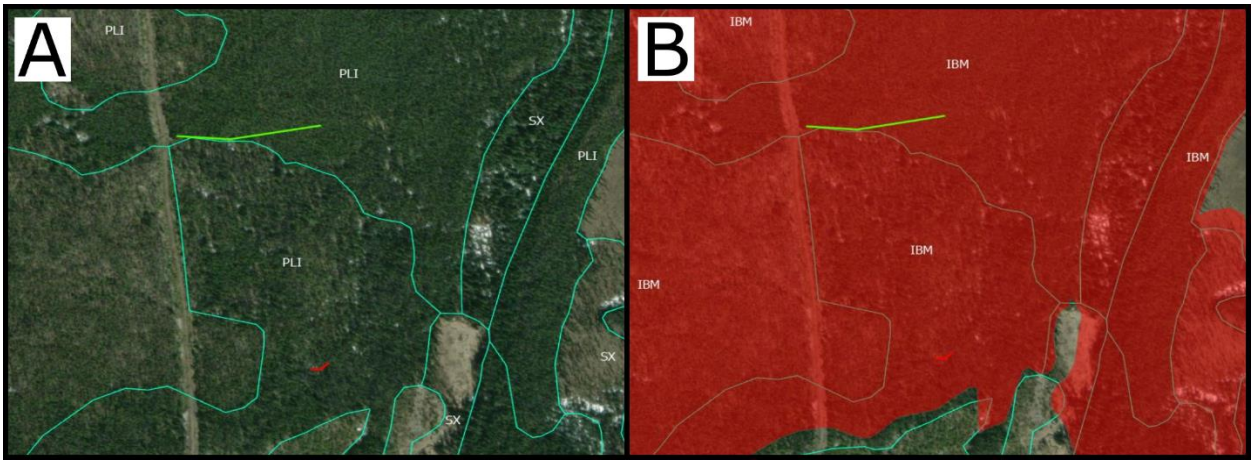

Figure 4.3. (A) The VRI dataset of Site 6 displaying 75% interior lodgepole pine forest stands (PLI). (B) The MPB dataset of Site 6 displaying a recorded MPB-outbreak (IBM) with a stand percentage dead of 57%.

Together, the wildfire photographs supported by the GIS analysis, using the MPB and VRI datasets, supported the informed decision that the ten selected fire sites contained grey-attack MPB-affected forest stands, a combination of lodgepole pine-dominated stands (greater than 63%), as well as pine-spruce and pine-fir (*Abies lasiocarpa*) mixed stands (lodgepole pine proportions 46 to 53%). Additionally, the MPB assessment provided the headfire front positions required for the following observed ROS calculation.

4.2.3 Observed and Predicted Headfire ROS Calculation

I estimated the observed ROS of each site using the headfire front positions extracted from MPT during the MPB assessment. As detailed by Hart et al. (2021), this process uses the distance between headfire front positions referred to here as the headfire spread distance (HSD) and timestamps (T1, T2) from both photographs to calculate the headfire rate of spread (HROS):

$$HROS = \frac{HSD}{(T2-T1)} \quad (1)$$

The predicted headfire ROS for the C-3 fuel type of each site was calculated using the FBP System, a subsystem of the CFFDRS. In the FBP System, predicted ROS values are calculated from empirical models related to weather conditions and fuel type. The FBP System uses FWI System codes and indices as inputs. These include the Fine Fuel Moisture Code (FFMC), an index representing the moisture content of the surface litter; the Buildup Index (BUI), an index associated with drought in organic forest floor layers; and the Initial Spread Index (ISI), which combines the FFMC and wind speed in an empirical function as a broad measure of initial expected rate of spread (Van Wagner, 1987). I identified the closest BCWS weather station for each fire site and obtained initial spring start up values, i.e. FFMC, Duff Moisture Code (DMC), and Drought Code (DC), for the given year from BCWS records (as per Lawson & Armitage, 2008). I calculated the FFMC and BUI of each site using the CFFDRS R Package (v1.8.18) with the associated historical daily weather taken at 1200 LST and start up values (Cantin et al., 2020). I extracted the wind speed and direction at the time of the respective wildfire photograph rounded to the nearest hour from the nearest BCWS weather station. The slope and aspect were determined from the DEM associated with each site. With respect to fuel type, I classified all sites as the C-3 (mature jack or lodgepole pine) fuel type which represents the fuel structure of healthy green jack and lodgepole pine stands, including stands with varying amounts (~0-30% of overstory density) of black spruce, white spruce and other conifers (e.g. Lawson, 1972; Stocks, 1989). The spread data behind the C-3 ROS function includes several decades of experimental burn and wildfire behaviour observations over a wide range of weather conditions (FCFDG, 1992). Fire behaviour in MPB-affected forest stands can therefore be compared with the C-3 fuel type predictions to demonstrate the effect of MPB on fire behaviour, such as ROS (Perrakis et al., 2014). After collecting all of the required fuel type and fire weather

data, I calculated the predicted ROS using RedApp (v6.2.4), the Universal Fire Behaviour Calculator support tool (Mcloughlin, 2016).

4.2.4 Spread Rate and Site Specific Attribute Analysis

I compared the observed ROS against FBP-predicted ROS at each site to identify (1) the differences between predicted and observed ROS, and (2) if differences in ROS were related to any potential MPB or stand structure attributes. For the latter, I performed regression analyses using the R package stats (v3.5.0) on the difference between the observed and predicted ROS to highlight how much variability in the FBP System C-3 ROS model predictions could be explained by potential stand structure factors. Variables tested included MPB severity rating, time since peak MPB-outbreak, stand percentage of lodgepole pine, stand percentage dead, crown closure percentage, forest stand height, and tree age (R Core Team, 2013). MPB-related variables were chosen to highlight the nature of influence of beetle-caused mortality on fire spread. With respect to the remaining factors, the crown closure represents the average percentage cover of the tree canopy in the forest stand, whereas the forest stand height and age represents the height and age of the forest stand, respectively. I chose these factors due to their function as important indicators of forest structure as well as their potential effect on fire behaviour in forest stands (Banerjee, 2020; Boulanger et al., 2017; Shang et al., 2020; Tao et al., 2016). For example, a lower crown closure percentage could increase the amount of solar radiation and in-stand wind of a forest stand, thus decreasing the moisture content of the surface fuels (Wotton & Beverly, 2007). Whereas stand height and age are potentially related to crown base height (CBH) and therefore crown fire initiation which can significantly affect ROS (Cruz et al., 2003; Rothermel, 1991).

4.3 Results

4.3.1 MPT Accuracy Assessment and MPB Status

I assessed the accuracy of the georeferenced oblique aerial wildfire photographs of the ten sites by analyzing the angle error and 3D error of each photograph as detailed in Hart et al. (2021). For all photographs, mean 3D error was less than 3m and mean angle error was less than 0.045º, values I considered to be reasonable given previously published guidance (Bozzini 2018; Hart et al., 2021; Stockdale et al., 2015; Table 4.2).

Table 4.2 MPT errors for each georeferenced wildfire photograph.

Image #	Aerial Photograph Time Stamp	Mean Angle Error (º)	Mean 3D Error (range, m)
1A	13:16	0.017	0.68 (0.35 - 0.94)
1B	13:51	0.022	0.49 (0.16 – 1.00)
2A	17:54	0.022	0.80 (0.19 - 1.73)
2B	20:02	0.044	1.30 (0.52 - 2.46)
3A	18:38	0.041	1.53 (0.63 - 2.36)
3B	19:07	0.018	1.17 (0.15 - 3.56)
3C	20:47	0.045	1.98 (0.52 - 3.81)
4A	17:45	0.010	0.90 (0.12 - 2.37)
4B	19:15	0.032	2.15 (0.30 - 3.76)
5A	13:45	0.017	0.84 (0.48 - 2.10)
5B	14:15	0.006	0.75 (0.44 - 1.07)
6A	15:40	0.021	1.90 (0.82 - 3.45)
6B	16:19	0.042	1.34 (0.92 - 1.67)
7A	15:52	0.015	0.74 (0.05 - 1.96)
7B	16:27	0.018	0.88 (0.28 - 1.51)
8A	17:55	0.014	1.20 (0.63 - 2.50)
8B	20:08	0.023	1.06 (0.46 - 2.41)
9A	16:13	0.044	1.30 (0.41 - 2.83)
9B	18:39	0.041	1.49 (0.73 - 1.88)
10A	18:18	0.036	1.26 (0.84 - 2.13)
10B	19:42	0.015	1.12 (0.90 - 1.42)

I used the headfire front positions from the georeferenced photographs to estimate the fire spread distance of each site. Spread distances and burning periods ranged from 130 m to 985 m,

and 29 minutes to 146 minutes, respectively, representing ROS values from 1.02 m/min to 11.72 m/min (Table 4.3). The range of max HROS error ranged from 0.36% to 3.21% across all sites.

Table 4.3 Fire behaviour characteristics extracted from the wildfire photographs included in the observed ROS calculations.

Site #	Fire Year	Fire Spread Distance (m)	Burning Period (min)	Max Total 3D Error (m)	Max HROS Error (%)	HROS (m/min)
1	2018	197.96	35	1.943	0.98	5.67
2	2018	130.74	128	4.192	3.21	1.02
3A	2017	236.69	29	5.919	2.50	8.16
3B	2017	370.29	100	7.363	1.99	3.70
4	2018	482.26	90	6.126	1.27	5.36
5	2018	335.19	30	3.170	0.95	11.17
6	2017	321.52	39	5.115	1.59	8.24
7	2017	144.6	35	3.470	2.40	4.13
8	2018	818.82	133	4.917	0.60	6.16
9	2018	506.47	146	4.713	0.93	3.47
10	2018	984.78	84	3.546	0.36	11.72

4.3.2 Fire Spread Distance and Spread Estimates

I calculated the predicted ROS for the C-3 fuel type using the FFMC, BUI, wind speed, slope and aspect at each site (Table 4.4), in order to compare with the observed ROS from the image analysis. The fire weather I used to calculate the variables was collected from weather stations within 40 km of the wildfire location. FFMC values ranged from 88.9 to 95.5, representing moderately dry to extremely dry forest fuel conditions in pine fuels (Beverly & Wotton, 2007). The BUI across all sites ranged from 11.6 to 127.5, suggesting relatively moist to extremely dry conditions in the forest floor. Wind speeds from nearest stations ranged from 4 km/hr to 11 km/hr, generally considered ‘light air’ to ‘light breeze’ conditions (Fogarty & Alexander, 1999). The highest ISI values, 10.2 and 10.3, were observed in Sites 1 and 5 respectively and can be attributed to high FFMC. The slope of Sites 1, 5, and 7 were larger than 5%, and thus slope and aspect are included in the respective ISI calculations, whereas the other

sites were flat (slope less than 5%) and not accounted for in the ISI calculations. The resulting C-3 ROS model predictions were all less than 6.14 m/min which is considered relatively low end as crown fires routinely spread at over 50 m/min (Alexander & Cruz, 2016; Stocks et al., 2004).

Table 4.4. Fire inputs and spread rate predictions for the 10 sites. ISIsw is the slope-wind adjusted ISI; and HROSp is the predicted rate of spread.

Site #	FFMC	BUI	Wind Speed (km/hr)	Wind Observation (LST)	Distance (km)	Slope, Aspect	ISI_{sw}	Fuel Type	$HROS_p$ (m/min)
1	95.5	117	6.8	1400	5	26.77%, 62	10.2	C-3	5.99
2	89.6	51.6	7.4[c]	1800-2000	8	< 5%	5.9	C-3	1.29
3A	91.3	62.4	4.4	1900	14	< 5%	6.5	C-3	1.72
3B	91.3	62.4	3.1[c]	1900-2000	14	< 5%	6.1	C-3	1.45
4	88.9	33.3	7.1[c]	1800-1900	39	< 5%	5.2	C-3	0.81
5	92.4	127.5	9.7	1400[a]	20	26.85, 185	10.3	C-3	6.14
6	92.8	60[b]	6	1600[a]	17	< 5%	8.6	C-3	3.47
7	92.3	48.3	10.3	1600[a]	28	38.73, 275	7.7	C-3	2.46
8	92.3	11.6	7.2[c]	1800-1900[a]	36	< 5%	8.5	C-3	3.78
9	91.5	60[b]	10.3[c]	1600-1800[a]	23	< 5%	8.9	C-3	3.80
10	92.9	86.3	4.4[c]	1800-1900[a]	23	< 5%	8.1	C-3	3.25

Notes: [a] Wind direction adjusted based on smoke column characteristics in the photographs.
[b] BUI adjusted based on conditions in the Cariboo region.
[c] The wind speed calculated as the average of the respective times shown (LST).

The observed HROS, extracted from the wildfire photographs, and predicted HROS calculated using the FBP System C-3 ROS model, are compared in Table 4.5. The majority of observed spread rates in this study indicated significantly faster fire spread than expected in healthy mature pine stands. The C-3 ROS model predictions for Sites 5, 6, 8, and 10 displayed significant differences in observed and predicted ROS, ranging from -38.64% to -72.27%, indicating faster spread rates than expected despite having ROS greater than 3.0 m/min (Table 4.5). The C-3 ROS model predictions for Site 1 and 9, which also had ROS greater than 3.0 m/min, were relatively close to the observed ROS with differences of +5.64% and +9.51%, respectively, indicating a close match with the C-3 ROS predictions. Meanwhile, although they had a ROS of less than 3.0 m/min, the C-3 ROS model predictions of Sites 3A, 3B, 4, and 7,

were significantly different than expected with respect to the observed ROS with percent differences ranging from -40.44% to -84.89%, further indicating faster than expected spread rates in the C-3 fuel type (Table 4.5). It was important to consider the difference in ROS as percentage as it provides detail regarding the FBP System C-3 ROS model predictions. For example, although the observed ROS of Site 4 and 5 were faster than the C-3 model predictions by 4.77 m/min and 5.03 m/min, their percentage difference was -84.89% and -45.03%, respectively, indicating a relatively faster observed ROS in Site 4 than in Site 5 with respect to the C-3 model predictions (Table 4.5). Furthermore, to yield how much higher (or lower) the ROS is in MPB-affected forest stand when compared against the predicted ROS in an unaffected C-3 fuel type forest stand, I calculated the relative change values between the observed and predicted ROS ranging from 79.07% to 661.73%.

Table 4.5 The observed and predicted spread rates from MPT and FBP System respectively. The HROSp represents the predicted spread rate and HROSo represented the observed ROS. The sites with faster observed ROS than predicted by the FBP C-3 model are highlighted in grey.

Site #	$HROS_p$ (m/min)	$HROS_o$ (m/min)	Difference (m/min)	Difference (%)	Relative ROS Change in MPB vs C-3 fuel type (%)
1	5.99	5.67	+0.32	+5.64	94.66
2	1.29	1.02	+0.27	+26.47	79.07
3A	1.72	8.16	-6.44	-78.92	474.42
3B	1.45	3.70	-2.25	-60.81	255.17
4	0.81	5.36	-4.55	-84.89	661.73
5	6.14	11.17	-5.03	-45.03	181.92
6	3.47	8.24	-4.77	-57.89	237.46
7	2.46	4.13	-1.67	-40.44	167.89
8	3.78	6.16	-2.38	-38.64	162.96
9	3.80	3.47	+0.33	+9.51	91.32
10	3.25	11.72	-8.47	-72.27	360.62

The observed and predicted ROS differences are further illustrated in in Figure 4.4, where eight out of eleven observations are left of the black line (representing a 1:1 correlation) and outside the grey dotted line (representing the +/- 25% confidence band), further indicating

faster fire spread than expected in healthy mature pine stands. Specifically, the observed ROS was 1.7 times faster than the FBP System C-3 model predictions when observing the linear trend of the observed and predicted ROS data (Figure 4.4). Considering the mean of the relative change in ROS between the predicted and observed, the observed ROS was 2.5 times faster than the FBP System C-3 model predictions.

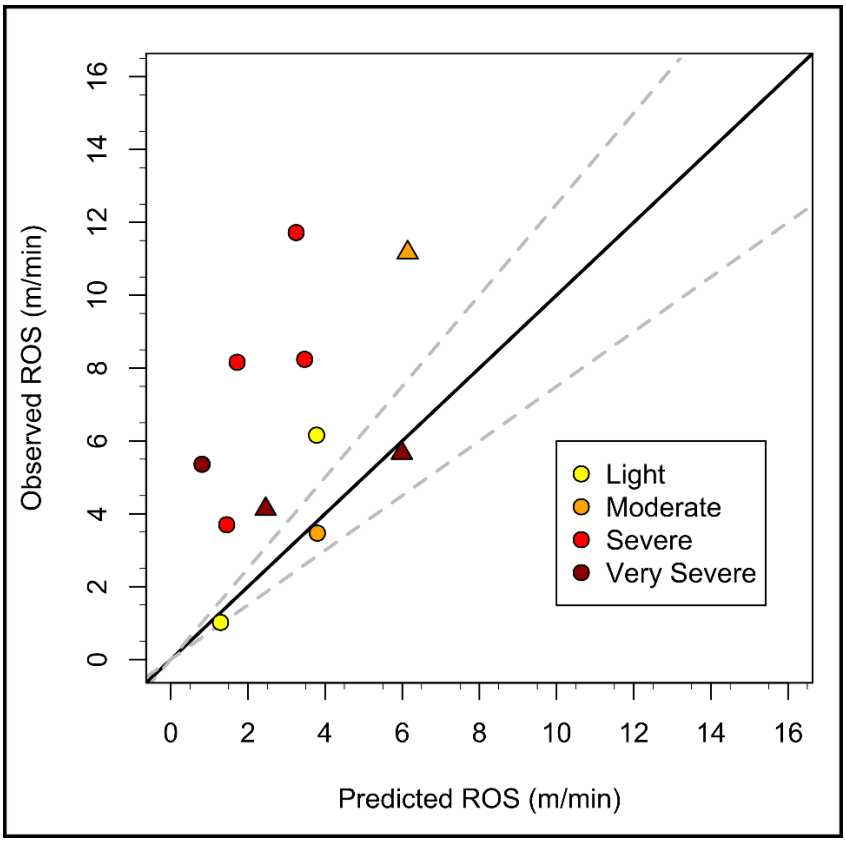

Figure 4.4. The predicted and observed ROS based on the FBP System C-3 fuel type, for each fire site with colour representing the level of MPB-affectedness; solid (black) and dotted lines (grey) represent perfect linear correlation and +/- 25% confidence band; triangle shape observations represent sites with slope-adjusted ISI.

4.3.3 Stand Structure Attribute Analysis

I extracted the peak MPB severity, number of years since peak MPB, stand percentage of lodgepole pine, and stand percentage of dead trees, to investigate potential MPB-related factors that could be influencing the overall fire behaviour (Table 4.6). The peak MPB severity and

number of years since peak MPB varied across all sites, from light to very severe and from nine to fifteen years, respectively (Table 4.6). The number of sites was relatively even across severity levels. The percentage of lodgepole pine within the forest stands varied from site to site. Sites 1, 4, 7, 9, and 10 were mixed-species stands, with 46% to 53% overstory lodgepole pine, while Sites 2, 3, 5, 6, and 8 were more clearly dominated by lodgepole pine, i.e. 63% to 85%. All sites displayed significant levels of stand percentage dead ranging from 32% to 57%. In addition to overstory lodgepole pine, other conifer species included Engelmann spruce (*Picea engelmannii*), black spruce (*Picea mariana*), Douglas-fir (*Pseudotsuga menziesii*), and subalpine fir (*Abies lasiocarpa*). Species with lower pine proportions would be more likely to be considered 'fair' matches with the C-3 fuel type before MPB attack, while the pine-dominated stands would be more likely to be good to excellent matches with C-3 (FCFDG, 1992).

Table 4.6. Potential MPB-related factors effecting the FBP System C-3 model predictions, including MPB severity, severity year, years since peak MPB, and forest stand percentage of lodgepole pine and dead trees.

Site #	MPB Severity	MPB Severity Year	Years Since Peak MPB	Stand Percentage Lodgepole Pine (%)	Stand Percentage Dead (%)
1	Very Severe	2005	13	50	33[a]
2	Light	2008	10	67[b]	34[b]
3A	Severe	2008	9	85	39[b]
3B	Severe	2008	9	85	40
4	Very Severe	2007	11	47[a,b]	38[a]
5	Moderate	2006	12	63[b]	35
6	Severe	2006	11	75	57
7	Very Severe	2006	11	50	35[a]
8	Light	2008	10	72[b]	45[a]
9	Moderate	2003	15	53[b]	40[a]
10	Severe	2004	14	46[b]	32[b]

Notes: [a] Stand percentage dead estimate from aerial photographs and neighbouring VRI data.
[b] Value determined by averaging more than one VRI polygon.

In addition, I extracted the percentage of crown closure, height, and age of each site to investigate potential site specific forest attributes influencing the FBP System C-3 model predictions (Table 4.7). The crown closure of Site 9 (23%) was considered sparse (10% to 25%)

according to the British Columbia Land Cover Classification Scheme (Table 4.7; VRI Data Standards, 2022). Whereas the remaining crown closures of Sites 1, 2, 3, 4, 5, 6, 7, 8, and 10 were considered open (26% to 60%), with crown closures ranging from 29% to 60%. The average height and age of the site forest stands ranged from 16.3 m to 26.6 m and 74 years to 160 years, all within the expected height and age range of mature lodgepole pine forests (Thrower, 1994).

Table 4.7. Potential site specific forest conditions effecting the FBP System C-3 model predictions, including crown closure, stand height, and age.

Site #	Crown Closure	Height	Age
1	55	16.3	104
2	43	26.6	141
3A	60	21.3	76
3B	60	21.3	76
4	36	22.2	152
5	55	17.6	74
6	29	20.2	103
7	40	23.3	130
8	29	17.5	160
9	23	16.4	135
10	36	16.8	91

I performed regression analyses on the number of years since peak MPB, percentage of lodgepole pine, and stand percentage dead to identify if site specific MPB factors had an impact on the difference between observed and predicted ROS (Figure A4). The results from these regression analyses were not significant (p-values greater than 0.1) across all observations (Table 4.8). In addition, I performed regression analyses on site specific stand structure attributes to investigate if crown closure percentage, stand height, and stand age were effective at explaining the difference in ROS. Similar to the previous regression analyses, no significant relationships were found (p-values greater than 0.1; Table 4.8).

Table 4.8. Regression model p-value and R^2 value results between the differences in observed and predicted ROS for all sites and the following attributes: years since peak MPB, percentage of lodgepole pine, stand percentage dead, crown closure, stand height, and stand age.

	Difference (m/min)	Difference (m/min)	Difference (%)	Difference (%)
Site Specific Attributes	**p-value**	**R^2**	**p-value**	**R^2**
Years Since Peak MPB	0.855	0.004	0.336	0.103
Percentage of Lodgepole Pine	0.800	0.007	0.575	0.036
Stand Percentage Dead	0.803	0.007	0.510	0.050
Crown Closure	0.784	0.009	0.664	0.022
Stand Height	0.650	0.024	0.959	0.0003
Stand Age	0.144	0.222	0.302	0.117

4.4 Discussion

The goal of this study was to analyze the observed and predicted spread rates from wildfires dominated by grey-attack forest stands. I selected 10 sites from the 2017 and 2018 BC fire seasons from aerial wildfire photographs based on visible features and provincial health survey data. Fire front positions were extracted from MPT georeferenced wildfire photographs and observed ROS measured at each site; ROS ranged from 1.02 m/min to 11.72 m/min (Table 4.3). I used the FBP System C-3 ROS model to calculate the predicted ROS values in the absence of MPB attack, which ranged from 0.81 m/min to 6.14 m/min (Table 4.4). Comparing the observed and predicted ROS resulted in spread rate differences ranging from -8.47 m/min (underprediction) to +0.33 m/min (slight overprediction) with percent differences of -84.89% to +26.47% (Table 4.5). The comparison displayed significant differences between the observed spread rates and the C-3 ROS model predictions, with a majority of observations indicating faster fire spread than expected in healthy mature pine stands. Perhaps the most telling result from this study is that, in a small but well-extracted and precise dataset, the observed ROS was 1.7 times faster than the FBP System C-3 model predictions (Figure 4.4).

The fire behaviour literature provides evidence that insect outbreaks such as MPB have a significant effect on the fuel conditions, in stand weather, and future fire risk of forest stands (Dhar et al., 2016; Jolly et al., 2012; Moriarty et al., 2019; Page et al., 2012; Perrakis et al., 2014; Schoennagel et al., 2012). The effects of MPB on a forest stand vary with respect to the attack-stage of a MPB-outbreak, i.e. green-attack (less than 1 year since MPB), red-attack (1-3 years since MPB), and grey-attack (greater than 4 years since MPB). Although the aforementioned stages are described as three static outbreak stages, it is worth noting that a MPB-outbreak is a complex and heterogeneous process with varying levels of affectedness with respect to the years since attack. For example, the effects of MPB on the forest stand characteristics may change considerably from 5 to 15 years since a MPB-outbreak, i.e. increased amount of coarse woody debris over time, however for the purposes of defining the attack stage in this study both 5 and 15 years since attacked are considered grey-attack. During the early stages of a MPB-outbreak, as trees die and foliage transitions from green to red, there is a substantial reduction in foliar moisture content resulting in increased flammability of crown and canopy fuels of the forest stand (Jolly et al., 2012; Page et al., 2012). Meanwhile, chemical changes in the needles are also known to occur during this stage, such as the increased emission of terpenoids which are correlated with needle flammability and likelihood of ignition (Page et al., 2014). As canopy foliage dies throughout the red-attack phase, the needle retention ability of the forest stand decreases to the point where the needles drop off and the forest stand enters the grey-attack phase (Natural Resources Canada, 2022). Although needle drop off reduces the canopy bulk density (CBD), this ultimately increases the needle litter and surface fuel load on the forest floor (Jenkins et al., 2014). Additionally, needle drop off increases the solar input available to the surface fuels, in turn increasing the surface fuel temperature and decreasing its moisture content. In late stages

of the grey-attack stage, i.e. post epidemic phase, the increase in sunlight can also increase the abundance of understory vegetation through advanced regeneration and enhanced growth rates (Steinke et al., 2020). Furthermore, Hoffman et al. (2015) found that the reduction in canopy bulk density associated with needle drop off significantly decreased the canopy imposed drag on wind flow thus increasing the surface to mid-canopy wind speeds. During the post outbreak, (late grey-attack) stage, studies have found considerable increases in coarse woody debris and fuel depth (Collins et al., 2012; Klutsch et al., 2009; Page & Jenkins, 2007).

The effects of MPB attack on the fuel and in stand weather conditions of forest stands presents a significant fire risk with respect to crown fire potential and crown fire spread. From the perspective of wildfire managers, crown fires are the most intense and hard to control with serious risk implications for fire fighters, public safety, and properties (Alexander & Cruz, 2011). Crown fires occur when surface fires transition from the surface into the crown of trees and burn from crown to crown (Alexander & Cruz, 2016). The three types of crown fire are dependent on their respective degree of dependence on the surface fire; passive crown fire, the spread rate is largely dependant on the surface fire; active crown fire, the fire behaviour is linked to the surface fire yet largely dependant on the crown fire; and independent crown fire; the crown fire does not rely on the surface fire. The initial surface fire intensity, foliar moisture content, and CBH determine whether a surface fire will ignite a crown fire whereas the CBD and crown fire ROS determine whether the crown fire will be sustained (Van Wagner, 1977). The initial surface fire intensity and crown fire ROS used in determining the ignitability and sustainability of crown fire also introduces the effects of wind speed, slope, fuel dryness, air temperature, relative humidity, fuel complex characteristics, and presence of ladder fuels (Alexander & Cruz, 2016).

Previous research exploring the effect of MPB on fire behaviour has primarily consisted of simulation studies using custom fuel and physics-based models (Jenkins et al., 2014; Stephens et al., 2018). However, there are challenges with using such methods for example; major sources of model error, i.e. underlying prediction biases as identified by Cruz and Alexander (2010); and limited field validation concerns as stated by Alexander and Cruz (2013). The lack of recent research, aforementioned challenges, and the limited number of studies using empirical-based observations presents a clear gap in the evidence of fire behaviour in MPB-affected forest stands (Hoffman et al., 2015; Meigs et al., 2015; Moriarty et al., 2019). One of the only studies to incorporate empirically-based data was accomplished by Perrakis et al. (2014), who extracted spread rate data from naturally occurring wildfires and prescribed burns in MPB-affect forests to observe the effect of MPB on ROS. In their study, Perrakis et al. (2014) observed that headfire spread rates, primarily in the active crown fire phase, were 2.7 times faster in recently-attack (1 to 5 years) MPB-affected forest stands using the FBP System ROS models. The difference between the 1.7 times faster observed spread rates determined in this study and the 2.7 times faster spread rates observed Perrakis' study could be the result of their focus on red-attack stage forest stands and crown fire dominant wildfires. As suggested by Hoffman et al. (2015), following a reduction in CBD, as MPB-outbreak progresses, the rate of spread declines yet still remains above pre-outbreak levels in high wind cases. Considering the existing knowledge of fire behaviour and effects of grey-attack stage MPB on the fuel and weather conditions of forest stands, the faster spread rates observed in this study could be associated with mechanisms such as; increased in stand wind speed; increased needle litter and surface fuel load; increased surface fuel temperature; decreased surface fuel moisture content; and increased coarse woody debris and fuel depth.

I also performed an in-depth analysis exploring potential MPB-related factors influencing the C-3 ROS model predictions. The MPB severity and years since MPB-attack fundamentally change the fuel composition of a forest stand, such as the forest floor fuels, foliar moisture content, and drying of surface fuels (Dhar et al., 2016; Jenkins et al., 2014; Jolly et al., 2012). The peak MPB severity level as shown in Figure A4-B displayed the largest difference in ROS (%) in the area identified as very severe with respect to the peak MPB severity level. Regarding years since peak MPB-attack, although the results were not significant it nonetheless appears likely that as the MPB-outbreak progresses the fuel depth and amount of coarse woody debris would increase thus increasing the amount of surface and ladder fuels available for combustion. Combined with an increase in surface to mid-canopy wind speed, an increased surface rate of spread with higher likelihood of passive crown fire would be expected. Similarly, the percentage of lodgepole pine and stand percentage dead of each site were analyzed and results were not-significant. However, in all likelihood with an increased number of observations, a larger percentage of lodgepole pine and dead trees should result in faster spread rates than expected with regards to the effects of late-stage MPB on the potential of fire behaviour, such as increased ROS due to faster in-stand wind speeds, drier surface fuels, and increased fuel depth (e.g. Jenkins et al., 2012; Linn et al., 2013). In addition, I examined site specific stand structure attributes for significance with respect to C-3 ROS model predictions. However, the forest stand structure complexity and site-specific nature of wildfire conditions make it difficult to determine the overall effect of crown closure, tree stand height, and age which is further emphasized by the non-significant results across all stand structure attributes from this analysis.

There are several confounding factors that potentially introduce sources of uncertainty into the analytical process. The process of determining the MPB attack severity of each site

required multiple stages of visual and spatial analysis with the VRI and MPB datasets. As mentioned previously, the VRI and MPB datasets contain both location and attribute uncertainty due to the difficulty of collecting accurate aerial surveys across vast areas of BC. However, when used together with the BCWS image archive, these data can help inform classification decisions regarding MPB effects and fuel composition. The sites in this study are not 100% grey-attack forest stands as shown in the photographs of the different sites (Figure 4.2). The composition of the sites may include, but are not limited to, green healthy pine, secondary conifer species, and red-attack forests. In addition, we acknowledge that the fire weather for each site was based on weather station data up to 39km away. This introduces variability, such as wind speeds, in the fire weather calculations that the FBP System is highly dependant on. Although the FBP System is effective for fire behaviour prediction across Canada, the overall influence of fuel type on fire behaviour is secondary to the impact of fire weather on fire behaviour (Hély et al., 2001). Furthermore, the fire observations in this study occurred during relatively low ISI conditions across all sites; the analysis could be greatly improved by including a wider range of ISI, including fire spread in more extreme conditions (e.g. wind speed greater than 25 km/h). Considering the complexity of assessing the MPB status, forest stand composition, and fire weather variables, this study was able to demonstrate the utility of the monoplotting method for extracting wildfire spread rates in MPB-affected forest stands and that grey stage MPB-affected stands do burn significantly faster than models suggest for unaffected stands.

4.5 Conclusion

The ability to generate useful findings from the monoplotting process to collect empirically based MPB-affected fire behaviour data provides a range of potential for future analysis, especially coupled with more location-specific fire weather data following practices

(for example, see Nadeem et al., 2019). More importantly, future studies would benefit from collecting additional MPB-affected ROS observations in grey-attack stage forest stands and seeking to improve the areas of uncertainty in this study, such as the MPB-validation and forest stand composition analysis, through additional data and resources. For example, enhanced forestry inventory techniques using LiDAR systems to collect highly accurate key inventory variables such as, tree height, volume, basal area, and fibre attributes linked to wood composition (NRCAN, 2022).

The escalating severity of disturbance events combined with the complexity of post-disturbance landscapes exemplifies the necessity of research that explores the effect of disturbances in our dynamic forests. Providing novel sources of empirical fire behaviour data affected by disturbance events can provide invaluable resources for the development and validation of empirically based fire behaviour models to help fire management and researchers better understand and predict fire behaviour.

Appendix A

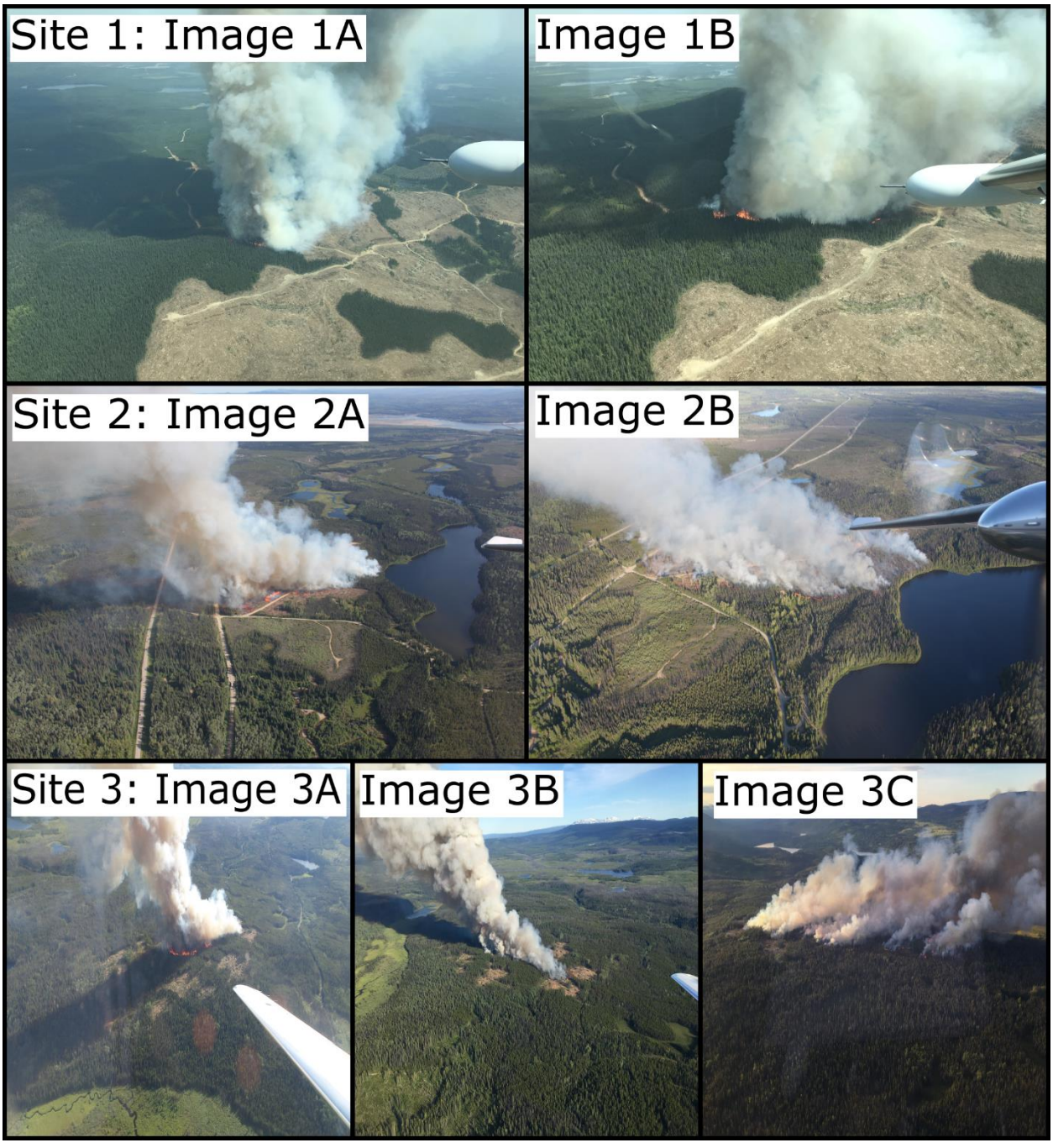

Figure A1. The study site image pairs displaying wildfire in grey-attack forest stands: 1A, 1B, 2A, 2B, 3A, 3B, and 3C.

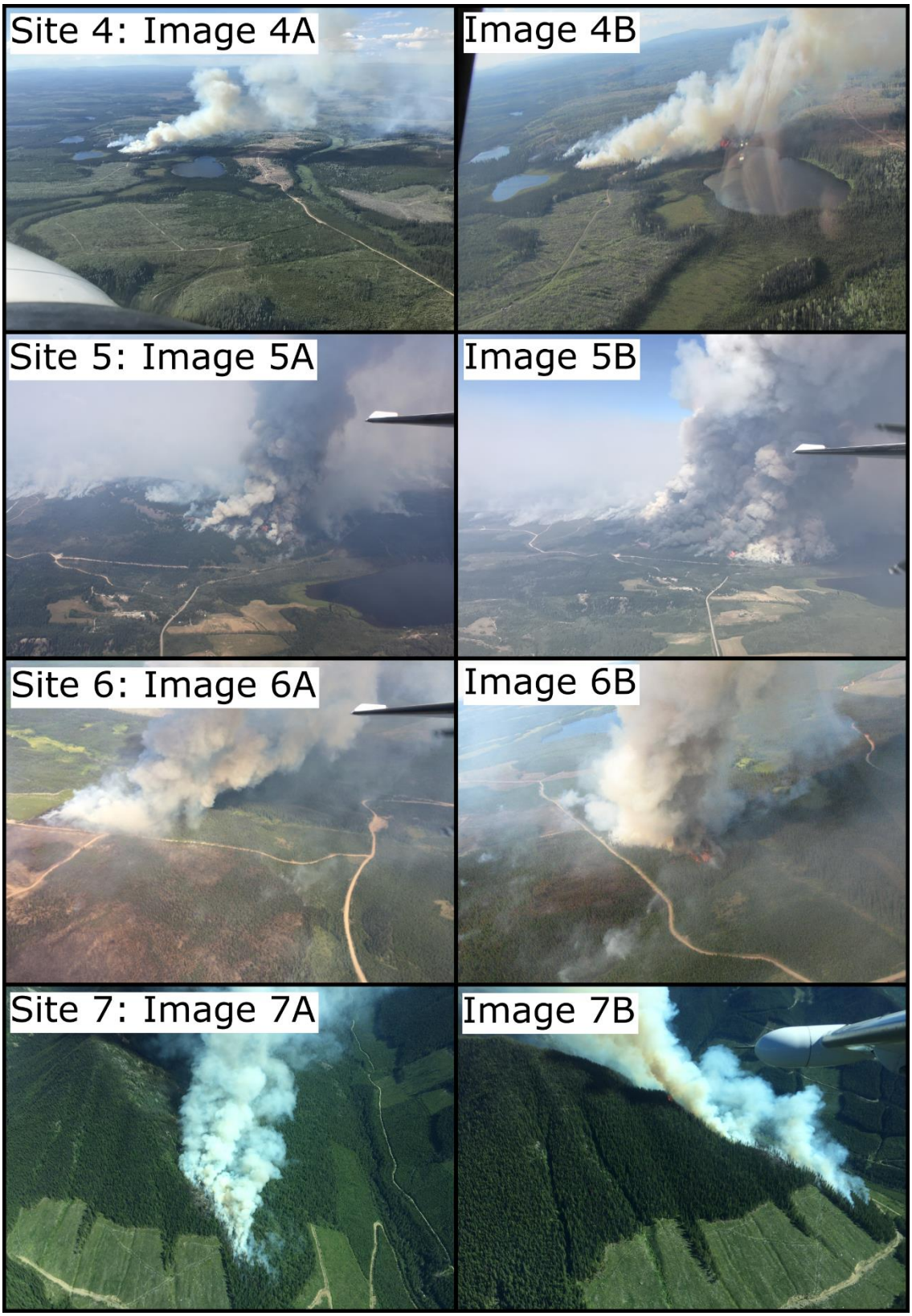

Figure A2. The study site image pairs displaying wildfire in grey-attack forest stands: 4A, 4B, 5A, 5B, 6A, 6B, 7A, and 7B.

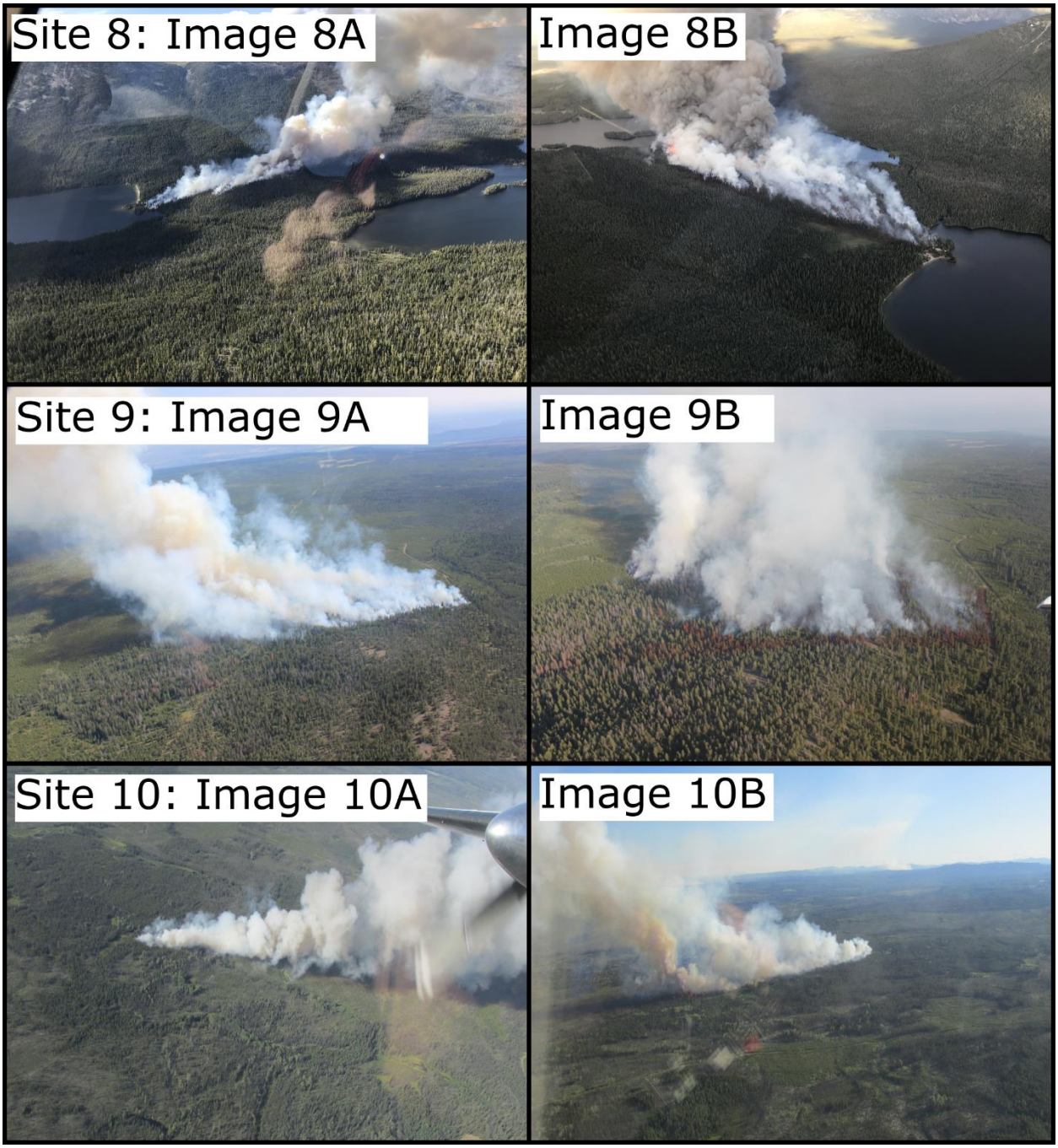

Figure A3. The study site image pairs displaying wildfire in grey-attack forest stands: 8A, 8B, 9A, 9B, 10A, and 10B.

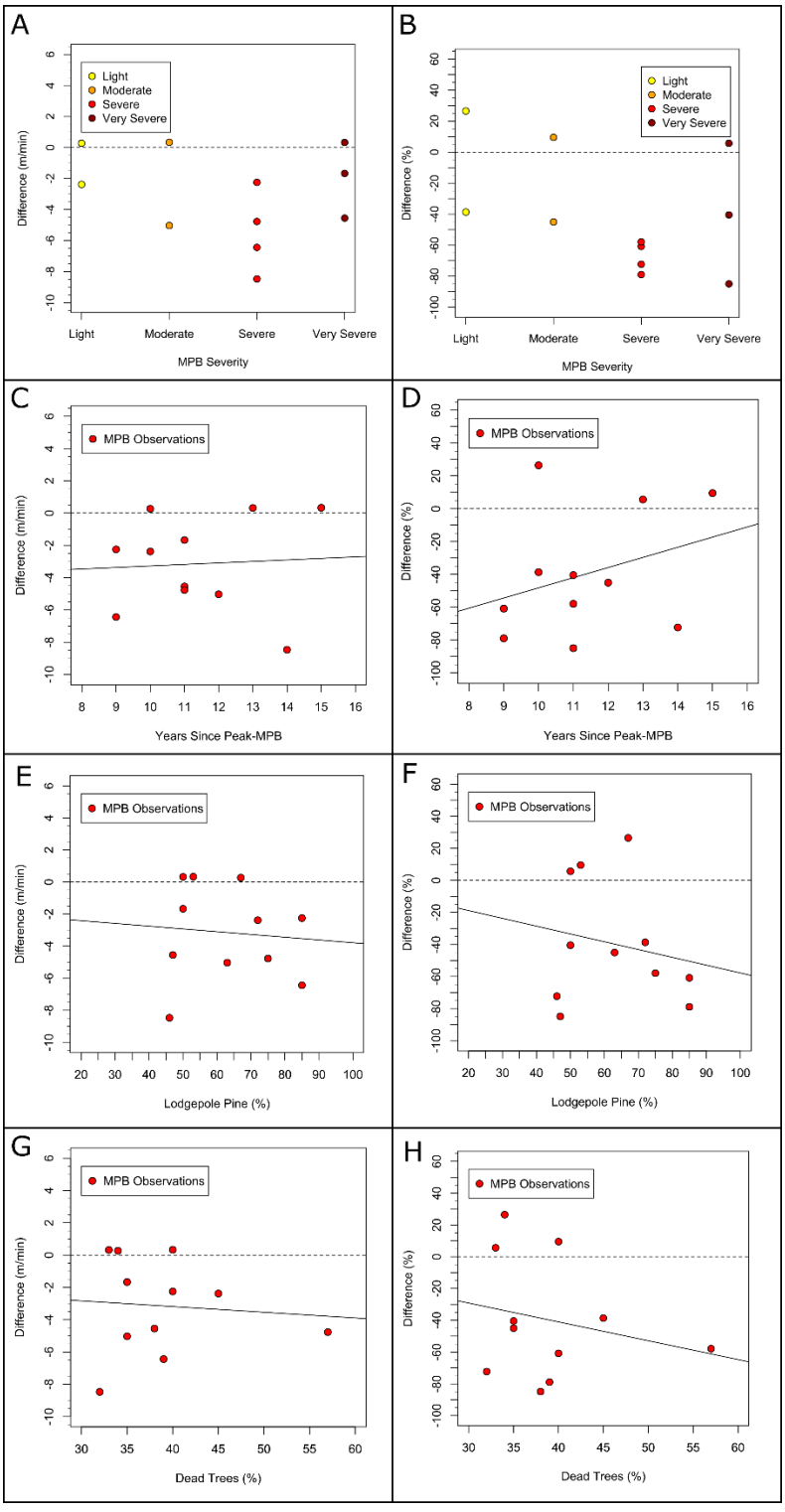

Figure A4. The m/min and percent difference between the predicted and observed ROS of the MPB observations (yellow, orange, red, and dark red points) against the MPB severity level (A/B); the years since peak MPB (C/D); (E/F) the percentage of lodgepole pine; (G/H) the stand percentage dead. The dotted line represents perfect linear correlation, the solid line (black) represents the regression line between the two variables.

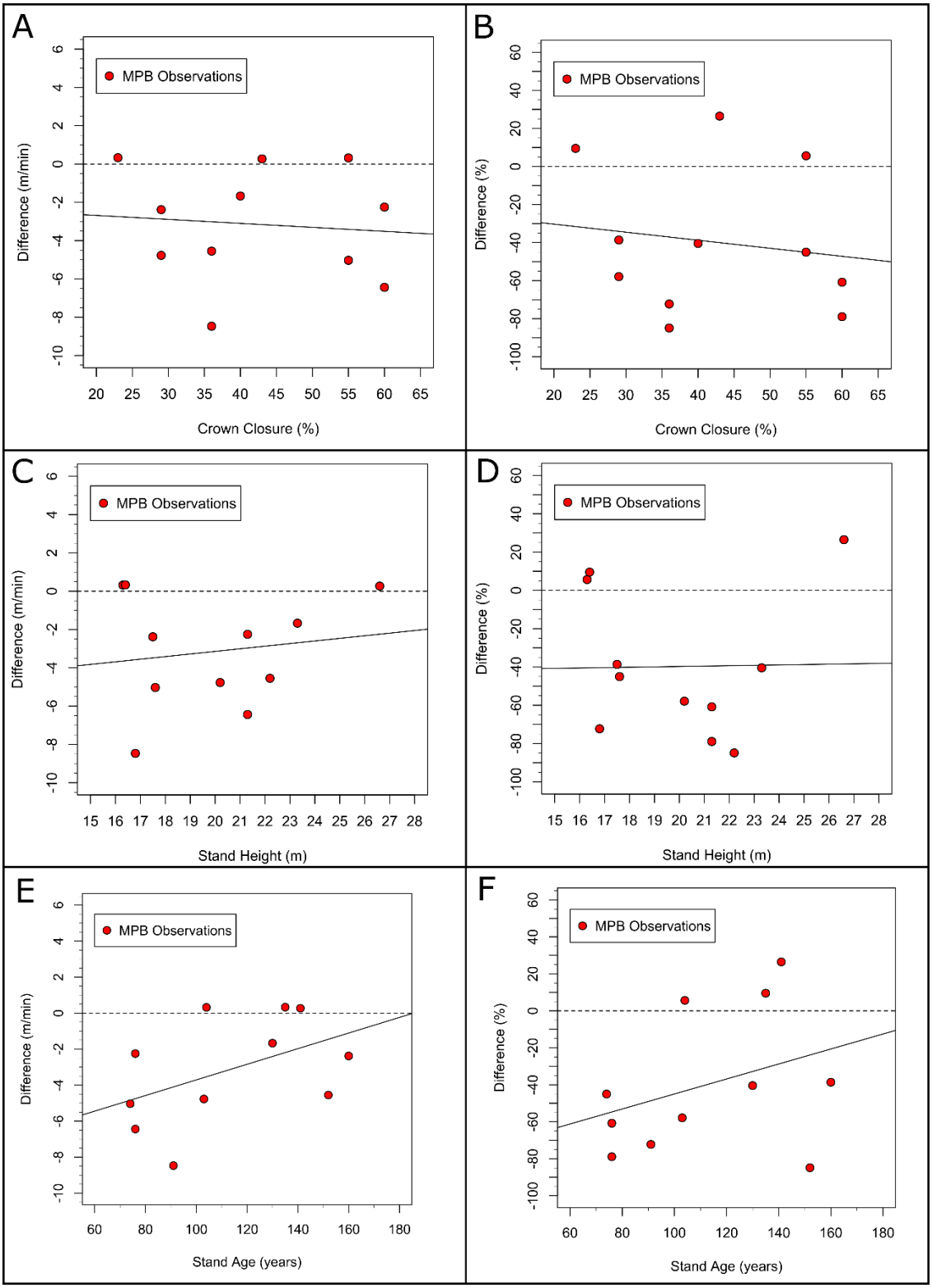

Figure A5. The m/min and percent difference between the predicted and observed ROS of the MPB observations (red points) against the average crown closure (A/B), stand height (C/D), and stand age (E/F). The dotted line represents perfect linear correlation, the solid line (black) represents the regression line including all observations.

References

Alexander, M. E., & Cruz, M. G. (2011). What are the safety implications of crown fires? In Proceedings of 11th International Wildland Fire Safety Summit, Missoula, Montana, USA, 4–8 April 2011. https://publications.csiro.au/rpr/download?pid=csiro:EP114880&dsid=DS2

Alexander, M. E., & Cruz, M. G. (2013). Are the applications of wildland fire behaviour models getting ahead of their evaluation again? *Environmental Modelling and Software*, *41*, 65–71. https://doi.org/10.1016/j.envsoft.2012.11.001

Alexander, M. E., & Cruz, M. G. (2016). Chapter 9: Crown Fire Dynamics in Conifer Forests (General Technical Report PNW-GTR-891). In *Synthesis of knowledge of extreme fire behavior: volume 2 for fire behavior specialists, researchers, and meteorologists.* US Forest Service, Pacific Northwest Research Station: Portland, Oregon, USA. https://doi.org/10.2737/PNW-GTR-891

Aukema, B.H, L. Carroll, A., Zheng, Y., Zhu, J., F. Raffa, K., Dan Moore, R., Stahl, K., & Taylor, S.W (2008). Movement of outbreak populations of mountain pine beetle: influences of spatiotemporal patterns and climate. *Ecography, 31*(3), 348-358. http://dx.doi.org/10.1111/j.0906-7590.2007.05453.x

Banerjee, T. (2020). Impacts of forest thinning on wildland fire behavior. *Forests*, *11*(9), 918. https://doi.org/10.3390/F11090918

BC Data Catalogue. (2022a). *DEM*. Available online: https://catalogue.data.gov.bc.ca/dataset/digital-elevation-model-for-british-columbia-cded-1-250-000 (accessed 15 March 2020).

BC Data Catalogue. (2022b). *Pest Infestation Polygons*. Available online: https://catalogue.data.gov.bc.ca/dataset/450b67bb-02d5-4526-8bc0-ac7924125a1e#edc-pow (accessed 15 March 2020).

BC Data Catalogue. (2022c). *VRI Data*. Available online: https://catalogue.data.gov.bc.ca/dataset/vri-historical-vegetation-resource-inventory-2002-2019- (accessed 15 March 2020).

BC Ministry of Forests Lands & Natural Resource Operations. (2022). *The 1999-2015 mountain pine beetle outbreak - Province of British Columbia*. Available online: https://www2.gov.bc.ca/gov/content/industry/forestry/managing-our-forest-resources/forest-health/forest-pests/bark-beetles/mountain-pine-beetle/responding-to-the-1999-2015-outbreak (accessed 15 March 2020).

BC Wildfire Service. (2020). *2017 Wildfire Season*. Available online: https://www2.gov.bc.ca/gov/content/safety/wildfire-status/about-bcws/wildfire-history/wildfire-season-summary (accessed 15 March 2020).

Beverly, J. L., & Wotton, B. M. (2007). Modelling the probability of sustained flaming: Predictive value of fire weather index components compared with observations of site weather and fuel moisture conditions. *International Journal of Wildland Fire*, *16*(2), 161–173. https://doi.org/10.1071/WF06072

Boulanger, Y., Girardin, M., Bernier, P. Y., Gauthier, S., Beaudoin, A., & Guindon, L. (2017). Changes in mean forest age in Canada's forests could limit future increases in area burned but compromise potential harvestable conifer volumes. *Canadian Journal of Forest Research*, *47*(6), 755–764. https://doi.org/10.1139/cjfr-2016-0445

Bozzini, C. (2018). *WSL Monoplotting Tool: User Manual*. Swiss Federal Research Institute WSL. Available online: https://www.wsl.ch/fileadmin/user_upload/WSL/Services_Produkte/Software_Apps/Monoplotting/MPT_-_2.0_-_User_manual_-_E.pdf (accessed 15 March 2020).

Canelles, Q., Aquilué, N., James, P. M. A., Lawler, J., & Brotons, L. (2021). Global review on interactions between insect pests and other forest disturbances. *Landscape Ecology*, *36*(4), 945–972. https://doi.org/10.1007/s10980-021-01209-7

Cantin, A., Wang, X., Parisien, M.-A., Wotton, M., Anderson, K., Moore, B., Schiks, T., & Flannigan, M. D. (2020). *CFFDRS R Package*. https://cran.r-project.org/web/packages/cffdrs/index.html

Collins, B. J., Rhoades, C. C., Battaglia, M. A., & Hubbard, R. M. (2012). The effects of bark beetle outbreaks on forest development, fuel loads and potential fire behavior in salvage logged and untreated lodgepole pine forests. *Forest Ecology and Management*, *284*, 260–268. https://doi.org/10.1016/j.foreco.2012.07.027

Coogan, S. C. P., Robinne, F. N., Jain, P., & Flannigan, M. D. (2019). Scientists' warning on wildfire — a canadian perspective. *Canadian Journal of Forest Research*, *49*(9), 1015–1023. https://doi.org/10.1139/cjfr-2019-0094

Corbett, L. J., Withey, P., Lantz, V. A., & Ochuodho, T. O. (2016). The economic impact of the mountain pine beetle infestation in British Columbia: Provincial estimates from a CGE analysis. *Forestry*, *89*(1), 100–105. https://doi.org/10.1093/forestry/cpv042

Cruz, M. G., & Alexander, M. E. (2010). Assessing crown fire potential in coniferous forests of western North America: A critique of current approaches and recent simulation studies. *International Journal of Wildland Fire*, *19*(4), 377–398. https://doi.org/10.1071/WF08132

Cruz, M. G., Alexander, M. E., & Wakimoto, R. H. (2003). Assessing the probability of crown fire initiation based on fire danger indices. *Forestry Chronicle*, *79*(5), 976–983. https://doi.org/10.5558/tfc79976-5

Dhar, A., Parrott, L., & Hawkins, C. D. B. (2016). Aftermath of mountain pine beetle outbreak in british columbia: Stand dynamics, management response and ecosystem resilience. *Forests*, *7*(8), 1–19. https://doi.org/10.3390/f7080171

Dhar, A., Parrott, L., & Heckbert, S. (2016). Consequences of mountain pine beetle outbreak on forest ecosystem services in western Canada. *Canadian Journal of Forest Research*, *46*(8), 987–999. https://doi.org/10.1139/cjfr-2016-0137

ESRI. (2020). *ESRI World Imagery (For Export)*. Available online: https://www.arcgis.com/home/item.html?id=226d23f076da478bba4589e7eae95952 (accessed 15 March 2020).

Forestry Canada Fire Danger Group. (1992). Development and structure of the Canadian Forest Fire Behavior Prediction System (Information Report ST-X-3). Forestry Canada, Science and Sustainable Development Directorate: Ottawa, Ontario, Canada. https://cfs.nrcan.gc.ca/publications?id=10068

Fogarty, L. G., & Alexander, M. E. (1999). *A field guide for predicting grassland fire potential: derivation and use.* Available online: https://www.frames.gov/documents/catalog/fogarty_and_alexander_1999.pdf (accessed 15 March 2020).

Halofsky, J. E., Peterson, D. L., & Harvey, B. J. (2020). Changing wildfire, changing forests: the effects of climate change on fire regimes and vegetation in the Pacific Northwest, USA. *Fire Ecology*, *16*(1). https://doi.org/10.1186/s42408-019-0062-8

Hart, H., Perrakis, D. D. B., Taylor, S. W., Bone, C., & Bozzini, C. (2021). Georeferencing oblique aerial wildfire photographs: An untapped source of fire behaviour data. *Fire*, *4*(4). https://doi.org/10.3390/fire4040081

Hart, S. J., & Preston, D. L. (2020). Fire weather drives daily area burned and observations of fire behavior in mountain pine beetle affected landscapes. *Environmental Research Letters*, *15*(5). https://doi.org/10.1088/1748-9326/ab7953

Hély, C., Flannigan, M., Bergeron, Y., & McRae, D. (2001). Role of vegetation and weather on fire behavior in the Canadian mixedwood boreal forest using two fire behavior prediction systems. *Canadian Journal of Forest Research*, *31*(3), 430–441. https://doi.org/10.1139/x00-192

Hessburg, P. F., Miller, C. L., Parks, S. A., Povak, N. A., Taylor, A. H., Higuera, P. E., Prichard, S. J., North, M. P., Collins, B. M., Hurteau, M. D., Larson, A. J., Allen, C. D., Stephens, S. L., Rivera-Huerta, H., Stevens-Rumann, C. S., Daniels, L. D., Gedalof, Z., Gray, R. W., Kane, V. R., … Salter, R. B. (2019). Climate, Environment, and Disturbance History Govern Resilience of Western North American Forests. *Frontiers in Ecology and Evolution*, *7*, 239. https://doi.org/10.3389/fevo.2019.00239

Hicke, J. A., Johnson, M. C., Hayes, J. L., & Preisler, H. K. (2012). Effects of bark beetle-caused tree mortality on wildfire. *Forest Ecology and Management*, *271*, 81–90. https://doi.org/10.1016/j.foreco.2012.02.005

Hirsch, K. (1996). Canadian Forest Fire Behavior Prediction (FBP) System: User's Guide (Special Report 7). Natural Resources Canada, Canadian Forest Service, Northwest Region, Northern Forestry Centre: Edmonton, Alberta, Canada. https://www.frames.gov/documents/catalog/hirsch_1996.pdf

Hoffman, C. M., Linn, R., Parsons, R., Sieg, C., & Winterkamp, J. (2015). Modeling spatial and temporal dynamics of wind flow and potential fire behavior following a mountain pine beetle outbreak in a lodgepole pine forest. *Agricultural and Forest Meteorology*, *204*, 79–93. https://doi.org/10.1016/j.agrformet.2015.01.018

Jactel, H., Koricheva, J., & Castagneyrol, B. (2019). Responses of forest insect pests to climate change: not so simple. *Current Opinion in Insect Science*, *35*, 103–108. https://doi.org/10.1016/j.cois.2019.07.010

Jenkins, M. J., Page, W. G., Hebertson, E. G., & Alexander, M. E. (2012). Fuels and fire behavior dynamics in bark beetle-attacked forests in Western North America and implications for fire management. *Forest Ecology and Management*, *275*, 23–34. https://doi.org/10.1016/j.foreco.2012.02.036

Jenkins, M. J., Runyon, J. B., Fettig, C. J., Page, W. G., & Bentz, B. J. (2014). Interactions among the mountain pine beetle, fires, and fuels. *Forest Science*, *60*(3), 489–501. https://doi.org/10.5849/forsci.13-017

Johnston, L. M., Wang, X., Erni, S., Taylor, S. W., McFayden, C. B., Oliver, J. A., Stockdale, C., Christianson, A., Boulanger, Y., Gauthier, S., Arseneault, D., Wotton, B. M., Parisien, M. A., & Flannigan, M. D. (2020). Wildland fire risk research in Canada. *Environmental Reviews*, *28*(2), 164–186. https://doi.org/10.1139/er-2019-0046

Jolly, W. M., Parsons, R. A., Hadlow, A. M., Cohn, G. M., McAllister, S. S., Popp, J. B., Hubbard, R. M., & Negron, J. F. (2012). Relationships between moisture, chemistry, and ignition of Pinus contorta needles during the early stages of mountain pine beetle attack. *Forest Ecology and Management*, *269*, 52–59. https://doi.org/10.1016/j.foreco.2011.12.022

Kirchmeier-Young, M. C., Gillett, N. P., Zwiers, F. W., Cannon, A. J., & Anslow, F. S. (2019). Attribution of the Influence of Human-Induced Climate Change on an Extreme Fire Season. *Earth's Future*, *7*(1), 2–10. https://doi.org/10.1029/2018EF001050

Klutsch, J. G., Negrón, J. F., Costello, S. L., Rhoades, C. C., West, D. R., Popp, J., & Caissie, R. (2009). Stand characteristics and downed woody debris accumulations associated with a mountain pine beetle (Dendroctonus ponderosae Hopkins) outbreak in Colorado. *Forest Ecology and Management*, *258*(5), 641–649. https://doi.org/10.1016/j.foreco.2009.04.034

Lawson, B. D. (1972). An interpretive guide to the Canadian forest fire behavior system (Information Report BC-P-03). Environment Canada, Canadian Forestry Service, Pacific Research Centre: Victoria, British Columbia, Canada. https://cfs.nrcan.gc.ca/publications?id=28451

Lawson, B. D., & Armitage, O. B. (2008). Weather Guide Canadian Forest Fire Danger Rating System. Canadian Forest Service, Northern Forestry Centre: Edmonton, Alberta, Canada. https://cfs.nrcan.gc.ca/pubwarehouse/pdfs/29152.pdf

Linn, R. R., Sieg, C. H., Hoffman, C. M., Winterkamp, J. L., & McMillin, J. D. (2013). Modeling wind fields and fire propagation following bark beetle outbreaks in spatially-heterogeneous pinyon-juniper woodland fuel complexes. *Agricultural and Forest Meteorology*, *173*, 139–153. https://doi.org/10.1016/j.agrformet.2012.11.007

Martin, D., Tomida, M., & Meacham, B. (2016). Environmental impact of fire. *Fire Science Reviews*, *5*(5), 1–21. https://doi.org/10.1186/s40038-016-0014-1

McGee, T., McFarlane, B., & Tymstra, C. (2015). Chapter 3 - Wildfire: A Canadian Perspective. In J. Schroder & D. Paton (Eds.), *Wildfire Hazards, Risks, and Disasters*. Elsevier Inc. https://doi.org/10.1016/B978-0-12-410434-1.00003-8

Mcloughlin, N. (2016). *The Universal Fire Behavior Calculator*. Available online: https://redapp.org/system/files/private_files/REDapp_6.2_User_Guide_1.pdf (accessed 15 March 2020).

Meigs, G. W., Campbell, J. L., Zald, H. S. J., Bailey, J. D., Shaw, D. C., & Kennedy, R. E. (2015). Does wildfire likelihood increase following insect outbreaks in conifer forests? *Ecosphere*, *6*(7), 1-24. https://doi.org/10.1890/es15-00037.1

Moriarty, K., Cheng, A. S., Hoffman, C. M., Cottrell, S. P., & Alexander, M. E. (2019). Firefighter Observations of "Surprising" Fire Behavior in Mountain Pine Beetle-Attacked Lodgepole Pine Forests. *Fire*, *2*(2), 34. https://doi.org/10.3390/fire2020034

Nadeem, K., Taylor, S. W., Woolford, D. G., & Dean, C. B. (2019). Mesoscale spatiotemporal predictive models of daily human- and lightning-caused wildland fire occurrence in British Columbia. *International Journal of Wildland Fire*, *29*(1), 11–27. https://doi.org/10.1071/WF19058

Natural Resources Canada. (2022). *Mountain pine beetle (factsheet)*. Available online: https://www.nrcan.gc.ca/forests/fire-insects-disturbances/top-insects/13397 (accessed 15 March 2020).

NRCAN. (2022). *Enhanced forest inventory techniques.* Available online: https://www.nrcan.gc.ca/our-natural-resources/forests/sustainable-forest-management/measuring-and-reporting/forest-inventory/enhanced-forest-inventory-techniques/13421 (accessed 15 March 2020).

Pacific Climate Impacts Consortium. (2022). *Weather Station Data*. Available online: https://pacificclimate.org/data/bc-station-data (accessed 15 March 2020).

Page, Wesley G., Jenkins, M. J., & Alexander, M. E. (2014). Crown fire potential in lodgepole pine forests during the red stage of mountain pine beetle attack. *Forestry*, *87*(3), 347–361. https://doi.org/10.1093/forestry/cpu003

Page, Wesley G., Jenkins, M. J., & Runyon, J. B. (2012). Mountain pine beetle attack alters the chemistry and flammability of lodgepole pine foliage. *Canadian Journal of Forest Research*, *42*(8), 1631–1647. https://doi.org/10.1139/X2012-094

Page, Wesley Green, & Jenkins, M. J. (2007). Mountain pine beetle-induced changes to selected lodgepole pine fuel complexes within the intermountain region. *Forest Science*, *53*(4), 507–518. https://doi.org/10.1093/forestscience/53.4.507

Perrakis, D. B., Lanoville, R. A., Taylor, S. W., & Hicks, D. (2014). Modeling wildfire spread in mountain pine beetle-affected forest stands, British Columbia, Canada. *Fire Ecology*, *10*(2), 10–35. https://doi.org/10.4996/fireecology.1002010

Plucinski, M. P., Sullivan, A. L., Rucinski, C. J., & Prakash, M. (2017). Improving the reliability and utility of operational bushfire behaviour predictions in Australian vegetation. *Environmental Modelling and Software*, *91*, 1–12. https://doi.org/10.1016/j.envsoft.2017.01.019

Pureswaran, D. S., Roques, A., & Battisti, A. (2018). Forest insects and climate change. *Current Forestry Reports*, *4*(2), 35–50. https://doi.org/10.1007/s40725-018-0075-6

R Core Team. (2013). *A language and environment for statistical computing*. R Foundation for Statistical Computing: Vienna. http://www.R-project.org/

Rothermel, R. C. (1991). Predicting behavior and size of crown fires in the northern Rocky Mountains (Research Paper INT-438). USDA Forest Service, Intermountain Research Station*:* Ogden, Utah, USA. https://www.fs.fed.us/rm/pubs_int/int_rp438.pdf

Saab, V. A., Latif, Q. S., Rowland, M. M., Johnson, T. N., Chalfoun, A. D., Buskirk, S. W., Heyward, J. E., & Dresser, M. A. (2014). Ecological consequences of mountain pine beetle outbreaks for wildlife in Western North American forests. *Forest Science*, *60*(3), 539–559. https://doi.org/10.5849/forsci.13-022

Schoennagel, T., Balch, J. K., Brenkert-Smith, H., Dennison, P. E., Harvey, B. J., Krawchuk, M. A., Mietkiewicz, N., Morgan, P., Moritz, M. A., Rasker, R., Turner, M. G., & Whitlock, C. (2017). Adapt tomore wildfire in western North American forests as climate changes. *Proceedings of the National Academy of Sciences of the United States of America*, *114*(18), 4582–4590. https://doi.org/10.1073/pnas.1617464114

Schoennagel, T., Veblen, T. T., Negron, J. F., & Smith, J. M. (2012). Effects of mountain pine beetle on fuels and expected fire behavior in lodgepole pine forests, Colorado, USA. *PLoS ONE*, *7*(1). https://doi.org/10.1371/journal.pone.0030002

Seidl, R., Fernandes, P. M., Fonseca, T. F., Gillet, F., Jönsson, A. M., Merganičová, K., Netherer, S., Arpaci, A., Bontemps, J. D., Bugmann, H., González-Olabarria, J. R., Lasch, P., Meredieu, C., Moreira, F., Schelhaas, M. J., & Mohren, F. (2011). Modelling natural disturbances in forest ecosystems: A review. *Ecological Modelling*, *222*(4), 903–924. https://doi.org/10.1016/j.ecolmodel.2010.09.040

Shang, C., Wulder, M. A., Coops, N. C., White, J. C., & Hermosilla, T. (2020). Spatially-Explicit Prediction of Wildfire Burn Probability Using Remotely-Sensed and Ancillary Data. *Canadian Journal of Remote Sensing*, *46*(3), 313–329. https://doi.org/10.1080/07038992.2020.1788385

Statistics Canada. (2019). *Environment Facts Sheet: British Columbia's forest fires, 2018*. Available online: https://www150.statcan.gc.ca/n1/en/pub/16-508-x/16-508-x2019002-eng.pdf?st=HAo2klaO (accessed 15 March 2020).

Steinke, J., McIntosh, A., Schroeder, L., & Macdonald, S. (2020). Understory vegetation responses to simulated mountain pine beetle attack and salvage logging in grey attack stage lodgepole pine stands. *Forest Ecology and Management, 474*. https://doi.org/10.1016/j.foreco.2020.118373.

Stephens, S. L., Collins, B. M., Fettig, C. J., Finney, M. A., Hoffman, C. M., Knapp, E. E., North, M. P., Safford, H., & Wayman, R. B. (2018). Drought, Tree Mortality, and Wildfire in Forests Adapted to Frequent Fire. *BioScience*, *68*(2), 77–88. https://doi.org/10.1093/biosci/bix146

Stockdale, C. A., Bozzini, C., Macdonald, S. E., & Higgs, E. (2015). Extracting ecological information from oblique angle terrestrial landscape photographs: Performance evaluation of the WSL Monoplotting Tool. *Applied Geography*, *63*, 315–325. https://doi.org/10.1016/j.apgeog.2015.07.012

Stocks, B. J. (1989). Fire behavior in mature jack pine. *Canadian Journal of Forest Research, 19*(6), 783-790. https://doi.org/10.1139/x89-119

Stocks, B. J., Alexander, M. E., Wotton, B. M., Stefner, C. N., Flannigan, M. D., Taylor, S. W., Lavoie, N., Mason, J. A., Hartley, G. R., Maffey, M. E., Dalrymple, G. N., Blake, T. W., Cruz, M. G., & Lanoville, R. A. (2004). Crown fire behaviour in a northern jack pine - Black spruce forest. *Canadian Journal of Forest Research*, *34*(8), 1548–1560. https://doi.org/10.1139/X04-054

Stocks, B. J., Lynham, T. J., Lawson, B. D., Alexander, M. E., Wagner, C. E. Van, McAlpine, R. S., & Dubé, D. E. (1989). The Canadian Forest Fire Danger Rating System: An Overview. *The Forestry Chronicle*, *65*(6), 450–457. https://doi.org/10.5558/tfc65450-6

Tao, S., Guo, Q., Li, C., Wang, Z., & Fang, J. (2016). Global patterns and determinants of forest canopy height. *Ecology*, *97*(12), 3265–3270. https://doi.org/10.1002/ecy.1580

Thrower, J. S. (1994). Revised height-age curves for lodgepole pine and interior spruce in British Columbia (Report). J.S. Thrower & Associates Ltd. Consulting Foresters: Vancouver, British Columbia, Canada. https://www.for.gov.bc.ca/hfd/library/documents/bib9049.pdf

Van Wagner, C. E. (1977). Conditions for the start and spread of crown fire. *Canadian Journal of Forest Research*, *7*, 23–34.

Van Wagner, C. E. (1987). Development and structure of the Canadian forest fire weather index system (Forestry Technical Report 35). Natural Resources Canada, Canadian Forest Service: Ottawa, Ontario, Canada. https://cfs.nrcan.gc.ca/pubwarehouse/pdfs/19927.pdf

VRI Data Standards. (2022). *VRI*. Available online: https://www2.gov.bc.ca/gov/content/industry/forestry/managing-our-forest-resources/forest-inventory/data-management-and-access/vri-data-standards (accessed 15 March 2020).

Woods, A. J., Heppner, D., Kope, H. H., Burleigh, J., & Maclauchlan, L. (2010). Forest health and climate change: A British Columbia perspective. *Forestry Chronicle*, *86*(4), 412–422. https://doi.org/10.5558/tfc86412-4

Wotton, B. M., & Beverly, J. L. (2007). Stand-specific litter moisture content calibrations for the Canadian Fine Fuel Moisture Code. *International Journal of Wildland Fire*, *16*(4), 463–472. https://doi.org/10.1071/WF06087

Xu, R., Yu, P., Abramson, M. J., Johnston, F. H., Samet, J. M., Bell, M. L., Haines, A., Ebi, K. L., Li, S., & Guo, Y. (2020). Wildfires, Global Climate Change, and Human Health. *New England Journal of Medicine*. https://doi.org/10.1056/nejmsr2028985

Chapter 5: Conclusion

5.1 Summary

Wildfire is an essential ecological process that has been a dominant factor in shaping the natural history of earth through acts of renewal and change (Pausas & Keeley, 2009). This is further demonstrated through the fundamental role wildfire plays in the composition and distribution of global ecosystems (McLauchlan et al., 2020). However, the increasingly destructive nature of wildfire as a result of climate change poses a serious risk to public health, the natural environment, and socio-economic structure of communities (Harrison et al., 2010; Reid et al., 2016). The collective impacts of wildfire contribute to the vital importance of investigating novel methodologies to further understand and predict fire behaviour.

The overall focus of this thesis was to develop a methodology for acquiring empirically-based fire behaviour data to further inform fire behaviour prediction. This was successfully accomplished by evaluating the utility of mono-photogrammetry to extract fire behaviour data from oblique aerial wildfire photographs, and by performing an empirical wildfire spread analysis on grey-attack stage mountain pine beetle (MPB)-affected forest stands. The aim of the first study (Chapter 3) was to develop a process of georeferencing oblique aerial wildfire photographs to determine the geographic coordinates of fire behaviour features and to use such features in calculating wildfire spread rates as a means for providing additional data for fire behaviour models, such as the Canadian Fire Behaviour Prediction (FBP) System. The Monoplotting Tool (MPT), a mono-photogrammetric software tool developed by the WSL Research Institute (Bozzini et al., 2012), was used to georeference and extract spatial fire behaviour data from ten wildfire photographs. Specifically, MPT was used to successfully

extract the headfire front positions, spread distance, and burning period of five wildfires, which were used to calculate their respective spread rates. The successful observed rate of spread (ROS) results were compared against the FBP System predicted ROS with differences attributed mainly to model error or uncertainty in weather and fuel inputs, findings that have been discussed by other studies (Cheney et al., 2012; Filkov et al., 2018; Gould et al., 2011), yet remain difficult to resolve. Additionally, the georeferenced images were assessed to determine if the landscape features, fuel type, distance to fire front, elevation above ground level, or angle of incidence exerted an impact on the georeferencing accuracy. Results indicate that the camera angle of incidence influences the accuracy of each georeferenced image, a finding that is in accordance with existing literature (Stockdale et al., 2015). Taking these types of issues into account, applying mono-photogrammetry to wildfire photographs taken during airtanker response shows promise for providing reproducible estimates of headfire front position, spread distance, and ROS with relatively high accuracy.

The second study was focused on utilizing the monoplotting method to perform an empirical wildfire spread analysis on wildfire spread rates in grey-attack stage of MPB-affected forest stands. This study further demonstrates the utility of the monoplotting methodology while providing rare empirical-based evidence of fire behaviour data in MPB-affected forest stands. A combination of visual and GIS analyses were completed on ten wildfires to confirm that their forest stands contained grey-attack forest stands. The monoplotting method was used to extract the headfire front positions and subsequent ROS calculations were executed to collect the observed ROS from each MPB-affected wildfire. In addition, the predicted ROS of each wildfire was calculated using the Canadian FBP System C-3 ROS model. The results from this study showed promise that the monoplotting method can be applied to various areas of fire behaviour

research and that the observed ROS were 1.7 times faster than the predicted ROS, a result that aligns with existing research (Hoffman et al., 2015; Perrakis et al., 2014). Aside from the direct comparison between the predicted and observed ROS, a regression analysis between the difference in observed and predicted ROS and potential variables regarding the MPB and forest stand characteristics was performed. Results from this regression analysis indicate that MPB severity level, years since peak MPB, stand percentage of lodgepole pine, stand percentage dead, forest canopy closure, stand age, and stand height are not significant factors with respect to explaining variability in the difference between observed and predicted ROS. Additional findings from this study highlight potential factors that may have introduced uncertainty into this study, such as the identification of MPB-affected forest stands and variability in the FBP System calculations, findings that are consistent with existing research (Hart et al., 2021; Perrakis et al., 2014).

5.2 Contributions

The successful application of the photogrammetric monoplotting technique displayed in this research provides the fire science community with a significant contribution with regards to informing fire behaviour prediction and other aspects of wildland fire science. The main contributions were 1) an established method to acquire new and accurate fire behaviour observations using monoplotting, and 2) novel and empirically-based headfire ROS data in grey-attack MPB-affected forest stands.

In the context of informing fire behaviour prediction, the monoplotting approach demonstrated in Chapter 3 offers an established method to extract highly accurate fire behaviour data and fire spread observations, such as headfire front position, spread distance, and headfire ROS. In addition, this method has the potential to characterize other aspects of fire behaviour,

such as flame height, flame depth, smoke plume dimensions, and spotting. This is highly desirable for fire managers and researchers due to the scarcity of reliable fire behaviour observations to evaluate fire behaviour models (Alexander & Cruz, 2013; Gould et al., 2011; Sullivan, 2009). Furthermore, the knowledge of wildfire behaviour has never been more important due to the recent increase in the severity and frequency of wildfire events (Halofsky et al., 2020). The monoplotting method can advance fire behaviour prediction systems through providing accurate and rare empirical fire behaviour data in a diverse range of landscape settings under a variety of weather conditions. More so, the rise in availability of low-cost, high resolution input data, such as the LidarBC Open LiDAR Data Portal (Government of BC, 2022) and smartphone imaging technology (Blahnik & Schindelbeck, 2021) should increase the amount and availability of high resolution input data for the monoplotting method. Larger image archives with higher resolution input data, such as LiDAR DEM, not only leads to increasingly accurate fire behaviour data, but also builds the foundation for a broad range of future fire science research, such as the effect of varying pest insect outbreaks on fire behaviour and the discovery fire behaviour data in unexplored fuel complexes.

The utility of the monoplotting approach, with respect to its ability of collecting observable fire behaviour data, is further demonstrated wildfire spread rate analysis in grey-attack MPB-affected forest stands (Chapter 4). This research is desirable in the fire science community as there are significant gaps in the knowledge of fire behaviour in MPB-affected forest stands (Coogan et al., 2019; Jenkins et al., 2014), and limited studies using empirical evidence (Hoffman et al., 2015; Meigs et al., 2015; Moriarty et al., 2019). Aside from providing rare empirical spread rate data in grey-attack forest stands, this research performed a comparison between the grey-attack observed ROS and FBP System predicted ROS. The faster than expected

spread rates in grey-attack MPB-affected forest stands presented in this study highlighted the importance of investigating unexplored fuel complexes. Under or overpredicting fire behaviour can significantly impact the decision making ability of wildfire managers with potentially life threatening consequences. Similar to Chapter 3, the results of Chapter 4 showed that the applications of monoplotting are not limited to validating existing fire behaviour systems and known fuel types. Specifically, monoplotting can be applied to other areas of wildland fire science, such as exploring the relationship between pest insect outbreaks.

5.3 Future Research

Future research using the monoplotting method to obtain fire spread data from oblique aerial wildfire photographs should consider methodological recommendations and data improvements. In the context of future wildfire photograph acquisition, findings from Chapter 3 recommend that the photographs should display a highly visible fire front and be taken closer to fire front at a lower elevation to increase the accuracy of georeferenced photographs using MPT. Future research should also focus on acquiring and testing higher resolution data input data for their study area, such as high resolution photographs, orthoimagery, and LiDAR DEMs. This should increase the reliability of extracted fire behaviour data using MPT, such as headfire front positions, as it is known that the MPT georeferencing accuracy increases with increased resolution of input data (Bozzini et al., 2012). Additionally, future research regarding spread rate analyses should direct more efforts to identifying the fire front, as this is a complex process that must consider the visible flame depth, shape of fire front, location of smoke plume base, and direction of smoke spread.

Future research regarding wildfire spread analysis in grey-attack stage forest stands would benefit from advanced fire weather to reduce the uncertainty of spread rates predicted by

the FBP-System C-3 ROS model. In addition, this research would benefit from additional MPB-related data and advanced analyses to validate the presence and stage of MPB in the respective forest stands due to the temporal and spatial complexity of MPB-outbreaks in forest stands. Additional MPB-related data could arise from techniques using terrestrial LiDAR systems could generate statistically based estimates of forest stand variables such as tree volume, basal area, and fibre attributes regarding wood quality. Whereas advanced analyses considering the MPB-affectedness of a forest stand could include an automated grid cell landscape classification to estimate the stand percentage affected by MPB. The study presented in Chapter 4 used the closest weather stations to estimate the weather input variables, such as wind speed, precipitation, and relative humidity. While this was beneficial for providing the FBP System weather inputs of each site, the distance (up to 39km) limited the accuracy of the reported weather data for certain sites. Therefore, utilizing interpolated datasets will improve the reliability of weather data associated with wildfire sites that are not close to weather stations. Finally, this study used a small sample size with relatively low end range of fire spread rates largely due to their light wind conditions. This limited the ability to observe extreme fire behaviour, in particular the crown fire effects of MPB on forest stands. As such, it is important that future studies focus on a broader range of fire characteristics i.e. low to high ISI, and fire types, i.e. surface to crown fire, to explore the complete spectrum of fire behaviour in MPB-affected forest stands.

Overall, the research presented in this thesis demonstrated a novel application of monoplotting to acquire observational fire behaviour data from oblique aerial wildfire photographs captured during airtanker response. This work further demonstrates how monoplotting can be used to obtain novel empirical fire behaviour data while investigating fire

behaviour in unexplored fuel complexes. Additional findings from this research indicate that there are numerous opportunities that have yet to be explored with respect to monoplotting and wildland fire science, such as flame and smoke plume characteristic measurements or fire behaviour analyses in unexplored fuel complexes. It is evident that while there is room for improvements with regards to data, monoplotting can provide accurate fire behaviour data to inform fire behaviour prediction systems or other areas of wildland fire science where databases of such wildfire photographs exist. Fire behaviour prediction research will become more critical in the future as the severity and frequency of disturbance events, such as wildfire and pest insect outbreaks, increases as a result of climate change. Ultimately, the methods presented in this research provide fire management and researchers with invaluable resources to better understand and predict fire behaviour which are essential in making critical wildfire management decisions.

References

Alexander, M. E., & Cruz, M. G. (2013). Are the applications of wildland fire behaviour models getting ahead of their evaluation again? *Environmental Modelling and Software, 41*, 65–71. https://doi.org/10.1016/j.envsoft.2012.11.001

Blahnik, V., & Schindelbeck, O. (2021). Smartphone imaging technology and its applications. *Advanced Optical Technologies, 10*(3), 145–232. https://doi.org/10.1515/aot-2021-0023

Bozzini, C., Conedera, M., & Krebs, P. (2012). A New Monoplotting Tool to Extract Georeferenced Vector Data and Orthorectified Raster Data from Oblique Non-Metric Photographs. *International Journal of Heritage in the Digital Era, 1*(3), 499–518. https://doi.org/10.1260/2047-4970.1.3.499

Cheney, N. P., Gould, J. S., McCaw, W. L., & Anderson, W. R. (2012). Predicting fire behaviour in dry eucalypt forest in southern Australia. *Forest Ecology and Management, 280*, 120–131. https://doi.org/10.1016/j.foreco.2012.06.012

Coogan, S. C. P., Robinne, F. N., Jain, P., & Flannigan, M. D. (2019). Scientists' warning on wildfire — a canadian perspective. *Canadian Journal of Forest Research, 49*(9), 1015–1023. https://doi.org/10.1139/cjfr-2019-0094

Filkov, A., Duff, T., & Penman, T. (2018). Improving Fire Behaviour Data Obtained from Wildfires. *Forests, 9*(2), 81. https://doi.org/10.3390/f9020081

Gould, J., McCaw, M., Cruz, M. ., & Anderson, W. (2011). How good are fire behaviour models? Validation of eucalypt forest fire spread model (unpublished conference paper). Wildfire 2011, the 5th International Wildland Fire Conference, Sun City, South Africa.

Government of BC. (2022). *LidarBC Open LiDAR Data Portal*. Available online: https://governmentofbc.maps.arcgis.com/apps/MapSeries/index.html?appid=d06b37979b0c4709b7fcf2a1ed458e03 (accessed 15 March 2020).

Halofsky, J. E., Peterson, D. L., & Harvey, B. J. (2020). Changing wildfire, changing forests: the effects of climate change on fire regimes and vegetation in the Pacific Northwest, USA. *Fire Ecology*, *16*(1). https://doi.org/10.1186/s42408-019-0062-8

Harrison, S., Marlon, J., & Bartlein, P. (2010). Fire in the Earth System. In Dodson J. (Eds.) *Changing Climates, Earth Systems and Society. International Year of Planet Earth.* Springer. https://doi.org/https://doi.org/10.1007/978-90-481-8716-4_3

Hart, H., Perrakis, D. D. B., Taylor, S. W., Bone, C., & Bozzini, C. (2021). Georeferencing oblique aerial wildfire photographs: An untapped source of fire behaviour data. *Fire*, *4*(4). https://doi.org/10.3390/fire4040081

Hoffman, C. M., Linn, R., Parsons, R., Sieg, C., & Winterkamp, J. (2015). Modeling spatial and temporal dynamics of wind flow and potential fire behavior following a mountain pine beetle outbreak in a lodgepole pine forest. *Agricultural and Forest Meteorology*, *204*, 79–93. https://doi.org/10.1016/j.agrformet.2015.01.018

Jenkins, M. J., Runyon, J. B., Fettig, C. J., Page, W. G., & Bentz, B. J. (2014). Interactions among the mountain pine beetle, fires, and fuels. *Forest Science*, *60*(3), 489–501. https://doi.org/10.5849/forsci.13-017

McLauchlan, K. K., Higuera, P. E., Miesel, J., Rogers, B. M., Schweitzer, J., Shuman, J. K., Tepley, A. J., Varner, J. M., Veblen, T. T., Adalsteinsson, S. A., Balch, J. K., Baker, P., Batllori, E., Bigio, E., Brando, P., Cattau, M., Chipman, M. L., Coen, J., Crandall, R., … Watts, A. C. (2020). Fire as a fundamental ecological process: Research advances and frontiers. *Journal of Ecology*, *108*(5), 2047–2069. https://doi.org/10.1111/1365-2745.13403

Meigs, G. W., Campbell, J. L., Zald, H. S. J., Bailey, J. D., Shaw, D. C., & Kennedy, R. E. (2015). Does wildfire likelihood increase following insect outbreaks in conifer forests? *Ecosphere*, *6*(7), 1-24. https://doi.org/10.1890/es15-00037.1

Moriarty, K., Cheng, A. S., Hoffman, C. M., Cottrell, S. P., & Alexander, M. E. (2019). Firefighter Observations of "Surprising" Fire Behavior in Mountain Pine Beetle-Attacked Lodgepole Pine Forests. *Fire*, *2*(2), 34. https://doi.org/10.3390/fire2020034

Pausas, J. G., & Keeley, J. E. (2009). A burning story: The role of fire in the history of life. *BioScience*, *59*(7), 593–601. https://doi.org/10.1525/bio.2009.59.7.10

Perrakis, D. B., Lanoville, R. A., Taylor, S. W., & Hicks, D. (2014). Modeling wildfire spread in mountain pine beetle-affected forest stands, British Columbia, Canada. *Fire Ecology*, *10*(2), 10–35. https://doi.org/10.4996/fireecology.1002010

Reid, C. E., Brauer, M., Johnston, F. H., Jerrett, M., Balmes, J. R., & Elliott, C. T. (2016). Critical Review of Health Impacts of Wildfire Smoke Exposure. *Environmental Health Perspectives*, *124*(9), 1334–1343. https://doi.org/10.1289/ehp.1409277

Stockdale, C. A., Bozzini, C., Macdonald, S. E., & Higgs, E. (2015). Extracting ecological information from oblique angle terrestrial landscape photographs: Performance evaluation of the WSL Monoplotting Tool. *Applied Geography*, *63*, 315–325. https://doi.org/10.1016/j.apgeog.2015.07.012

Sullivan, A. L. (2009). Wildland surface fire spread modelling, 1990 - 2007. 2: Empirical and quasi-empirical models. *International Journal of Wildland Fire*, *18*(4), 369. https://doi.org/10.1071/wf06142